Engineering PLGA Particles for Advanced Drug Delivery

Elizabeth Enlow

A dissertation submitted to the faculty of the University of North Carolina at Chapel Hill in partial fulfillment of the requirements for the degree of Doctor of Philosophy in the Department of Chemistry

Chapel Hill
2010

Approved by

Professor Joseph M. DeSimone

Professor Valerie Ashby

Professor Sergei Sheiko

Professor Nancy Allbritton

Professor Moo Cho

Abstract

Elizabeth Enlow: Engineering PLGA Particles for Advanced Drug Delivery
(under the direction of Professor Joseph M. DeSimone)

Many effective therapeutics fail to meet their full potential *in vivo* due to toxic side effects, degradation under physiological conditions, poor bioavailability, and/or poor accumulation at the site of disease which has led to the development of particulate drug carriers. Of particular interest are biodegradable polymer particles which can be tailored to meet a wide range of needs, are biocompatible and leave no residuals *in vivo*. Herein the fabrication of engineered poly(lactic acid-co-glycolic acid) (PLGA) nanoparticles via the PRINT® (Particle Replication In Non-wetting Templates) process is reported. Complete control of size, shape, and composition was demonstrated. Biodistribution characterization of PLGA PRINT nanoparticles showed 10-15% tumor accumulation, suggesting these particles would make excellent drug delivery vehicles for advanced cancer therapy. Two approaches to cancer therapy were investigated: RNAi therapy and chemotherapy. These two therapies have different modes of action, different delivery requirements, and different cargo sensitivities. By exploring these dissimilar systems the true versatility of the PRINT process is demonstrated. To demonstrate gene delivery, nanoparticles were loaded with siRNA and knockdown was measured *in vitro*. Particles with poly(ethyleneimine) (PEI) as a complexing agent achieve knockdown with an EC_{50} of 184 nM, while particles coated with lipid achieve knockdown with an EC_{50} of 7 nM, rivaling the best systems reported. To illustrate chemotherapeutic efficacy, nanoparticles were fabricated with high and efficient loadings of docetaxel, up to 40% (w/w) with

encapsulation efficiencies >90%. These particles display cellular toxicity at sub-femtomolar docetaxel concentrations, displaying better *in vitro* efficacy than the standard of care, Taxotere®. *In vivo* these particles were shown to delay tumor progression in a xenograft mouse model. Fabrication of PLGA particles via the PRINT process enables independent control of particle properties (size, shape, cargo, polymer molecular weight, polymer lactic acid to glycolic acid ratio, and stabilizer) leading to a higher degree of tailorability than traditional methods and is versatile enough to be applied to dissimilar therapeutics. This system therefore shows great promise as a platform drug delivery technology.

The author would like to acknowledge those individuals who assisted the work herein: Dr. J. Christopher Luft, Dr. Patricia Ropp, and Dr. Shaomin Tian for *in vitro* work and biology advice, and specifically Dr. Luft for cell culture training; Charlene Ross and the animal core facility whose help was invaluable on all *in vivo* work; Dr. Warefta Hasan for countless hours of particle making on both chemotherapy and siRNA projects; William Hinson for assistance with the early biodistribution experiments; Dr. Victoria Madden and Dr. Wallace Ambrose for TEM analysis; and Dr. Chuanzhen Zhou at North Carolina State University for TOF SIMS analysis. A list of those who've assisted would not be complete without acknowledging Dr. Kevin Herlihy and Dr. Janine Nunes for innumerable scientific discussions over the years and for keeping me sane; Dr. Mary Napier for everything she does and whose door is always open; and Kelly Chang and Dr. Christine Conwell for their friendship in and out of lab.

Of course none of this would be possible without my advisor, Prof. Joseph DeSimone who took me in with no polymer or biology experience and taught me how to move forward in unfamiliar territory, to always keep the big picture in mind, and that diversity in expertise and experience is fertile grounds for innovation. Getting to participate in the development of this new and promising technology has been a privilege and I thank you.

Finally I owe everything to my incredible parents, Phillip and Sharon Enlow, and to my sister and best friend, Ashleigh Enlow Lewis. Thank you for being my biggest supporters and my most trusted confidants. My cup runneth over.

Table of Contents

List of Tables

List of Figures

List of Abbreviations

ASPC-1 – human pancreas adenocarcinoma cell line

AUC – area under the curve

DCM – dichloromethane

DiD – 1,1'-dioctadecyl-3,3,3',3'-tetramethylindodicarbocyanine perchlorate

DLS – dynamic light scattering

DMF – dimethylformamide

DMSO – dimethyl sulfoxide

DOPE – 1,2-dioleoyl-sn-glycero-3-phophoethanolamine

DOTAP – 1,2-dioleoyl-3-trimethylammonium-propane

DSC – differential scanning calorimetry

EC_{50} – half maximal effective concentration

H460 – human non-small cell lung carcinoma cell line

HeLa – human cervical adenocarcinoma cell line

HPLC – high performance liquid chromatography

IC_{50} – half maximal inhibitory concentration

IL-12 – interleukin 12

I.T. – intratumoral

I.V. – intravenous

kDa – kilodaltons (equivalent to 1,000 grams per mole)

LNCaP – human prostate carcinoma cell line

mPEG – methoxy terminated poly(ethylene glycol)

PBS – phosphate buffered saline

PDI – polydispersity index

PDMS – poly(dimethyl siloxane)

PEG – poly(ethylene glycol)

PEI – poly(ethyleneimine)

PET – poly(ethylene terephthalate)

PFPE – perfluoropolyether

PK – pharmacokinetics

PLGA – poly(lactic-co-glycolic acid)

PLLA – poly(L-lactic acid)

PRINT – particle replication in non-wetting templates

PVOH – poly(vinyl alcohol)

RNAi – ribonucleic acid interference

SEM – scanning electron microscopy

siRNA – small interfering ribonucleic acid

SKOV3 – human ovarian adenocarcinoma cell line

TEM – transmission electron microscopy

T_g – glass transition temperature

TNFα – tumor necrosis factor alpha

(w/w) – denotes a percentage expressed as weight per weight

(w/v) – denotes a percentage expressed as weight per volume

CHAPTER 1

INTRODUCTION TO ADVANCED DRUG DELIVERY

1.1 Introduction to Advanced Drug Delivery

Advanced drug delivery is the growing effort to take existing therapeutics with low efficacy or highly undesirable side effects and improve their localization to the site of disease thereby limiting systemic exposure and increasing therapeutic concentrations. The most common treatments in today's healthcare system are drugs administered orally or parenterally. Both result in the drug circulating in the bloodstream, reaching all tissues in the body. For some therapies this results in unwelcome side effects. This consequence is common for therapies where the drug is a cytotoxin, such as chemotherapies. Alternatively there are therapies where this exposure is not harmful for the body but degrades or destroys the activity of the therapeutic. This is common for therapeutics which are unstable or can be degraded by the body, such as RNA. For these reasons, the medical community is seeking new ways of delivering drugs. The most widespread application of these advanced therapies is in the treatment of cancer.

1.2 Cancer and therapeutic options

Cancer is a family of disease in which cells at almost any location in the body, though typically in organs, mutate. These cells loose the ability to perform their function, rapidly divide and eventually form a tumor. Cells can exit the tumor, enter the circulation, and lodge elsewhere spreading the cancer (termed metastasis). Cancer is difficult to treat because the body recognizes the tumor as self and therefore mounts no defense. Fatality results when the affected organ(s) fail. Treatment of cancer fall into three main categories: surgery to remove the tumor (resection), radiation therapy, and chemotherapy. Chemotherapy is the administration of cytotoxic agents whose purpose is

to kill the cells in the tumor. Unfortunately these cytotoxins reach not only the tumor, but the rest of the body as well, killing healthy cells and resulting in unwanted side effects. The reason this is effective to a degree is that chemotherapeutics tend to act more heavily on faster dividing cancer cells than healthy cells dividing at a normal rate. However, some healthy cells naturally have a high growth rate, such as hair, which is why people undergoing chemotherapy experience hair loss. Other common side effects include nausea, neuropathy, fluid retention, stomatitis, nail disorders, weakness, hypersensitivity reactions, and infection.[1] These harsh side effects limit the amount of therapy that can be administered and the frequency of administration. This limits the effectiveness of the treatment. If drug could be delivered to the tumor with limited systemic exposure then higher concentrations of drug in the tumor could be maintained and efficacy could be increased. Another method being investigated for cancer treatment is gene therapy. The administration of RNA or DNA can alter the production of proteins which are abnormally expressed in tumor cells leading to drug resistance, rapid division, and metastasis. However, these therapies will need an effective delivery vehicle to have clinical applications. Gene therapy can be used alone or to sensitize cells to chemotherapeutics.

1.3 Systemic administration of solubilized drug and drug conjugates

Two ways to deliver therapeutics more effectively to the tumor are passive targeting and active targeting. In passive targeting the unique attributes of tumor tissue are exploited. Since tumors grow more rapidly than normal tissue they are disordered and several systems are compromised. First the junctions of the endothelial cells in the vasculature are larger than in normal tissue. Therefore larger particles and moieties can

escape the vasculature than can in healthy tissue. This vasculature is termed “leaky”. Second the lymphatic system which drains tissue is not properly formed which results in poor clearance. These combine to form the enhanced permeability and retention (EPR) effect. Particles accumulate in the tumor since more can exit the circulation and are not effectively cleared. Passive targeting is employed by some the most common cancer therapies in the clinic today; formulations designed to deliver hydrophobic chemotherapeutics which were initially passed over in preference to hydrophilic chemotherapeutics which could easily be administered intravenously. Stabilizers such as Cremphor EL and Tween 80 are mixed with the therapeutic in water with small amounts of solvent so that the drug can be administered through an infusion. These formulations tend to create nano-aggregates which enhance tumor accumulation via the EPR effect and as such are a step toward enhanced delivery. The stabilizers carry toxicities of their own, however, which cause side effects.

By contrast active targeting relies on ligands which bind to receptors either specifically expressed or over-expressed on tumor cells, resulting in higher accumulation. The first therapies to take advantage of active targeting were drug conjugates. These chemically bound systems have a 1:1 payload to ligand ratio so for each recognition event only one molecule of therapeutic is administered. In addition to the low ratios of payload to ligand, these conjugates can elicit an immunoresponse and offer no protection to the cargo.

1.4 Enhanced drug delivery with liposomes and polymeric micelles

Liposomes, discovered in 1965[2] and proposed as drug delivery vehicles in 1976,[3, 4] took the idea of drug delivery beyond simple targeting of single therapeutic molecules to carrier systems which could deliver many therapeutic molecules and which could be multi-functional.[5] Liposomes are made up of a lipid bilayer which has wrapped around on itself to form a vesicle. Drugs can be encapsulated in these vesicles and can be released by diffusion or by the dissolution of the liposome. Hydrophilic drugs can be carried in the core, while hydrophobic drugs can be carried in the lipid bilayer. These carriers can take advantage of the EPR effect. One example of this technology currently in the clinic is Doxil®, a liposome that contains doxorubicin. This is a product of ALZA Pharmaceuticals (http://www.alza.com), and is marketed as STEALTH® liposomal technology. These liposomal systems are not without problems. There are instability and leakage issues, since the individual lipids are not covalently bound together. Liposomes also have a tendency to elicit the body's immunoresponse unless they include a poly(ethylene gycol) (PEG) coating. Finally, liposomes cannot completely protect cargo from degradation as they are not solid and have a certain flux of fluids and lipid molecules. Surfactant and polymeric micelles have been investigated as synthetic substitutes for liposomes.[6] Micelles can typically access a smaller size range than liposomes and can be produced at lower costs; some phospholipids are expensive. However, micelles still exhibit stability problems and incomplete cargo protection for the same reasons as liposomes. In addition, both liposomes and micelles have a critical micelle concentration (CMC), below which they disband. When a dose of micelles or liposomes is administered to a patient, the concentration is greatly lowered and special

care must be taken that this does not drop below the CMC. Finally, both micelles and liposomes are limited in the polymers/lipids that can be used for their formation as they require an amphiphile with specific subunit lengths, which restricts specific tailoring of delivery vehicles. Despite the disadvantages many therapeutics employing conjugate, liposome, and micelle technologies are approved by the FDA or are in clinical trials (Table 1.1).

Table 1.1 Examples advanced chemotherapy systems in clinical stages.[7]

Therapeutic Name	Platform	Chemotherapeutic	Clinical Stage
Smancs	Polymer conjugate	Neocarzinostatin	Approved
PK1	Polymer conjugate	Doxorubicin	Phase 2
hT-101	Polymer conjugate	Camptothecin	Phase 2
Xyota	Polymer conjugate	Paclitaxel	Phase 3
CT-2106	Polymer conjugate	Camptothecin	Phase 2
MAG-CPT	Polymer conjugate	Camptothecin	Phase 1
Doxil	Liposome	Doxorubicin	Approved
EndoTAG	Liposome	Paclitaxel	Phase 2
LE-SN-38	Liposome	SN-38	Phase 2
CPX-1	Liposome	CPT-11, floxuridine	Phase 2
NK105	Micelle	Paclitaxel	Phase 2
NC-6004	Micelle	Cisplatin	Phase 1/2
NK012	Micelle	SN-38	Phase 2
SP1049C	Micelle	Doxorubicin	Phase 3

1.5 Drug delivery using polymer particles

Recently, the interest in using solid polymer particles for medical purposes has grown considerably. Therapeutics can be encapsulated in polymer particles that can then be targeted to the appropriate site just as with liposomes and micelles. The advantages to

using solid polymer particles as vehicles for drug delivery are their ability to reduce the immunoresponse, give more protection to the cargo, reach a wider range of sizes, and tailor the release kinetics by specifically tailoring the polymer matrix.[8]

1.5.1 Bioabsorbable polymers

Of particular interest for solid polymer particles are bioabsorbable polymers. The use of bioabsorbable polymers in medical applications can be traced back to 150 A.D. when catgut was used to suture injured gladiators. Since then a range of synthetic polymers which degrade in situ have been discovered. These polymers are mainly polyesters which degrade hydrolytically and include poly(glycolic acid), poly(L-lactic acid), poly(D-lactic acid), poly(dioxanone), poly(ε-caprolactone), poly(β-hydroxybutyrate), poly(β-valerolactone), and their copolymers (Figure 1.1).

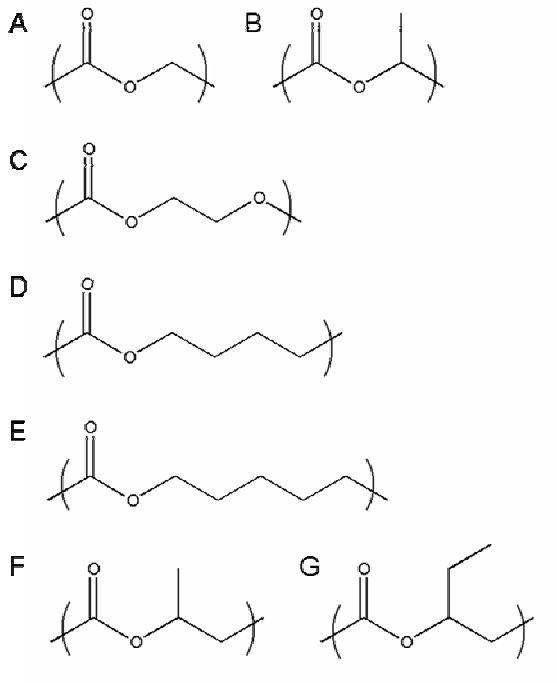

Figure 1.1 The chemical structure of biodegradable polyesters A) poly(glycolic acid), B) poly(lactic acid), C) poly(dioxanone), D) poly(valerolactone), E) poly(ε-caprolactone), F) poly(β-hydroxybutyrate), and G) poly(β-hydroxyvalerate).

As homopolymers, all the above polymers are semi-crystalline. The degradation of these semi-crystalline polymers varies according to the degree to which the ester in the backbone is susceptible to hydrolysis. Poly(L-lactic acid) degrades slower than the other mentioned homopolymers because of steric hindrance to hydrolysis created by the methyl groups off the backbone and because it alone is glassy at physiological temperatures, giving less mobility to the amorphous chains. Copolymers tend to be completely amorphous; however, at low percent incorporation of the second monomer they can retain some crystallinity. Random copolymers can be created by ring-opening polymerizations with incorporation ratios close to that of the feed ratios. When considering which polymer would be best for a specific purpose, the degradation rate is often the deciding factor. Amorphous polymers degrade faster than their semi-crystalline counterparts. This is due to the accessibility of the amorphous chains to water compared to the inaccessibility of close-packed crystalline chains. The most commonly used polyester is poly(lactic-co-glycolic acid) (PLGA). This polymer can be tailored by changing the lactic acid to glycolic acid ratios, yielding polymers which degrade anywhere from weeks to months. These polymers are identified by their lactic acid to glycolic acid ratios with the lactic acid, usually equal or higher, first (e.g. 85:15 PLGA is 85% lactic acid and 15% glycolic acid). Furthermore they degrade hydrolytically to produce lactic acid and glycolic acid which are naturally occurring and readily metabolized by the citric acid cycle. High molecular weight PLGA can be produced by a ring-opening polymerization of D,L-lactide and glycolide using an FDA approved stannous octoate catalyst. There are 17 medical uses of PLGA approved by the FDA. Prior approval makes this material very attractive as a drug delivery matrix.

1.5.2 Fabricating PLGA particles

Various methods for fabricating PLGA particles, including emulsions, precipitations, spray drying, and flow focusing, are currently under investigation by a large number of research groups.[9-14] A substantial volume of literature has been dedicated to investigating the effects of process parameters on particle properties and the attempts to develop trends to guide particle design have been reviewed.[15, 16] PLGA particles are, for the most part, currently being made by either emulsion solvent evaporation methods or supercritical processing techniques.

1.5.2.1 Emulsion/solvent evaporation methods

In emulsion solvent evaporation methods, PLGA is dissolved in a good solvent, typically dichloromethane. This solution is then added to water which contains a surfactant, typically poly(vinyl alcohol) (PVOH). By controlling the speed with which this mixture is stirred, the concentration of surfactant, and the specific PLGA used the size of the particles is roughly controlled. The solvent is then evaporated and the PLGA hardens into spheres.[9, 17-26] There are variations on this method involving double emulsions[27-30] and oil-in-oil emulsions[11, 31] that attempt to improve encapsulation of water-soluble drugs which tend to partition into the main water phase during the emulsion process.

1.5.2.2 Supercritical solvent/anti-solvent methods

Supercritical processing techniques used to produce PLGA particles can be divided into two main categories, those in which the supercritical fluid is the solvent and

those in which the supercritical fluid acts as an antisolvent. RESS (precipitation by rapid expansion of supercritical solutions) and RESOLV (rapid expansion of a supercritical solution into a liquid solvent) are two methods that have been used to produce PLGA particles in which the supercritical fluid acts as the solvent.[32-34] In these methods, PLGA is dissolved in $scCO_2$ with ethanol as a cosolvent. This solution is then sprayed into air (RESS) or an aqueous media (RESOLV). The rapid expansion of CO_2 lowers its ability to solubilize the polymer and particles precipitate. ASES (aerosol solvent extraction system) and PCA (precipitation with a compressed antisolvent) are two methods that have been used to produce PLGA particles in which the supercritical fluid acts as an antisolvent.[35-40] In supercritical antisolvent processes, PLGA is dissolved in a good solvent, typically dichloromethane. This is then sprayed into a chamber of supercritical CO_2. The solvent's ability to solvate the polymer is reduced as the solvent swells with the supercritical phase and the polymer hardens into spheres. For all supercritical processing techniques, the particle size is roughly controlled by the type of spray generated.

1.5.2.3 Methods to non-spherical particles

More recently investigation into non-spherical PLGA particles has been conducted including the fabrication of micron scale PLGA features by imprint lithography which can contain a reservoir[41, 42] and the deformation of PLGA microspheres into a wide variety of non-spherical shapes using a film stretching technique[43]. The former technique can only produce large particles while the latter technique requires starting with particles fabricated by emulsion methods so while shape can be imparted, the disadvantages of the emulsion method limit this technology.

Recently a hydrogel template method was demonstrated for the fabrication of PLGA particles. Microparticles were fabricated in a wide range of sizes and shapes, including a micron scale reproduction of a computer keyboard. Cylindrical 500 nm and 200 nm particles were also demonstrated. In this method gelatin is used as a mold, generated by pouring warmed gelatin over a silicon template and cooling in the refrigerator to "solidify". The so called hydrogel template is then filled with a high solids (40%) solution of PLGA in dichloromethane. After the dichloromethane evaporates the hydrogel template containing PLGA particles is warmed to dissolve the gelatin and release isolated PLGA particles.[44] These technologies clearly point to the desire to have more control over PLGA drug carriers, but have yet to produce nanoparticles with independent control over all key parameters and demonstrated efficacy as delivery vehicles.

1.5.3 PLGA-PEG particles: A popular variation on solid PLGA particles

While many researchers have studied solid PLGA particles, others have turned their attention to particles containing poly(ethylene glycol) (PEG) in the form of PLGA-PEG block copolymers. These block copolymers are most commonly synthesized using a carbodiimide coupling reaction between PLGA and commercially available amine-functional PEG[45, 46] but can be synthesized by using an methoxy-PEG (mPEG) to initiate a ring opening polymerization of lactide and glycolide in the presence of a tin catalyst.[47] Particles are fabricated from these copolymers by emulsion or nanoprecipitation processes. An emulsification agent such as PVOH is often still required since the PEG block, typically 2-5kDa, can be over an order of magnitude smaller than the PLGA block.

The goal is for the PEG block to orient to the surface of the particle, providing enhanced stability and stealth. The degree to which PEG appears on the surface, and to which residual PVOH remains, is more often presumed than measured. However, the effects are measured. For instance, Senthilkumar et al. compared solid PLGA particles to PLGA-PEG particles fabricated using the exact same method and saw some enhancement in circulation and tumor accumulation *in vivo*.[47] The additional considerations for PLGA-PEG particles are the liability of the bond between polymers and the ratio of PLGA to PEG.

1.5.4 Factors affecting encapsulation and release of therapeutics

The two most studied properties of PLGA particles for drug delivery are their ability to encapsulate drug and the release profile of this drug. These properties depend strongly on the PLGA used and the method of fabrication. The encapsulation efficiency of a drug is defined as the amount of drug in the particle over the amount of drug charged to the system. This is a crucial parameter because in all the previously described systems there are two phases and any cargo can partition between these two phases based on its specific solubility characteristics. Furthermore it has been reported that in the case of emulsion fabrication methods, by far the most common methods, the more drug charged to the system the higher the loss.[48] This limits the payload of the particles. Attempts to increase the encapsulation efficiency include moving from oil-in-water (o/w) emulsions to water-in-oil-in-water (w/o/w) double emulsions, increasing interfacial tension between the dispersion of polymer/drug and the second phase, modifying the therapeutic to increase its hydrophobicity, and modifying the process to generate particles which harden

faster.[16] Another characteristic of the particle which is affected by the process parameters is the release profile. Studies have shown that particle release and degradation properties are affected by solvents, emulsifier/stabilizer, cargo, molecular weight of polymer, lactic acid to glycolic acid ratio and particle size.[49-53] There is no simple formula as all these parameters are interrelated, however, three trends do emerge from the body of literature: smaller particles release faster, high lactic acid content slows release, and higher molecular weight slows release. Smaller particles show faster release due to their increased surface area to volume ratio and reduced distance to the surface from the core of the particle.[16] A polymer with a higher lactic acid content slows the degradation and release rates due to the increased hydrophobicity of the lactic acid unit which reduces water diffusion into the particle. The methyl group which distinguishes this unit from the glycolic acid unit also adds steric hindrance so that access to the backbone of the polymer by water is decreased resulting in slower degradation.[54] Finally, higher molecular weight polymers exhibit slower release and degradation characteristics due to higher entanglement, higher T_g, and longer times to soluble fractions.[54] Other variables that relate to the rate the drug diffuses through the PLGA matrix include the properties of the drug, the amount of drug loaded, drug/polymer interactions, plastization of the polymer by the drug or residual solvents, and initial porosity.[16] Despite all these differences, most PLGA particles display a burst release of 10-30%. This is attributed to the fast dissolution of drug on and near the surface of the particles. This is then typically followed by a slow release phase as drug diffuses from the center of the particle and the polymer degrades.[16]

1.5.5 *In vitro* toxicity and internalization of PLGA particles

Once a formulation is chosen, particles are typically tested first for their *in vitro* behavior using cell culture and then for their *in vivo* behavior using mouse models. The most common *in vitro* measurements are for toxicity of the matrix material, internalization of particles, and efficacy. PLGA is such an attractive choice because it has a long history of safety in humans. Specifically micro- and nanoparticles fabricated from PLGA have proven to be non-toxic on a wide variety of human cell lines.[55] After vehicle safety is determined, the internalization of PLGA nanoparticles is important to characterize for each formulation being considered. The specific cell line under investigation affects the degree and rate of particle internalization.[56] The specific therapeutic being delivered is also important to consider. For some treatments the therapeutic can cross the cellular membrane on its own and particle internalization is not necessary, however, can potentially improve efficacy. In these instances particles can be used as local depots of drug, delivering drug to the extracellular space of the tumor. For other treatments the therapeutic can not cross the cellular membrane on its own and must be transported across the membrane by the particle. This is common with negatively charged therapeutics such as siRNA because the cell membrane is also negatively charged and the two repel each other. For particles which are internalized, intracellular trafficking is also important. The particles are typically endocytosed via pathways that join with or evolve into endosomes. The therapeutic or particle must escape the endosome before it evolves into a lysosome, in which the therapeutic will most likely be degraded. Most studies of internalization and transport use a hydrophobic fluorescent dye which has been encapsulated or physically entrapped in the particle as a marker of

location. It is believed that this dye will not be released from the particle due to hydrophobic interactions with PLGA and poor solubility in the surrounding media. Confocal microscopy or flow cytometry are then used to determine if dye can be observed inside the cells. These studies predominately show rapid internalization of PLGA nanoparticles.[57] In most cases the particles are not targeted and have a coating of PVOH which was used in the fabrication of the particles or a coating of PEG incorporated via PLGA-PEG block copolymers. Since PLGA, PVOH and PEG can only contribute negative charge it is not surprising that these particles are always negatively charged. What is surprising is that the cells would be rapidly internalizing negatively charged particles based on the aforementioned repulsion with the cell membrane. In fact many other studies have shown that positively charged particles are rapidly endocytosed while negatively charged particles are not.[58] While some researchers have accepted a positive internalization result using these methods without further investigation, some recent findings are suggesting a closer look may be warranted.[57] An alternative explanation of contact transfer of dye from the particles to the cellular membrane has been suggested by Xu et al. They propose particles in contact with the cell membrane transfer dye directly into the lipid bilayer. A thorough set of experiments was conducted to test the contact transfer theory. First two sets of particles were fabricated: one with a physically entrapped hydrophobic dye and one with a dye chemically bound to the PLGA. The particles with physically entrapped dye showed very high cellular internalization at very short time points whereas the particles with bound dye showed almost no internalization out to 24 hours. In time course studies with physically entrapped dye they saw very rapid internalization followed by a drop in intracellular

fluorescence once the media was changed. This implied the dye was partitioning back out of cells into the media over time. This is important to note as some groups report this same observation and attribute it to particle exocytosis. This can be substantial with observations of a 65% drop of fluorescence at 30 minutes after replacing media being reported.[59] Xu et al. further studied the contact transfer phenomena to determine whether the dye is first released from the particles and then internalized by cells or whether the dye is transferred to the lipophilic membrane via direct contact. To study this they compared release in phosphate buffered saline (PBS) to release in PBS with fetal bovine serum (FBS) and release in PBS containing liposomes to simulate the cell membrane. They found almost no dye released in PBS, increased slightly by the addition of FBS to simulate media, but increased by 5-fold with the inclusion of liposomes. This supports the mechanism of contact transfer and is a crucial observation as some groups demonstrate no release in PBS as evidence that the dye does not leach from the particle.[57] This is not to say that all positive internalization measurements are false readings and that under no circumstances are PLGA particles internalized by cells. Several variables could be playing a role to this point missed due to an over-estimation of internalization. For example, the amount of residual PVOH on the surface of particles is highly varied and not well controlled. This could affect internalization by modifying the hydrophilicity of the particle and the degree of surface shielding. It has been demonstrated that particles with higher amounts of PVOH associated with the surface show lower cellular internalization.[60] Although fluorescence may not be reliable there are other methods available for the determination of cellular internalization. These methods require more sample preparation and more sophisticated equipment so are used less often.

Transmission electron microscopy (TEM) is an example of a more reliable method which has been used to observe particle internalization.[61] In addition this method has been used to look at the intracellular fate of particles. The most important aspect of intracellular trafficking is escape from the endosome. In a study by Panyam et al. rapid endosomal escape (10 minutes) of 70 nm PVOH stabilized PLGA particles was observed using fluorescent microscopy supported by TEM analysis. Further investigation into the mechanism of this escape revealed the PLGA particles exhibited a charge reversal at pH 5 from negative to positive. As an endosome matures the pH drops to 5 from initial physiological pH. This would reverse the charge on the particle once internalized and this charge reversal would result in interaction with the endosomal membrane and generate a proton sponge effect.[61] Other groups have observed endosomal escape with PLGA nanoparticles as well.[62]

The investigation into non-spherical particle internalization is a relatively unexplored arena as most fabrication methods result in spherical particles. Champion et al. looked at the internalization of particles which were on the micron scale and found the angle of curvature where the cell encounters the particle determines whether the cell will attempt to phagocytos the particle. Whether it succeeds then depends on how large the particle is in relation to the cell.[63] Whether the angle of curvature theory holds for nanoparticles is unknown. The internalization of non-spherical nanoparticles with controlled shape and size is a relatively new field as technologies capable of fabricating these particles emerge. A study looking at cationically charged PEG hydrogel particles fabricated by the PRINT® process has demonstrated the importance of shape and size on the nanoscale. It was shown that particles 1 micron and smaller were readily taken by

HeLa cells within 4 hours. It was furthermore demonstrated that 150 nm particles with an aspect ratio of 3 were taken up more rapidly than particles of a similar volume with an aspect ratio of 1.[58] A particle with a high aspect ratio can deliver a higher payload per internalization event than a particle with the same critical dimension and an aspect ratio of 1. This could be used to achieve higher efficacy at a lower total dose.

1.5.6 Biodistribution

While the internalization of particles is necessary for some therapeutics and not for others, the biodistribution of the particles is always an important consideration. This has mostly been studied through the chemical attachment of a radioactive isotope to the polymer itself. Factors affecting the biodistribution of particles include size, shape, and stabilization method. There are several key aspects of biodistribution to consider for cancer therapy applications. First and foremost being the quantity of particles accumulating in the tumor over time. Particles <400 nm can take advantage of the EPR effect as previously discussed.[56] Secondly, circulation half lives are important since the longer particles circulate the more passes of the tumor vasculature and therefore the higher probability that they will be extravasated. Additionally the circulation half life of the particle must be considered when tailoring release and degradation characteristics. There are also organs where a lack of accumulation is desired. For example some chemotherapeutics are cardiotoxic when delivered systematically and therefore accumulation in the heart would preferably be decreased. Finally there is the avoidance of the clearance systems in the body. The main organs of clearance are the liver, spleen, and kidneys. The kidneys clear molecules and particles <10nm.[56] Almost all polymer

particles currently being investigated fall above this cut off and kidney clearance is not consider a major issue. The liver and spleen tend to clear particles which are >100nm.[56] The liver and spleen are therefore the main organs of accumulation for PLGA nanoparticle therapies which are typically 100 – 300 nm in size.[64-67] Naturally the level of particles in these organs drop over time as the particles are cleared.[64, 65, 68] The particles once cleared can accumulate further in the tumor or be cleared by the intestines and, once degraded, the kidneys.[64, 66] A comparison of PEGylated and sterically stabilized PLGA nanoparticles by Panagi et al. revealed similar distribution profiles between formulations over very different time scales. The PEGylated PLGA particles (113 nm; -4 mV) exhibited distribution over 24 hours while the sterically stabilized PLGA particles (154 nm; -45 mV) distributed over just 60 seconds. The majority of the particles (60%) accumulated in the liver and spleen. While organ accumulation was very similar the PEGylated particles showed enhanced circulation times which could be very beneficial in tumor accumulation; however this study was in healthy animals so tumor accumulation was not tested. Unlike most biodistribution studies which only look at major organs, this study looked at accumulation in the muscles, bone, and the carcass once all measured organs were removed. The authors report 5-10% of all formulations accumulating in both muscle and bone as well as 20% in the carcass. This demonstrates the potential for missing particles when only major organs are measured. Furthermore the effect of dose on biodistribution was investigated. Four doses over an order of magnitude were administered: 150-1050 μg for PEGylated and 63-750 μg for sterically stabilized. For PEGylated particles the dose had no effect, however, for sterically stabilized particles the higher dose resulted in slightly longer circulation and reduced liver and spleen uptake

with no other organs affected. This was attributed to saturation.[65] Many groups use PEGylated PLGA particles based on the touted advantages in circulation times. Li et al. demonstrated that 198 nm PLGA-PEG particles circulated for 24 hours, while 214 nm PLGA particles only circulated for 2 hours.[69]

Whenever considering the biodistribution profile of a specific formulation note should also be taken of lung accumulation. Larger particles or aggregates of particles can become physically entrapped in the lung. If there is too much accumulation this can result in inflammation or embolization. Generally lung accumulation is unwanted and may be a sign of stability problems with the formulation, however, some have considered this as a passive targeting strategy. Zhang et al. dosed mice with PLGA microparticles in three size ranges: <5 microns, 5-20 microns, and >20 microns. Particles 5-20 microns showed the highest lung accumulation, while all sizes showed lung accumulation higher than liver and spleen.[70] In addition to size, charge has been linked to lung accumulation. Xu et al. measured biodistribution of 192 nm PEGylated PLA particles which carried a positive charge (+5 mV) and observed lung accumulation 3 times higher than similarly sized negative PEGylated PLA particles (155nm, -36 mV) for which liver was the most prominent organ of accumulation as expected.[68]

1.5.7 *In vivo* internalization and tumor penetration

Some groups have taken the study of biodistribution further looking at the distribution of particles within the tumor and cell internalization *in vivo*. This information is important when designing therapies because some delivery systems will aim to destroy the vasculature of the tumor thereby cutting off its nutrient supply while other therapies

will need deeper tumor penetration. And as previously discussed some therapies require cell internalization while some do not. *In vitro* studies can not fully mimic the environment of a tumor. Lee et al. studied the tumor penetration of PEGylated poly(caprolactone) (PCL) nanoparticles, the second most prevalently used polyester after PLGA. They compared particles which were 25 nm and 60 nm. In addition they compared targeted versus non-targeted particles to investigate the theory of binding site barrier. This suggests that targeted particles will have less/slower diffusion through tumor tissue since they will bind to cell as soon as they leave the circulation. First they found that 25 nm particles had a 2-fold lower total tumor accumulation than 60 nm particles and that targeted particles had a slightly higher accumulation for both sizes. They attributed this to the smaller particles being easier to clear from the tumor. This further demonstrates that an optimum size is yet to be completely teased out, partly due to the heterogeneous sizes of traditionally fabricated particles. Next they looked at tumor penetration and found that the 25 nm particles penetrated tumor tissue 46 microns from the vasculature, reduced to 34 microns when targeted and that 60 nm particles penetrated tumor tissue only 20 microns, reduced to 14 microns when targeted. Finally they looked at cellular internalization observing most particles, targeted and non-targeted, were in extracellular space. This is in sharp contrast to their *in vitro* finding which showed high internalization of all particles.[71] This study clearly demonstrates the complex issues of tumor delivery, *in vivo* internalization, and the need for studies which have very well defined particle size.

While size effects on biodistribution have been investigated, shape has remained more elusive. Most particle fabrication techniques can not access non-spherical shapes

and most particle fabrication techniques that can produce micron-sized particles. Recently the Discher group developed a process for the fabrication of "filomicelles" which are flexible, filamentous micelles composed of PCL-PEG block copolymers. They studied the distribution of these filomicelles compared to spherical micelles of the same critical dimension and found increased circulation times and frustrated macrophage internalization. At 24 hours 63% of the filomicelles were still in circulation. They further showed that the filomicelles could encapsulate hydrophobic anti-cancer drugs and increase the maximum tolerated dose (MTD). These particles exhibited better *in vivo* efficacy than the standard of care therapy.[72] The enhanced efficacy of these particles over spherical particles further intensifies interest in non-spherical particles and the effect of shape on biodistribution.

1.6 Chemotherapeutic Delivery

Particles with promising biodistribution profiles are often tested for efficacy using standard of care chemotherapeutics. These systems are well documented in the literature, standard *in vitro* cytotoxicity assays can be used to screen formulations, and efficacy in *in vivo* models are well known. The most commonly used chemotherapeutics interfere with either microtubule assembly/disassembly or DNA replication to prevent mitosis. Taxanes are a group of compounds, natural and synthetic, which prevent mitosis by stabilizing microtubules, in essence "freezing" the cell. Docetaxel (Figure 1.2) is a semi-synthetic taxane; an esterified product extracted from the yew tree.

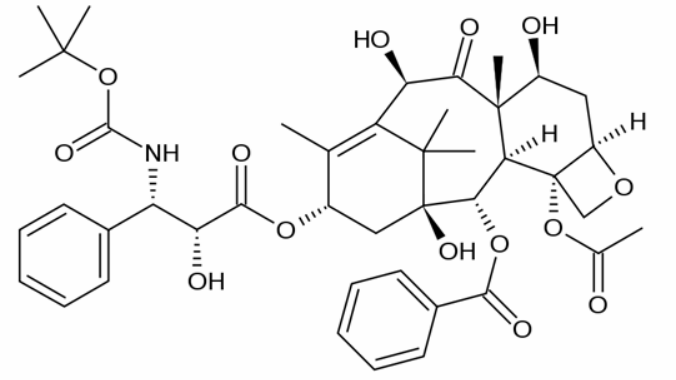

Figure 1.2 The chemical structure of docetaxel.

Docetaxel has been approved for the treatment of breast, lung, prostate, gastric, and head and neck cancer in the form of Taxotere®, a formulation of docetaxel in water and ethanol with poloxomer 188 (Tween 20) for stabilization. Docetaxel has shown promise over doxorubicin, paclitaxel and fluorouracil, however, it has dose limiting toxicities associated with systemic delivery, making it a prime candidate for improvement through encapsulation in a delivery vehicle.[73]

1.6.1 Docetaxel encapsulation

Several groups are investigating the use of PLGA particles as delivery vehicles for docetaxel. The first challenge is to load docetaxel into the nanoparticle. Using a block copolymer of PLGA and PEG to form micelles which encapsulate docetaxel in their hydrophobic core is the most common approach with maximum loadings at 15% (Table 1.2). The ability of a system to load docetaxel effectively is dictated by the partitioning of the docetaxel between the pre-particle phase and the secondary phase, usually water. The specific process parameters used will effect encapsulation.

Table 1.2 The encapsulation of docetaxel in PLGA/PLA particles.

Fabrication Method	Matrix	Theoretical Loading	Encapsulation Efficiency	Ref
Emulsion	PLGA	0.5-1%	17-23%	[74]
	PLA	0.5-1%	11-22%	[74]
	PLGA-mPEG	2%	77-83%	[47]
	PLGA-mPEG	2%	74%	[48]
	PVP-b-PLGA	4%	>95%	[75]
	PLGA-mPEG	6%	26%	[48]
	PLGA-lecithin-PEG	10%	62%	[49]
	PLGA	11%	70%	[53]
	PLGA/Poloxamer188	11%	88%	[53]
Nanoprecipitation	PLGA-PEG	10-15%	21-51%	[76]
Film Rehydration	PEG-b-PLA	12%	98%	[77]
Ultrasonication	NGR-PLA-PEG	5-15%	95-98%	[78]

1.6.2 Docetaxel release

In addition to being able to load a cargo efficiently, it is essential that the cargo is able to be released in an appropriate time frame. Release studies are typically carried out at 37^{o}C and pH 7.4 to mimic *in vivo* conditions. In addition it is important that the release is measured under so called "sink" conditions. Released drug is removed so that there is always a gradient which favors drug diffusion out of the particle into the surrounding media. PLGA particles release cargo through a combination of diffusion and degradation.[50] Although docetaxel has very low water solubility (14 ug/mL) these particles display a typical burst release followed by a extended release phase. The burst

phase typically represents 10-30% of the total encapsulated docetaxel, but can be higher with reports of 65% burst release (Table 1.3). Particles then release cargo at a slower rate over a week to a month.[45, 47, 74, 79]

Table 1.3 Examples of release from docetaxel loaded PLGA/PLA particles.

Matrix	Size (nm)	Docetaxel Loading*	Burst Release	Total Days of Release	Ref
PLGA	157	0.5%	65%	15	[74]
PLA	123	0.5%	45%	15	[74]
PLGA-mPEG	105	2%	30%	30	[47]
PLGA	105	2%	12%	30**	[48]
PLGA-lecithin-PEG	80	10%	20%	4	[49]
PLGA	275	11%	10%	30	[53]
PLGA/Poloxamer188	218	11%	15%	30	[53]
PEG-b-PLA	35	12%	20%	1	[77]

*See Table 1.2 for encapsulation values
**This particle released a maximum of 40%

1.6.3 *In vitro* cytotoxicity of docetaxel containing PLGA nanoparticles

Typically docetaxel containing PLGA nanoparticles are slightly less potent or equally potent to Taxotere® *in vitro*. It should be noted however that drug free nanoparticles show much less toxicity than Tween 80, therefore the toxicity comparison is somewhat clouded.[45, 52] When compared to free docetaxel instead of clinically formulated drug, docetaxel loaded PLGA nanoparticles have been shown to exhibit higher toxicity. Esmaeili et al. compared docetaxel loaded PLGA nanoparticles sterically stabilized with PVOH to free docetaxel which they solubilized using a stock solution in dimethyl sulfoxide (DMSO) instead of ethanol and Tween 80 (Taxotere®). They observed IC_{50} values up to 9 times lower than docetaxel with their particle formulation and showed enhanced toxicity in three different cell lines (T47D, SKOV3, and MCF7) with one cell

lines exhibiting similar toxicity (A549).[79] Targeting can further enhance docetaxel toxicity, presumably by enhancing internalization. Farokhzad et al. compared the toxicity of docetaxel loaded PLGA-PEG nanoparticles which were untargeted to nanoparticles targeted with a PMSA aptamer on LNCaP cells. Viability decreased from 61% to 42% at 30 minutes and from 48% to 30% at 2 hours with the addition of the targeting ligand.[46] Docetaxel can cross the cell membrane on its own so internalization is not necessary for cytotoxicity, but by delivering a higher payload directly into the cell higher toxicity can be achieved.

1.6.4 *In vivo* efficacy via intratumoral injection

Many researchers move from *in vitro* studies to *in vivo* studies by first testing particles directly injected into the tumor. This allows the cytotoxicity of the formulation to be tested under *in vivo* conditions without involving the additional issue of biodistribution. Farokhzad et al. investigated the efficacy of non-targeted versus targeted PLGA-PEG nanoparticles (153 nm) in LNCaP xenograft tumor bearing nude mice. Mice were dosed with 40 mg/kg docetaxel in one intratumoral injection. As such, accumulation in the tumor was the same for all formulations; however different clearance and delivery mechanisms were still in play. The results after almost 4 months of monitoring showed that the non-targeted particles were more effective than emulsified drug while the targeted particles were the most effective. Both particle formulations resulted in regression with subsequent growth at a slower rate than controls. After 110 days the non-targeted particle group had progressed back to the original tumor volume while the targeted particle group was still one third to one fourth the original volume. The

enhancement seen with targeting could be due to reduced clearance or to increased internalization or both.[46]

1.6.5 *In vivo* efficacy via intravenous injection

While higher potency *in vitro* is not always achieved, the enhanced tumor accumulation of the particle often leads to higher *in vivo* efficacy, while the decreased exposure to other organs reduces systemic toxicity. Senthilkumar et al. compared docetaxel loaded 100nm PLGA nanoparticles without PEG, with 2K PEG, and with 5K PEG to free docetaxel. The plasma elimination half lives of PLGA nanoparticle formulations with PEG were twice that of the formulation without PEG: 3.29 hours (no PEG) versus 6.90 hours (2K PEG) and 7.26 hours (5K PEG). All nanoparticle formulations outperformed free docetaxel which had a plasma elimination half life of 1.93 hours. At 12 hours post-administration PLGA-PEG (5K) particles showed tumor accumulation 8 times higher than free docetaxel and 3 times higher than nanoparticles without PEG. As expected the tumor accumulation increased from 1 hour post-administration to 12 hours post-administration. Interestingly by 24 hours docetaxel had been eliminated from the tumor for all particle formulations and free docetaxel. All formulations showed high liver and spleen accumulation at 1 hour which decreased over the following 24 hours. With all three particle formulation showing increased tumor accumulation, the anti-tumor efficacy of these formulations was tested in mice bearing xenograft C26 tumors (murine colon adenocarcinoma). Mice were dosed every other day until they had received a total of 5 doses (the dose is reported only as "a selected dose" throughout the manuscript). However it is clear that all mice treated with docetaxel

showed tumor regression while vehicle and saline treated mice did not. Furthermore the particle formulations showed enhanced efficacy, with the PEGylated formulations showing the most regression. As a measure of health the mice were also weighed during the course of the study. Mice which received free docetaxel exhibited significant weight loss. Mice which received nanoparticles without PEG also showed some weight loss while mice which received PEGylated nanoparticles did not. This is not addressed by the authors but could be due to increased accumulation in other organs as compared to the PEGylated formulations.[47]

In addition to increased tumor accumulation, avoidance of cardiotoxicity is a major concern with docetaxel therapy. Esmaeili et al. investigated the biodistribution of docetaxel loaded PLGA nanoparticles (175 nm) sterically stabilized with PVOH compared to Taxotere® in healthy mice. They showed decreased accumulation in the heart, kidneys, and interestingly the liver with nanoparticle formulations.[79] This could partly be due to the fact that Taxotere® forms nanoaggregates which would be trapped by the liver. The favorable comparison to Taxotere® makes PLGA nanoparticle systems even more attractive.

1.6.6 Chemotherapeutic PLGA particles in clinical trials

The benefits of these polyester delivery systems for chemotherapy have led to clinical applications. Genexol® is a PDLLA-PEG nanoparticle containing paclitaxel currently in Phase I/II/III trials for various cancers and combination therapies. Genexol® is already approved in Korea. Paclitaxel is the naturally occurring analog from which docetaxel was developed. It has been studied longer and is currently in patients as

Taxol®, a Cremaphor EL solubilized form similar to Taxotere®. Also approved is Abraxane®, a nanoassembly with albumin. Genexol® did not show enhanced *in vitro* cytotoxicity, but as previously discussed the anti-tumor efficacy was improved over Taxol® due to the improved tumor delivery. A combination of Genexol® with cisplatin is has proven more effective with less systemic toxicity in patients with advanced non-small cell lung cancer than Taxol® with cisplatin. Genexol® showed a higher response rate in women with metastatic breast cancer over Taxol®. This particular application has progressed to Phase III clinical trials and demonstrates the advances being made with PLGA drug delivery.[52]

1.7 RNA interference and siRNA delivery

In addition to the delivery of hydrophobic chemotherapeutics, PLGA nanoparticles have been explored for RNA therapies. RNA interference (RNAi) is a natural gene silencing process which can be induced by the introduction of small interfering RNA (siRNA), double stranded RNA molecules 20-22 nucleotides in length, to the cytoplasm. Once the siRNA enters the cytoplasm it is recognized and the active strand is incorporated in the RNA-induced silencing complex (RISC). This complex binds messenger RNA (mRNA) possessing the complementary sequence. This mRNA is then cleaved, preventing protein production. Many mRNA can be cleaved by a single siRNA/RISC. The reduction in the targeted protein levels is referred to as gene knockdown (Figure 1.3).

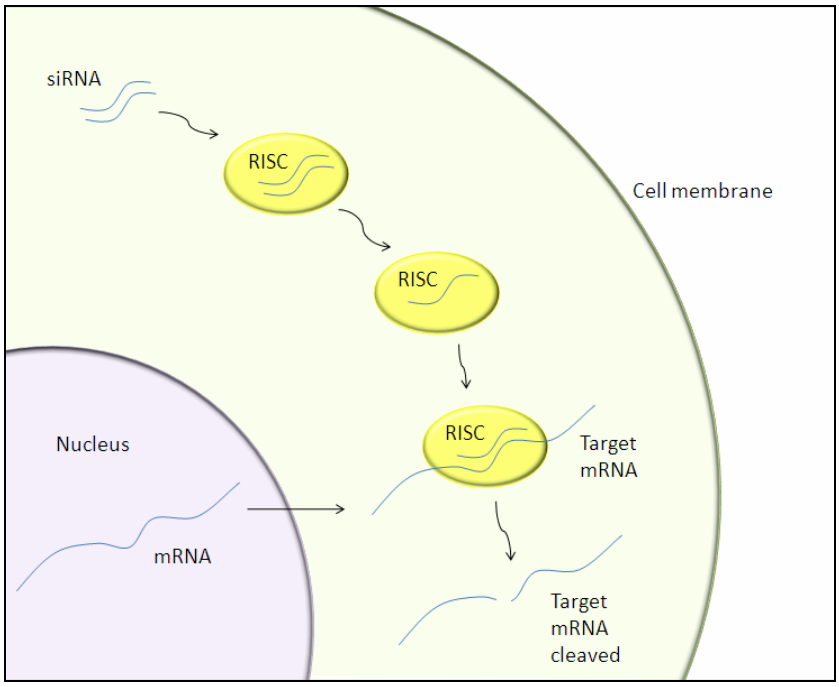

Figure 1.3 The RNAi pathway.

RNAi was first reported by Craig Mellow and Andrew Fire in 1998, who won the Nobel Prize in 2006 for this discovery. The RNAi pathway is a cell's defense against viruses and so called jumping genes. Viruses use a host cell to generate copies by injecting genetic information into the cell. Most RNA in our cells is single stranded. A major class of viruses (Class III) inject double-stranded RNA into cells. The cell recognizes this RNA material as foreign and the RNAi pathways acts to degrade the viral mRNA before proteins are produced generating copies of the virus. Exploiting this inherent pathway of gene knockdown is recognized as a therapeutic treatment options for a variety of diseases including cancer. The targets are oncogenes, genes that are mutated or expressed in abnormal levels in cancerous cells. Examples of genes over-expressed in cancerous cells are growth factors, transcription factors, tyrosine kinases, and regulatory GTPases. These genes regulate cell proliferation and can induce angiogenesis, the growth of new blood vessels. The over-expression of these genes leads to uncontrolled proliferation which

results in the formation of a tumor. Turning these genes off using siRNA therapy could be effective at fighting the disease; however siRNA is easily degraded *in vivo* and does not readily cross the cell membrane so the development of effective therapies will fully require the development of efficient delivery systems.

1.7.1 Incorporating siRNA in cationic PLGA nanoparticles for effective transfection

The design of PLGA nanoparticles for siRNA delivery is more complex than for the delivery of chemotherapeutics. First siRNA is hydrophilic making it more difficult to encapsulate using traditions two-phase processes that typically rely on water as the anti-solvent. For this reason modifications such as the use of double emulsions (w/o/w) have been employed. Secondly the delivery of chemotherapeutics does not require particle internalization, but the delivery of siRNA does. The siRNA must be introduced into the cytoplasm so both particle internalization and endosomal escape are necessary. The most common method used to achieve efficient delivery is the incorporation of poly(ethylene imine) (PEI) (Figure 1.4).

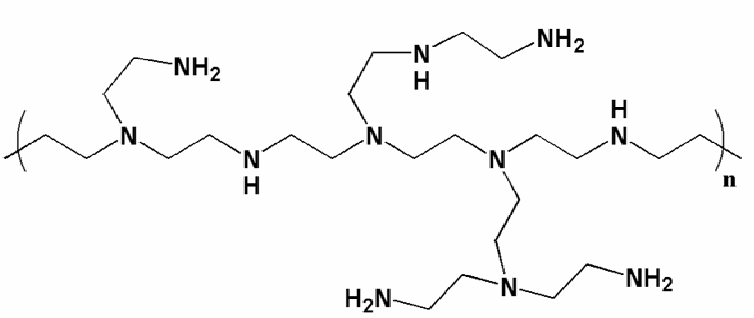

Figure 1.4 The chemical structure of branched poly(ethylene imine) (PEI).

PEI can be used alone as a transfection agent due its high water solubility and high density of primary amines which act to condense the negatively charged siRNA, induce

endocytosis, and promote endosomal escape through the proton sponge effect. PEI can be linear or branched, with the branched variation having primary, secondary, and tertiary amines. However there are toxicities associated with free PEI due to membrane disruption common to positively charged molecules. Combining PEI with PLGA in a nanoparticle form reduces toxicity.[80] The safety of PLGA/PEI particles with and without siRNA has been demonstrated by Patil et al. who observed no toxicity out to 500 ug/mL *in vitro* while PEI alone showed >90% cell death at doses an order of magnitude lower (<50 ug/mL).[81] Despite the ionic interactions with PEI, siRNA still exhibited a burst release from these particles followed by steady release over the next two weeks.[81] There are a variety of ways PEI can be incorporated in the particle. Zhang et al. compared three different methods using plasmid DNA (pDNA), a gene therapy tool for increasing protein expression. They compared 2 micron PLGA particles fabricated using a double emulsion technique encapsulating pDNA: composition one contained pDNA in the inner emulsion of PLGA without PEI, composition two contained pDNA in the inner emulsion of PLGA/PEI, composition three contained pre-formed PEI/pDNA complexes in the inner emulsion of PLGA, and composition four had pDNA adsorbed to the surface of PLGA/PEI particles. They determined the pDNA was effectively bound in/to the particles in all cases. They also showed all three methods of incorporating PEI in the PLGA particle greatly reduced associated toxicity on COS7 cells, a monkey kidney line, compared to free PEI. At 15 μg/mL viability was >80% for all particle compositions but at a comparable PEI concentration <15% viability was observed. The difference in the four compositions emerged when the transfection ability was tested. pDNA upregulates protein production and in this case a common model system, luciferase, was used. They

found that particles with pre-formed PEI/pDNA complexes had the most efficient transfection.[82] Cationic complexes are traditionally used for *in vitro* transfection, but can not be used in vivo due to toxicity and immunogenicity. Cationic complexes are commonly pre-formed for the incorporation in liposomes used as a drug delivery vehicle *in vivo*. This research demonstrates that though incorporated in a solid polymer particle, having a cationic complex may still provide benefits over a homogeneously mixed system.

Other groups have also demonstrated the enhancement in knockdown provided by a cationic PLGA particle. Andersen et al. compared PLGA particles to PLGA particles with PEI and cetylated PEI. They found that the PLGA particle did not result in gene knockdown while the PLGA/PEI and PLGA/cetylated PEI particles showed 62% and 41% knockdown respectively.[83] In addition to PEI, other cationic moieties have been investigated; the second most common being chitosan. Chitosan is a naturally occurring polymer with high primary amine density. Tahara et al. coated PLGA particles containing DOTAP/siRNA complexes in PVOH or a 1:1 mixture of PVOH and chitosan. They only observed gene knockdown in the sample coated with chitosan.[84]

1.7.2 The effect of N/P ratio on *in vitro* gene knockdown

The transfection of cationic PLGA nanoparticles *in vitro* often depends on the N/P ratio. This is a ratio of the number of nitrogens in the cationic moiety to the number of phosphorous groups in the gene. Some groups report N/P directly while other groups report the weight percent of the cationic moiety and siRNA in the solid particle. PEI and other cationic polymers tend to have a higher nitrogen density than lipids or synthetic

amphiphiles such as cetyl trimethylammonium bromide (CTAB). In general a higher N/P ratio results in higher transfection. Oster et al. compared the transfection capabilities of PLGA particles containing varying amounts of CTAB to particles containing varying amounts of PEI. In both cases pDNA was absorbed to the surface of the particle. They found that particles with PEI had much higher transfection than particles with CTAB at similar weight percents. Furthermore the higher the percentage PEI, the higher the transfection. Particles with 0-5% PEI showed transfection barely above background while particles with 10% and 50% PEI showed almost a 10 and 100 fold increase in protein respectively. Particle with 0-50% CTAB showed transfection barely above background.[80] Katas et al. also used adsorption of siRNA onto PLGA/PEI particles for transfection. They compared particles with varying N/P ratios and examined the often overlooked variable of PVOH molecule weight. They found that high levels of gene silencing were achieved at 24 hours; greater than 80% knockdown was achieved with 5 of the 6 formulations tested. Particles with higher molecular weight PVOH (30-70 kDa) exhibited a clear trend with higher N/P producing greater and more sustained knockdown (50:1 > 35:1 > 25:1). Particles with lower molecular weight PVOH (13-23 kDa) did not show a clear trend with the middle N/P tested, 35:1, exhibiting the greatest knockdown of all the formulations. while the others were not as effective as particles fabricated with higher molecular weight PVOH.[85] This could indicate a sweet spot in the formulation range investigated or a difference in that particular particle formulation as the emulsion process is heterogeneous.

1.7.3 *In vivo* gene knockdown by PLGA nanoparticles

A few groups have taken cationic PLGA siRNA systems *in vivo*. In 2008 Murata et al. reported anti-tumor efficacy using PLGA/PEI and PLGA/arginine microparticles. They chose an anti-VEGF siRNA as a therapeutic vector against S-180 (sarcoma) xenograft tumors. Vascular endothelial growth factor (VEGF) is responsible for angiogenesis which allows a tumor to grow and spread. By reducing VEGF and therefore the blood supply, many believe a tumor can be contained. They first examined the ability of PEI and arginine to complex with siRNA and produce knockdown. They found, as previously described, a higher N/P ratio resulted in higher knockdown and were able to reach 54% knockdown with arginine complexes and 68% knockdown with PEI complexes. They incorporated these complexes in microspheres that would act as injectable depots using a w/o/w emulsion. The two formulations showed similar release profiles with a burst of 20% and another 20% released over 3 weeks at a steady rate. *In vitro* these particles exhibited 60% and 43% knockdown with PLGA/arginine and PLGA/PEI respectively (formulation difference not significant; $p>0.05$). For *in vivo* evaluation the authors injected microspheres intratumorally and monitored tumor volume. They looked at vehicle controls and compared PLGA/siRNA particles to PLGA/arginine/siRNA particles and PLGA/PEI/siRNA particles. The PLGA/siRNA particles showed some significant growth inhibition ($p<0.05$), while the PLGA/arginine particles showed a higher level of growth inhibition ($p<0.01$), and the PLGA/PEI particles were the most efficient formulation with little growth over 21 days.[86]

In 2009 Woodrow et al. reported the investigation of intravaginal topical application of siRNA containing PLGA/spermidine nanoparticles as a topical microbicide

for defense against sexually transmitted diseases including human immunodeficiency virus (HIV). Using an N/P ratio of 8:1 they demonstrated PLGA/spermidine/siRNA particles were able to provide more sustained knockdown than commercial transfection agents *in vitro*, >14 days as compared to <7 days with the commercial agent. They tested particle distribution and found 7 days after *in vivo* application particles were detected throughout the reproductive tract. An EFGP reporter was used to test *in vivo* knockdown; 10 days after topical administration 50% knockdown was measured in the uterine horn, 60% knockdown was measured in the cervix, and 60% knockdown was measured in the vaginal tract. They compared these particles to lipid delivery systems which showed equal knockdown, but caused inflammation and epithelial disruption in the vaginal tissue whereas the PLGA nanoparticles did not.[87] While PLGA particles do not have a lot of clout as siRNA delivery systems yet, there is a growing body of evidence suggesting these particles can be tailored with varying cationic moieties and show equal knockdown with less toxicity than traditional carriers.

1.8 Future Directions

The use of PLGA nanoparticles for the treatment of cancer is under exploration by a wide variety of research groups. The future will see many of these therapies entering clinical trials. As the first generation of PLGA nanoparticles make their mark, the future of the technology is already starting to unfold. Next generation particles will be able to combine therapies for maximum efficacy and will have a higher degree of control.

1.8.1 Combination therapy

Amid PLGA carriers showing promise in both chemotherapy and siRNA, some researchers have started to consider the combination of the two for higher efficacy. Already patients are treated with cocktails of chemotherapeutics which have different mechanisms of toxicity. The combination of a cytotoxin with gene therapy aimed at reducing the cancer's ability to resist may bring about more rapid and more complete regression. Researchers have demonstrated that the knockdown of certain genes can sensitize cells to chemotherapeutics.[88, 89] Combination therapies without carriers have been shown to be more effective against tumor growth than the individual components.[90] Saad et al. developed a cationic liposome which incorporated doxorubicin, siRNA against MDR1/MRP1 (drug efflux pump) and siRNA against BCL2 (cellular anti-apoptotic defense) in the same nanoparticle. They achieved efficacy in multi-drug resistant cells which could not be approached by any of the individual components.[91]

1.8.2 Higher Degree of Control

In order to have more control over particle properties, a higher degree of control is needed in the fabrication process. A process would ideally generate monodisperse particles of a chosen size and geometry which could efficiently incorporate high loadings of therapeutic. Furthermore the process would allow the composition of the particle to be tailored independent of the size and geometry so that compositional effects could be explored with no uncontrolled variables. One way this can be accomplished is through the use of soft lithography. Currently two groups are exploring very different soft lithography technologies. The Park group at Purdue University has developed a hydrogel

template method which allows for the fabrication of PLGA particles fulfilling the necessary control requirements. They have demonstrated exquisite control on the micron scale achieving very high loadings and controlled release profiles. While not suitable for intravenous delivery, microparticles are useful for inhalation and depot applications. Furthermore they have shown the ability to fabricate drug free nanoparticles and are currently studying these particles for drug delivery.[44] The DeSimone group at the University of North Carolina at Chapel Hill has developed the PRINT process which allows for the fabrication of PLGA micro- and nanoparticles which fulfill all the above criteria and have demonstrated efficacy as drug delivery vehicles as is detailed herein.

References

1. E. J. Woodward, C. T., Scheduling of Taxanes: A Review. *Current Clinical Pharmacology* **2010**, Epub ahead of print.

2. A. D. Bangham, M. M. S., J. C. Watkins, Diffusion of univalent ions across the lamellae of swollen phospholipids. *Journal of Molecular Biology* **1965,** 13, (1), 238-252.

3. Gregoriadis, G., The Carrier Potential Of Liposomes In Biology And Medicine Part 2. *New England Journal of Medicine* **1976,** 295, (14), 765-770.

4. Gregoriadis, G., The Carrier Potential Of Liposomes In Biology And Medicine Part 1. *New England Journal of Medicine* **1976,** 295, (13), 704-710.

5. Gregoriadis, G., Engineering liposomes for drug delivery: progress and problems. *Trends in Biotechnology* **1995,** 13, (12), 527-537.

6. K. Kataoka, A. H., Y. Nagasaki, Block copolymer micelles for drug delivery: design, characterization and biological significance. *Advanced Drug Delivery Reviews* **2001,** 47, (1), 113-131.

7. Y. Matsumura, K. K., Preclinical and clinical studies of anticancer agent-incorporating polymer micelles. *Cancer Science* **2009,** 100, (4), 572-579.

8. A. Robert, J. F., Current Status of Nanomedicine and Medical Nanorobotics. *Journal of Computational and Theoretical Nanoscience* **2005,** 2, 1-25.

9. Chung, T. W.; Huang, Y. Y.; Liu, Y. Z., Effects of the rate of solvent evaporation on the characteristics of drug loaded PLLA and PDLLA microspheres. *International Journal of Pharmaceutics* **2001,** 212, (2), 161-169.

10. R. T. Liggins, H. M. B., Paclitaxel loaded poly(L-lactic acid) microspheres: properties of microspheres made with low molecular weight polymers. *International Journal of Pharmaceutics* **2001,** 222, 19-33.

11. Lin, S. Y.; Chen, K. S.; Teng, H. H.; Li, M. J., In vitro degradation and dissolution behaviours of microspheres prepared by three low molecular weight polyesters. *Journal of Microencapsulation* **2000,** 17, (5), 577-586.

12. Oster, C. G., Comparative study of DNA encapsulation into PLGA microparticles using modified double emulsion methods and spray drying techniques. *Journal of Microencapsulation* **2005,** 22, 235-244.

13. P. Patel, R. C. M., V. R. Babu, D. Jain, V. Rangaswamy, T. M. Aminabhavi, Microencapsulation of Doxycycline into Poly(lactide-coglycolide) by Spray Drying Technique: Effect of Polymer Molecular Weight on Process Parameters. *Journal of Applied Polymer Science* **2008,** 108, 4038-4046.

14. M. A. Holgado, J. L. A., M. J. C'ozar, J. Alvarez-Fuentes, Synthesis of lidocaine-loaded PLGA microparticles by flow focusing: Effects on drug loading and release properties. *International Journal of Pharmaceutics* **2008,** 358, 27-35.

15. C. E. Astete, C. M. S., Synthesis and characterization of PLGA nanoparticles. *Journal of Biomaterial Science* **2006,** 17, (3), 247-289.

16. C. Wischke, S. S., Principles of encapsulating hydrophobic drugs in PLA/PLGA microparticles. *International Journal of Pharmaceutics* **2008,** 364, 298-327.

17. Almeida, A. J.; Alpar, H. O.; Brown, M. R. W., Immune-Response to Nasal Delivery of Antigenically Intact Tetanus Toxoid Associated with Poly(L-Lactic Acid) Microspheres in Rats, Rabbits and Guinea-Pigs. *Journal of Pharmacy and Pharmacology* **1993,** 45, (3), 198-203.

18. Asmatulu, R.; Zalich, M. A.; Claus, R. O.; Riffle, J. S., Synthesis, characterization and targeting of biodegradable magnetic nanocomposite particles by external magnetic fields. *Journal of Magnetism and Magnetic Materials* **2005,** 292, 108-119.

19. Chiou, S. H.; Wu, W. T.; Huang, Y. Y.; Chung, T. W., Effects of the characteristics of chitosan on controlling drug release of chitosan coated PLLA microspheres. *Journal of Microencapsulation* **2001,** 18, (5), 613-625.

20. Liang, L. S.; Jackson, J.; Min, W. X.; Risovic, V.; Wasan, K. M.; Burt, H. M., Methotrexate loaded poly(L-lactic acid) microspheres for intra-articular delivery of methotrexate to the joint. *Journal of Pharmaceutical Sciences* **2004,** 93, (4), 943-956.

21. Liggins, R. T.; Burt, H. M., Paclitaxel loaded poly(L-lactic acid) microspheres: properties of microspheres made with low molecular weight polymers. *International Journal of Pharmaceutics* **2001,** 222, (1), 19-33.

22. Mumper, R. J.; Jay, M., Biodegradable Radiotherapeutic Polyester Microspheres - Optimization and Invitro Invivo Evaluation. *Journal of Controlled Release* **1992,** 18, (3), 193-204.

23. Nijsen, J. F. W.; Schip, A. D. V.; van Steenbergen, M. J.; Zielhuis, S. W.; Kroon-Batenburg, L. M. J.; van de Weert, M.; van Rijk, P. P.; Hennink, W. E., Influence of neutron irradiation on holmium acetylacetonate loaded poly(L-lactic acid) microspheres. *Biomaterials* **2002,** 23, (8), 1831-1839.

24. Uchida, M.; Jin, Y.; Natsume, H.; Kobayashi, D.; Sugibayashi, K.; Morimoto, Y., Introduction of poly-L-lactic acid microspheres into the skin using supersonic flow: effects of helium gas pressure, particle size and microparticle dose on the amount introduced into hairless rat skin. *Journal of Pharmacy and Pharmacology* **2002,** 54, (6), 781-790.

25. Wake, M. C.; Gerecht, P. D.; Lu, L. C.; Mikos, A. G., Effects of biodegradable polymer particles on rat marrow-derived stromal osteoblasts in vitro. *Biomaterials* **1998,** 19, (14), 1255-1268.

26. Zielhuis, S. W.; Nijsen, J. F. W.; Figueiredo, R.; Feddes, B.; Vredenberg, A. M.; van het Schip, A. D.; Hennink, W. E., Surface characteristics of holmium-loaded poly(L-lactic acid) microspheres. *Biomaterials* **2005,** 26, (8), 925-932.

27. Kim, H. K.; Park, T. G., Comparative study on sustained release of human growth hormone from semi-crystalline poly(L-lactic acid) and amorphous poly(D,L-lactic-co-glycolic acid) microspheres: morphological effect on protein release. *Journal of Controlled Release* **2004,** 98, (1), 115-125.

28. Chung, T. W.; Huang, Y. Y.; Tsai, Y. L.; Liu, Y. Z., Effects of solvent evaporation rate on the properties of protein-loaded PLLA and PDLLA microspheres fabricated by emulsion-solvent evaporation process. *Journal of Microencapsulation* **2002,** 19, (4), 463-471.

29. Han, K.; Lee, K. D.; Gao, Z. G.; Park, J. S., Preparation and evaluation of poly(L-lactic acid) microspheres containing rhEGF for chronic gastric ulcer healing. *Journal of Controlled Release* **2001,** 75, (3), 259-269.

30. Nakaoka, R.; Inoue, Y.; Tabata, Y.; Ikada, Y., Size effect on the antibody production induced by biodegradable microspheres containing antigen. *Vaccine* **1996,** 14, (13), 1251-1256.

31. Zhu, K. J. Z., J. X.; Wang, C.; Yasuda, H.; Ichimaru, A.; Yamamoto, K., Preparation and in vitro release behavior of 5-fluorouracil-loaded microspheres based on poly (L-lactide) and its carbonate copolymers. . *Journal of Microencapsulation* **2003,** 20, (6), 731-743.

32. Matsuyama, K.; Zhang, D. H.; Urabea, T.; Mishima, K., Formation of L-poly(lactic acid) microspheres by rapid expansion Of CO2 saturated polymer suspensions. *Journal of Supercritical Fluids* **2005,** 33, (3), 277-283.

33. Meziani, M. J. P., Pankaj; Desai, Tarang; Sun, Ya-Ping. , Supercritical Fluid Processing of Nanoscale Particles from Biodegradable and Biocompatible Polymers. *Industrial & Engineering Chemistry Research* **2005,** ACS ASAP.

34. Tom, J. W.; Debenedetti, P. G., Formation of Bioerodible Polymeric Microspheres and Microparticles by Rapid Expansion of Supercritical Solutions. *Biotechnology Progress* **1991,** 7, (5), 403-411.

35. Falk, R. F.; Randolph, T. W., Process variable implications for residual solvent removal and polymer morphology in the formation of gentamycin-loaded poly(L-lactide) microparticles. *Pharmaceutical Research* **1998,** 15, (8), 1233-1237.

36. Jarmer, D. J.; Lengsfeld, C. S.; Randolph, T. W., Manipulation of particle size distribution of poly(L-lactic acid) nanoparticles with a jet-swirl nozzle during precipitation with a compressed antisolvent. *Journal of Supercritical Fluids* **2003,** 27, (3), 317-336.

37. Tu, L. S. D., F.; Foster, N. R., Micronization and microencapsulation of pharmaceuticals using a carbon dioxide antisolvent. *Powder Technology* **2002,** 126, (2), 134-149.

38. Choi, S.; Lee, K.; Kim, H., Preparation of poly(L-lactic acid) nano- and micro-particles using supercritical antisolvent. *Journal of Chemical Engineering of Japan* **2005,** 38, (8), 571-577.

39. Kim, M. Y. L., Youn Woo; Byun, Hun-Soo; Lim, Jong Sung., Recrystallization of Poly(L-lactic acid) into Submicrometer Particles in Supercritical Carbon Dioxide. *Industrial & Engineering Chemistry Research* **2005,** ACS ASAP.

40. Patel, M. M.; Zeles, M. G.; Manning, M. C.; Randolph, T. W.; Anchordoquy, T. J., Degradation kinetics of high molecular weight poly (L-lactide) microspheres and release mechanism of lipid : DNA complexes. *Journal of Pharmaceutical Sciences* **2004,** 93, (10), 2573-2584.

41. J. Guan, N. F., L. J. Lee, D. J. Hansford, Fabrication of polymeric microparticles for drug delivery by soft lithography. *Biomaterials* **2006,** 27, 4034-4041.

42. J. Guan, H. H., L. J. Lee, D. J. Hansford, Fabrication of Particulate Reservior-Containing, Capsulelike, and Self-Folding Polymer Microstructures for Drug Delivery. *Small* **2007,** 3, 412-418.

43. J. A. Champion, Y. K. K., S. Mitragotri, Particle Shape: A new design parameter for micro- and nanoscale drug delivery systems. *Journal of Controlled Release* **2007,** 121, 3-9.

44. G. Acharya, C. S. S., M. McDermott, H. Mishra, H. Park, I. C. Kwon, K. Park, The hydrogel template method for the fabrication of homogeneous nano/microparticles. *Journal of Controlled Release* **2010,** 141, 314-319.

45. F. Esmaeili, M. H. G., S. N. Ostad, F. Atyabi, M. Seyedabadi, M. D. Malekshahi, M. Amini, and R. Dinarvnand, Folate-receptor-targeted delivery of docetaxel nanoparticles prepared by PLGA-PEG-folate conjugate. *Journal of Drug Targeting* **2008,** 16, (5), 415-423.

46. O. C. Farokhzad, J. C., B. A. Teply, I. Sherifi, S. Jon, P. W. Kantoff, J. P. Richie, and R. Langer, Targeted nanoparticle-aptamer bioconjugates for cancer chemotherapy in vivo. *PNAS* **2006,** 103, (16), 6315-6320.

47. M. Senthilkumar, P. M., and N. K. Jain, Long circulating PEGylated poly(D,L-lactide-co-glycolide) nanoparticulate delivery of docetaxel to solid tumors. *Journal of Drug Targeting* **2008,** 16, (5), 424-435.

48. S. Murugesan, S. G., R. K. Averinei, M. Nahar, P. Mishra, N. K. Jain, PEGylated Poly(lactide-co-glycolide) (PLGA) Nanoparticulate Delivery of Docetaxel: Synthesis of Diblock Copolymers, Optimization of Preparation Variables on Formulation Characteristics and In Vitro Release Studies. *Journal of Biomedical Nanotechnology* **2007,** 3, 52-60.

49. J. M. Chan, L. Z., K. P. Yuet, G. Liao, J. Rhee, R. Langer, O. C. Farokhzad, PLGA-lecithin-PEG core-shell nanoparticles for controlled drug delivery. *Biomaterials* **2009,** 30, 1627-1634.

50. Mittal, G. S., D. K.; Bhardwaj, V.; Ravi Kumar, M. N. V., Estradiol loaded PLGA nanoparticles for oral administration: effect of polymer molecular weight and copolymer composition on release behavior in vitro and in vivo. *Journal of Controlled Release* **2007,** 119, 77-85.

51. Lee, S. K., M. S.; Kim, J. S.; Park, H. J.; Woo, J. S.; Lee, B. C.; Hwang, S. J., Controlled delivery of a hydrophilic drug from a biodegradable microsphere system by supercritical anti-solvent precipitation technique. *Journal of Microencapsulation* **2006,** 23, 741-749.

52. G. Gaucher, R. H. M., and J. Leroux, Polyester-based micelles and nanoparticles for the parenteral delivery of taxanes. *Journal of Controlled Release* **2010,** 143, (1), 2-12.

53. Yan, F. Z., C.; Zheng, Y.; Mei, L.; Tang, L.; Song, C.; Sun, H.; Huang, L., The effect of poloxamer 188 on nanoparticle morphology, size, cancer cell uptake, and cytotoxicity. *Nanomedicine* **2010,** 6, 170-178.

54. G. Mittal, D. K. S., V. Bhardwaj, M.N.V. Ravi Kumar, Estradiol loaded PLGA nanoparticles for oral administration: Effect of polymer molecular weight and copolymer composition on release behavior in vitro and in vivo. *Journal of Controlled Release* **2007,** 119, 77-85.

55. J. Lu, X. W., C. Marin-Muller, H. Wang, P. H. Lin, Q. Yao, C. Chen, Current advances in research and clinical applications of PLGA-based nanotechnology. *Expert Reviews in Molecular Diagnostics* **2009,** 9, (4), 325-341.

56. F. Alexis, E. P., L. K. Molnar, and O. C. Farokzhad, Factors Affecting the Clearance and Biodistribution of Polymeric Nanoparticles. *Molecular Pharmaceutics* **2008,** 5, (4), 505-515.

57. P. Xu, E. G., L. Tong, C. B. Highley, D. R. Errabelli, T. Hasan, J. Cheng, D. S. Kohane, Y. Yeo, Intracellular Drug Delivery by poly(lactic-co-glycolic acid) Nanoparticles, Revisited. *Molecular Pharmaceutics* **2008,** 6, (1), 190-201.

58. S. E. A. Gratton, P. A. R., P. D. Pohlhaus, J. C. Luft, V. J. Madden, M. E. Napier, J. M. DeSimone, The effect of particle design on cellular internalization pathways. *PNAS* **2008,** 105, (33), 11613–11618.

59. J. Panyam, V. L., Biodegradable nanoparticles for drug and gene delivery to cells and tissue. *Advanced Drug Delivery Reviews* **2003,** 55, 329-347.

60. J. K. Vasir, V., Labhasetwar, Biodegradable nanoparticles for cytosolic delivery of therapeutics. *Advanced Drug Delivery Reviews* **2007,** 59, 718-728.

61. J. Panyam, W. Z., S. Prabha, S. K. Sahoo, V. Labhasetwar, Rapid endo-lysosomal escape of poly(D,L-lactide-co-glycolide) nanoparticles: implications for drug and gene delivery. *The FASEB Journal* **2002,** 16, 1217-1226.

62. M. S. Cartiera, K. M. J., V. Rajendran, M. J. Caplan, W. M. Saltzman, The uptake and intracellular fate of PLGA nanoparticles in epithelial cells. *Biomaterials* **2009,** 30, 2790-2798.

63. J. A. Champion, S. M., Role of target geometry in phagocytosis. *PNAS* **2006,** 103, (13), 4930-4934.

64. J. J. Yu, H. A. L., J. H. Kim, W. H. Kong, Y. Kim, Z. Y. Cui, K. G. Park, W. S. Kim, H. G. Lee, and S. W. Seo, Biodistribution and anti-tumor efficacy of PEG/PLA nanoparticles loaded doxorubicin. *Journal of Drug Targeting* **2007,** 15, (4), 279-284.

65. Z. Panagi, A. G., G. Evangelatos, E. Livaniou, D. S. Ithakissios, K. Avgoustakis, Effect of dose on the biodistrbution and pharmacokinetics and PLGA and PLGA-mPEG nanoparticles. *International Journal of Pharmaceutics* **2001,** 221, 143-152.

66. K. Avagoustakis, A. B., Z. Panagi, P, Klepetsanis, E. Livaniou, G. Evangelatos, D. S. Ithakissios Effect of copolymer composition on the physicochemical characteristics, in vitro stability, and biodistribution of PLGA-mPEG nanoparticles. *International Journal of Pharmaceutics* **2003,** 259, 115-127.

67. J. Cheng, B. A. T., I. Sherifi, J. Sung, G. Luther, F. X. Gu, E. Levy-Nissenbaum, A. F. Radovic-Moreno, R. Langer, O. C. Farokhzad, Formulation of functionalized PLGA-PET nanoparticles for in vivo targeted drug delivery. *Biomaterials* **2007,** 28, 869-876.

68. F. Xu, Y. Y., X. Shan, C. Liu, X. Tao, Y. Sheng, and H. Zhou, Long-circulation of hemoglobin-loaded polymeric nanoparticles as oxygen carriers with modulated surface charges. *International Journal of Pharmaceutics* **2009,** 377, 199-206.

69. Y. Li, Y. P., X. Zhang, Z. Gu, Z. H. Zhou , W. Yuan, J. Zhou, J. Zhu, X. Gao, PEGylated PLGA nanoparticles as protein carriers: synthesis, preparation and biodistribution in rats. *Journal of Controlled Release* **2001,** 71, 203-211.

70. S. Zhang, X. G., K. Shen, P. Yang, and X. Ju, Evaluation of poly(D,L-lactide-co-glycolide) microspheres for the lung-targeting of yuanhuacine, a novel DNA topoisomerase I inhibitor. *Journal of Drug Targeting* **2009,** 17, (4), 286-293.

71. H. Lee, H. F., B. Hoang, R. M. Reilly, and C. Allen, The Effects of Particle Size and Molecular Targeting on the Intratumoral and Subcellular Distribtuion of Polymeric Nanoparticles. *Molecular Pharmaceutics* ASAP.

72. D. A. Christian, S. C., O. B. Garbuzenko, T. Harada, A. L. Zajac, T. Minko, and D. E. Discher, Flexible Filaments for In Vivo Imaging and Delivery: Persistent Circulation of Filomicelles Opens the Dosage Window for Sustained Tumor Shrinkage. *Molecular Pharmaceutics* **2009,** 6, (5), 1343-1352.

73. Lyseng-Williamson, K. A. F., C., Docetaxel: A Review of its Use in Metastatic Breast Cancer. *Drugs* **2005,** 65, 2513-2531.

74. T. Musumeci, C. A. V., I. Giannone, B. Ruozi, L. Montenegro, R. Pignatello, and G. Puglisi, PLA/PLGA nanoparticles for sustained release of docetaxel. *International Journal of Pharmaceutics* **2006,** 325, 172-179.

75. Garrec, D. L. G., S.; Luo, L.; Lessard, D.; Smith, D. C.; Yessine, M. A.; Ranger, M.; Leroux, J. C., Poly(N-vinylpyrrolidone)-block-poly(D,L-lactide) as a new polymeric solubilizer for hydrophobic anticancer drugs: in vitro and in vivo evaluation. *Journal of Controlled Release* **2004,** 99, 83-101.

76. Karnik, R. G., F.; Basto, P.; Cannizzaro, C.; Dean, L.; Kyei-Manu, W.; Langer, R.; Farokhzad, O.C., Microfluidic platform for conrolled synthesis of polymeric nanoparticles. *Nanoletters* **2008,** 8, 2906-2912.

77. Shin, H. A., A. W. G.; Rao, D. A.; Rockich, N. C.; Kwon, G. S., Multi-drug loaded polymeric micelles for simultaneous delivery of poorly soluble anticancer drugs. *Journal of Controlled Release* **2009,** 140, 294-300.

78. Wang, X. W., Y.; Chen, X.; Wang, J.; Zhang, X.; Zhang, Q., NGR-modified micelles enhance their interaction with CD13-overexpressing tumor and endothelial cells. *Journal of Controlled Release* **2009,** 139, 56-62.

79. F. Esmaeili, R. D., M. H. Ghahremani, S. N. Ostad, H. Esmaily, and F. Atyabi, Cellular cytotoxicity and in-vivo biodistribution of docetaxel poly(lactide-co-glycolide) nanoparticles. *Anti-Cancer Drugs* **2010,** 21, (1), 43-52.

80. C. G. Oster, N. K., L, Grode, L. Barbu-Tudoran, A. K. Schaper, S. H. E. Kaufmann, T. Kissel, Cationic microparticles consisting of poly(lactide-co-glycolide) and polyethylenimine as carrier systems for parental DNA vaccination. *Journal of Controlled Release* **2005,** 104, 359-377.

81. Y. Patil, J. P., Polymeric nanoparticles for siRNA delivery and gene silencing. *International Journal of Pharmaceutics* **2009,** 367, 195-203.

82. X. Zhang, J. I., A. K. Salem, Comparative study of poly(lactic-co-glycolic acid)-polyethyleneimine-plasmid DNA microparticles prepared using double emulsion methods. *Journal of Microencapsulation* **2008,** 25, (1), 1-12.

83. M. Andersen, A. L., A. Arpanaei, S. M. R. Jensen, H. Kaur, D. Oupicky, F. Besenbacher, P. Kingshott, J. Kjems, K. A. Howard, Surface functionalization of PLGA nanoparticles for gene silencing. *Biomaterials* **2010,** 31, 5671-5677.

84. K. Tahara, H. Y., N. Hirashima, Y. Kawashima, Chitosan-modified poly(D,L-lactide-co-glycolide) nanospheres for improving siRNA delivery and gene-silencing effects. *European Journal of Pharmaceutics and Biopharmaceutics* **2010,** 74, 421-426.

85. H. Katas, E. C., H. O. Alpar, Preparation of polyethyleneimine incorporated poly(D,L-lactide-co-glycolide) nanoparticles by spontaneous emulsion diffusion method for small interfering RNA delivery *International Journal of Pharmaceutics* **2009,** 329, 144-154.

86. N. Murata, Y. T., K. Toyoshima, M. Yamamoto, H. Okada, Anti-tumor effects of anti-VEGF siRNA encapsulated with PLGA microspheres in mice. *Journal of Controlled Release* **2008,** 126, 246-254.

87. K. A. Woodrow, Y. C., C. J. Booth, J. K. Saucier-Sawyer, M. J. Wood, and W. M. Saltzman Intravaginal gene silencing using biodegradable polymer nanoparticles densely loaded with small-interfering RNA. *Nature Materials* **2009,** 8, 526-533.

88. J. Halder, C. N. L. J., S. K. Lutgendorf, Y. Li, N. B. Jennings, D. Fan, G. M. Nelkin, R. Schmandt, M. D. Schaller, A. K. Sood Focal Adhesion Kinase Silencing Augments Docetaxel-Mediated Apoptosis in Ovarian Cancer Cells. *Clinical Cancer Research* **2005,** 11, (24), 8829-88-36.

89. C. Gill, C. D., A. J. O'Neill, R. W. G. Watson, Effects of cIAP-1, cIAP-2, and XIAP triple knockdown on prostate cancer cell susceptibility to apoptosis, cell survival, and proliferation. *Molecular Cancer* **2009,** 8, (39), 1-12.

90. S. M. Thomas, M. J. O., M. L. Freilino, S. Strychor, D. R. Walsh, W. E. Gooding, J. R. Grandis, W. C. Zamboni, Antitumor Mechanisms of Systemically Administered Epidermal Growth Factor Receptor Antisense Oligonucleotides in Combination with Docetaxel in Squamous Cell Carcinoma of the Head and Neck. *Molecular Pharmacology* **2007,** 73, (3), 627-638.

91. M. Saad, O. B. G., T. Minko, Co-delivery of siRNA and an anticancer drug for treatment of multidrug-resistant cancer. *Nanomedicine* **2008,** 3, (6), 761-776.

CHAPTER 2

FABRICATION AND CHARATERIZATION OF ENGINEERED PLGA PRINT® PARTICLES

2.1 Introduction to the PRINT® Process

In 2004 the DeSimone lab reported a new material with low surface energy and high solvent resistance for the fabrication of microfluidic devices.[1] This material is a photocurable perfluorinated polyether oil which has since been trademarked Fluorocur® by Liquidia Technologies. This material demonstrated superior performance to poly(dimethyl siloxane) (PDMS), the most commonly used elastomer for the fabrication of microfluidic devices.[1, 2] Following this success, other applications in which PDMS plays a critical role were investigated, most notably imprint lithography. Imprint or "soft" lithography is family of patterning technologies where an elastomeric mold is fabricated from a hard template. This mold is then used to pattern another material either by inking the mold and transferring to a substrate to create a 2D pattern like a stamp or by pressing the mold into another material which fills the pattern, replicating the template in 3D. PDMS is the most common mold material due to its low surface energy (20 dyn/cm) and its low modulus. Once cured the flexible, low surface energy mold is easily peeled from the template without damage to the template. This is important because the template is typically created on silicon through standard lithography and is therefore expensive and delicate. By comparison Fluorocur has a surface energy of 8-10 dyn/cm and also has a low, tailorable modulus.[3] As such it was hypothesized that Fluorocur would outperform PDMS in soft lithography applications. In 2005 the DeSimone lab reported not only that Fluorocur was successfully used in imprint lithography to generate molds and replicate patterns in the same way that PDMS is used, but in addition Fluorocur could be used to create completely isolated particles.[4] This technology was termed the PRINT (Particle Replication In Non-wetting Templates) process. In typical PDMS molding there is a layer

of material which connects the cavities, termed the “scum” or “flash” layer, which must then be removed by an additional step such as etching. As feature size decreases this becomes an increasing problem as the layer being etched approximates the size of the feature being molded. Using Fluorocur instead of PDMS eliminates the connecting layer; the cavities of a Fluorocur mold can be filled without wetting the land area between. This versatile technology platform has applications from advanced drug delivery to energy collection and storage.

2.1.1 Control of Size, Shape, and Composition

Imprint or “soft” lithography in general offers many benefits over standard particle fabrication techniques and the PRINT process specifically enhances control over particle size, shape and composition. Standard lithography is very advanced due to the needs of the electronics industry. Therefore template fabrication is very precise. Size resolution is sub-100nm and shapes are largely unlimited. The PRINT process takes full advantage this state of the art technology. Figure 2.1 shows a selection of particles which have been fabricated using the PRINT process. These particles demonstrate the ability to design features into the particle which could affect cellular internalization, flow in air (inhalation) or in fluid (bloodstream), drug release profiles and biodistribution. Since there is always a flat spot generated from where the feature in the template joins the silicon wafer completely spherical particles can not be molded, however, spherical particles can be generated through an extra rounding step.

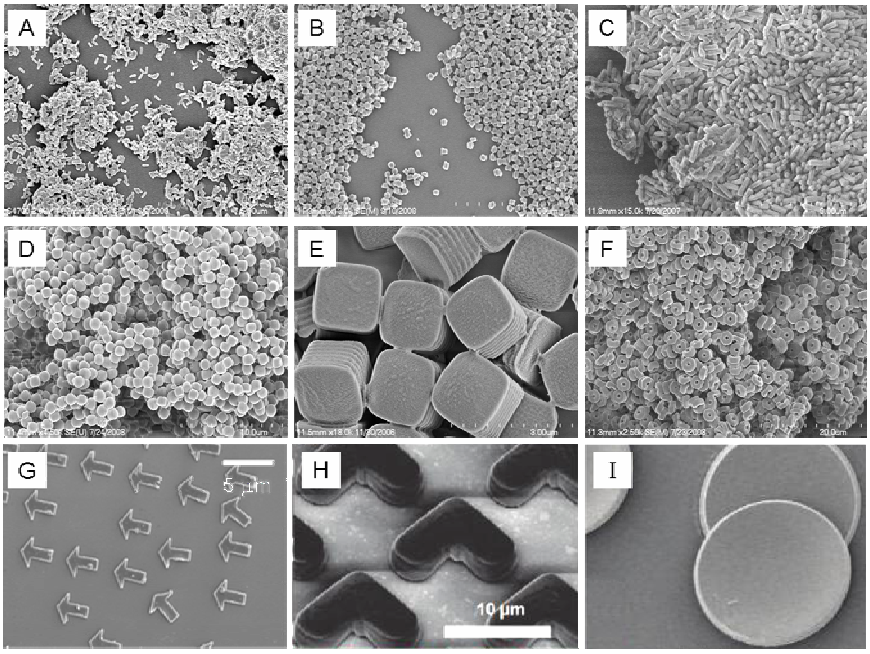

Figure 2.1 A variety of sizes and shapes generated using the PRINT process (A) 80nm x 360nm cylinders, (B) 200nm x 200nm cylinders, (C) 200nm x 600nm cylinders, (D) 1 µm sphere approximates, (E) 2 µm cubes with ridges on the sides, (F) 3 µm particles with center fenestrations, (G) 3 µm arrows, (H) 10 µm boomerangs, and (I) 7 µm discs.

In addition to control over size and shape, the PRINT process allows for unprecedented control over composition. The same size and shape can be generated from hydrogels, linear polymers, inorganics, small molecules, proteins, pure drug or a combination.[4-8] The method is gentle and biologicals as sensitive as proteins and siRNA can be molded and maintain biological activity. This is flexibility that other particle fabrication techniques simply do not possess and is why the PRINT process is truly a platform technology. Control over composition allows for the tailoring of the matrix to meet the specific needs of that delivery agent. For example, siRNA can be complexed with primary amine containing polymers for enhanced cytosolic delivery, different PLGA polymers can be used to tailor the release profiles of drug, and acid sensitive crosslinkers can be used to deliver drug to intracellular only locations. As a component of composition, targeting

ligands can be added to the particles for enhanced uptake specificity or markers of self can be added to the particles to prevent uptake. Control over composition independent of size and shape is unique since in most particle fabrication techniques the composition and size are interrelated. Complete and independent control over size, shape, and composition allows for the rational design of drug delivery vehicles with the PRINT process.

2.1.2 Mold Fabrication

The Fluorocur mold is the keystone in the PRINT process. Fluorocur is a mixture of a perfluorinated polyether oil (Figure 2.2) and a soluble photoinitiator.

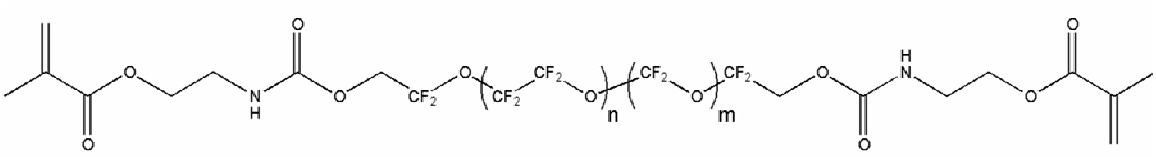

Figure 2.2 An example of the perfluorinated polyether oil structure. The chain length (n and m) can be varied as well as the end group functionalization.

Mold fabrication is the first step in the PRINT process. The Fluorocur oil is poured onto a silicon wafer that has been etched with the desired pattern (Figure 2.3 A). The oil wets the pattern completely due to the high spreading coefficient of Fluorocur. The wafer and photocurable oil are then placed in a chamber which is first purged with nitrogen for 2 minutes and then exposed to ultraviolet light under nitrogen purge for 2 additional minutes, at which point the oil crosslinks, forming a solid film (Figure 2.3 B). This elastomeric film is referred to as the mold and has the inverse pattern of the wafer. The mold is peeled off the silicon wafer, which can be used in this way repeatedly without damage (Figure 2.3 C). A smooth surface can be created in the same way with a silicon

wafer that does not have a pattern (Figure 2.3 D-F). This flat substrate is used in solvent evaporation, pressure fill methods as described below.

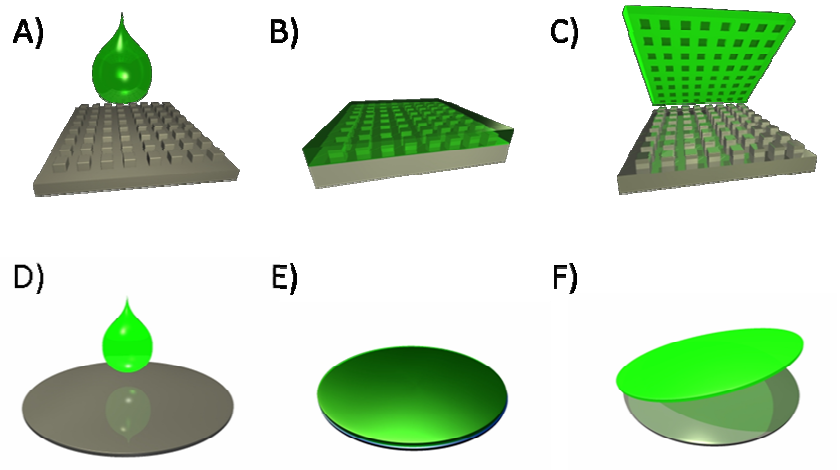

Figure 2.3 Mold and substrate fabrication (A) Fluorocur is poured onto a template, (B) The Fluorocur wets the template completely and crosslinks upon exposure to UV light, (C) The mold generated can be peeled from the template and now has the inverse pattern of the template, (D) Fluorocur is poured onto a flat silicon wafer, (E) The Fluorocur crosslinks upon exposure to UV light, (F) The substrate generated can be peeled from the template and is smooth on the wafer side.

2.2 The solvent evaporation, pressure fill PRINT method

In the first iteration of the PRINT process, a polymer dissolved in an organic solvent is sandwiched between a mold and a flat Fluorocur substrate. Pressure is applied and where the mold and substrate come in contact excess liquid is excluded. This allows the cavities to be filled without a connecting layer. The particles are then solidified by removing the solvent under vacuum. This method is particularly useful for making porous particles or particles with crystallinity.

2.2.1 Experimental

2.2.1.1 Materials

Poly(L-lactic acid) (PLLA; 130,000 g/mol), dichloromethane (DCM) and 1,4-dioxane were purchased from Sigma Aldrich. Fluorocur® was synthesized first in lab as previously reported[1] and then supplied by Liquidia Technologies.

2.2.1.2 Particle visualization and characterization

For visualization by scanning electron microscopy (SEM) samples were coated with 3 nm gold palladium alloy using a Cressington 108 auto sputter coater. Images were taken at an accelerating voltage of 2 kV using a Hitachi model S-4700 SEM. For thermal characterization, measurements were made on a Seiko 120 differential scanning calorimeter (DSC) using a heating rate of 10^{o}C/min. Electron diffraction measurements were made on a high resolution FEI-Philips Tecnai 12 transmission electron microscope (TEM).

2.2.1.3 Particle fabrication procedure

A mold of the desired features and a flat substrate are fabricated (Figure 2.4 A). A polymer is dissolved in an organic solvent. Solutions which are 1-5% (w/v) are typically used. The mold and substrate are placed in contact and the polymer solution is injected between the two using a needle and syringe (Figure 2.4 B). This prevents premature evaporation of the solvent. The mold/solution/substrate sandwich is then placed in a clamping device which applies pressure to ensure good contact between the mold and

substrate. The entire apparatus is then placed under vacuum at ambient temperature for 24 hours to thoroughly remove the solvent. When all the solvent evaporates, the polymer solidifies in the cavities of the mold (Figure 2.4 C). The apparatus can then be removed from vacuum, taken apart, and the mold can be peeled from the substrate (Figure 2.4 D). The particles remain in the mold due to the higher surface area contact with the mold compared to the substrate.

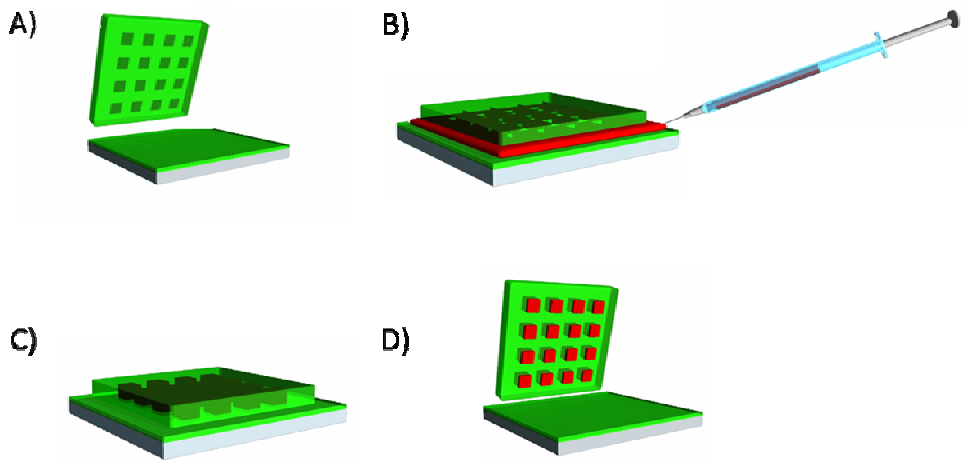

Figure 2.4 The solvent evaporation, pressure fill PRINT method (A) a mold and substrate are fabricated from Fluorocur, (B) a solution of polymer in organic solvent is injected between the mold and substrate, (C) pressure is applied to the sandwich which is placed under vacuum to remove the solvent solidifying the particles, and (D) the mold and substrate are separated revealing isolated particles in the mold.

2.2.2 Results

In this method particles are formed from linear polymers. Herein poly(L-lactic acid) (PLLA) is investigated due to its biocompatibility, record of safety in humans, and semi-crystalline nature. Since the cavities are filled with solvent/PLLA mixtures and the solvent is removed, the resulting particle is porous. The degree of porosity is affected by the initial ratio of PLLA to solvent. Solutions too high in concentration leave behind

polymer with very little evaporation and so create scum before pressure is applied and good contact is made between mold and substrate. Solutions too low in concentration do not fully replicate the size and shape of the mold. As shown in Figure 2.5 below, PLLA particles fabricated from 1% (w/v) are less solid than particles fabricated from 5% (w/v) solutions. The same solvent and mold were used for these two compositions. Particles fabricated from 1% (w/v) solutions do not replicate the full shape of the mold very well, though they are of similar size. Particles fabricated from 5% (w/v) solutions exhibit the shape of the 3 micron cylindrical mold, though large pores are still clearly evident. Interestingly, the particles in both cases appear more solid than expected if 95-99% of their volume was solvent and was removed during the PRINT process. While the particles could be highly porous on a scale below image resolution, it seems more likely that the particles actually contain more polymer than projected. During the solvent evaporation the vacuum pulls solvent out through the Fluorocur mold creating a vacuum within each individual cavity. This vacuum pulls more solvent and polymer from the interstitial spaces. The solvent evaporation, pressure fill method relies on the contact between the mold and the substrate to exclude material and create isolated particles. This excluded material could be increasing the density of the particles. Porosity in particles is useful for effecting release and degradation profiles, for affecting travel in air and lung deposition in inhalation products, and for imaging agents.

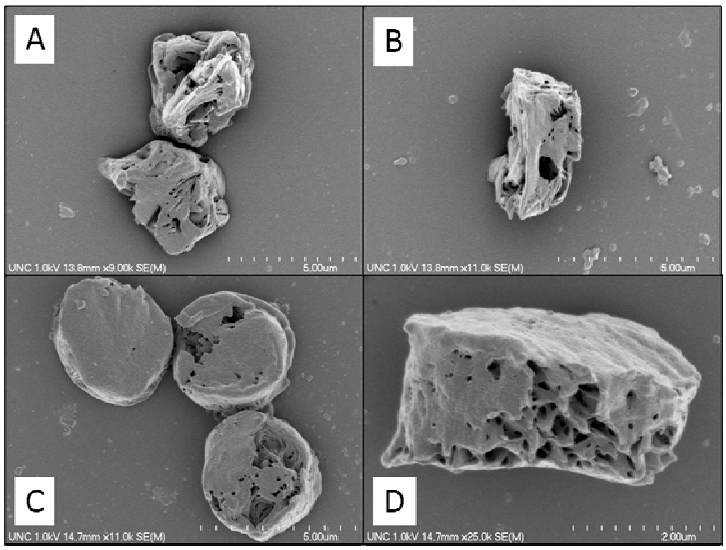

Figure 2.5 PLLA particles from 1,4 dioxane solutions. (A) 1% (w/v) top view, (B) 1% (w/v) side view, (C) 5% (w/v) top view, and (D) 5% (w/v) side view.

In addition to different polymer concentrations, different solvents can be used to fabricate particles. This also affects the porosity of the particles. A comparison between 1,4-dioxane and dichloromethane (DCM) highlights the affects the solvent has on the particle's porosity (Figure 2.6).

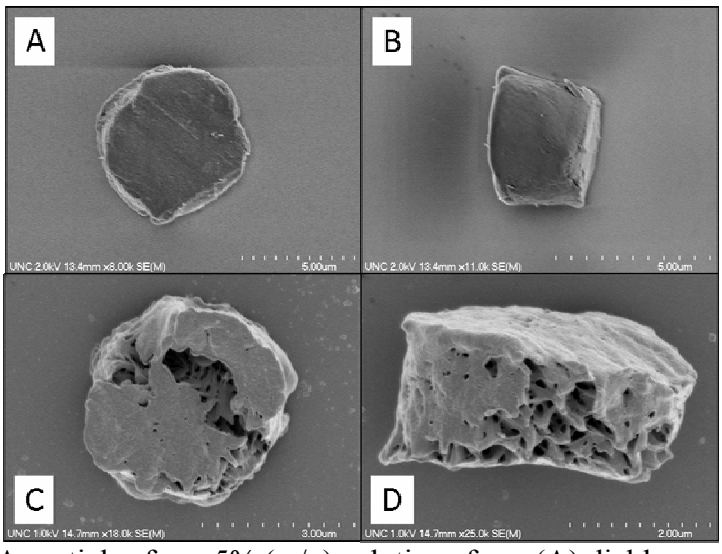

Figure 2.6 PLLA particles from 5% (w/v) solutions from (A) dichloromethane top view, (B) dichloromethane side view, (C) 1,4-dioxane top view, and (D) 1,4-dioxane side view.

The largest difference between the two solvents is their evaporation rate which is an order of magnitude different (Table 2.1). Importantly the contact angle with Fluorocur is similar so the solvents equally de-wet the mold and substrate.

Table 2.1 Relevant characteristics of solvents.

Solvent	Evaporation Rate (BuAc = 1)	Receding Contact Angle with PFPE	Viscosity (cP, 20°C)
Dichloromethane	27.5	42°	0.44
1,4-dioxane	2.7	51°	1.54

The particles from DCM have the shape of the original pattern with no visible external porosity. The particles could be more solid; as the solvent evaporates faster the vacuum created within the cavity pulls more polymer solution into the cavity. The lower viscosity of DCM could also contribute to more excess polymer solution entering the cavity. However it is also possible that the quality of the solvent is affecting the structure. Dichloromethane is a very good solvent for PLLA and, as the solvent evaporates through the walls of the cavity, it could pull solvated polymer to the wall. The polymer cannot escape the cavity, however, and a skin is formed. This would give the outward appearance of a more solid particle, however, the internal structure of the particle would still be porous. The particles from 1,4-dioxane are clearly porous. This can be explained by the fact that 1,4-dioxane is not as good a solvent as dichloromethane so not as much polymer is pulled to the walls. Alternatively, the slower evaporation and higher viscosity could result in less polymer solution being pulled into the cavity during evaporation. These structural differences have important implications. Porous PLLA degrades slower than non-porous PLLA.[9] As PLLA degrades acidic endgroups are generated. These

degradation products autocatalyze further degradation. When a particle is porous a flux of molecules out and water in keeps the microenvironment from becoming too acidic, in essence slowing degradation. It is believed that this affects not only the degradation of the polymer, but can affect the cargo as well. The acidic microenvironment in non-porous particles can damage acid sensitive cargos.[10] In order to determine the structural differences responsible for the differences in surface appearance of the particles, a freeze facture process would be needed to expose the inside of the particle.

In addition to porosity, the evaporation of solvent can crystallizes polymers which have crystalline or semi-crystalline natures. PLLA is a semi-crystalline polymer. PLLA can be thermally crystallized or crystallized by a solvent. PLLA has three crystal structures α, β and γ. The α-form occurs in thermally crystallized polymer samples and has a pseudo-orthorhombic crystalline structure. The β-form is typically obtained by hot-drawing fibers and has an orthorhombic crystalline structure. The γ-form occurs when PLLA is epitaxially crystallized.[11, 12] By evaporating the solvent through the mold, the PLLA crystallizes as it hardens to form particles. Differential scanning calorimetry (DSC) studies were conducted on a macroscopic scale to determine the degree to which crystallization occurs. A drop of solution was placed in a DSC sample pan and placed under vacuum to quickly evaporate the solvent. This sample was then tested for thermal transitions by DSC. The thermograms in Figure 2.7 show the results of these investigations. All thermograms are first heats because the temperature treatment of the polymer affects its crystallinity. In the second heat, all samples have had the same thermal treatment and the resulting thermograms are identical. Figure 2.7 A shows a thermogram of the raw material as received. There is a glass transition at 55^{o}C, a

crystallization exotherm at 108°C, and a melting endotherm at 172°C. The peak that accompanies the glass transition is an expansion peak from physical aging. As the polymer ages, it densifies. Once heated to the glass transition temperature, the polymer is given enough mobility to spread out from this packed state; this is common of PLLA. By integrating the area under the curves, the degree of crystallinity can be calculated. The heat of fusion of 100% crystalline PLLA polymer is 140 J/g.[13] The melting peak indicates a heat of fusion equal to 42 mJ/mg. This gives a crystallinity of 30%. Since the area under the crystallization peak approximately equals the area under the melting peak it can be determined that the sample was completely amorphous. All crystallinity in the sample was derived from thermal crystallization during the measurement. Figure 2.7 C shows the thermogram of an evaporated drop from 1,4-dioxane. The glass transition has remained approximately the same. The crystallization temperature has increased dramatically to 131°C. This implies crystals were present which, as the sample heated up, rearranged into a more thermodynamically preferred crystal state. Therefore this exotherm is more appropriately called a recrystallization peak. The polymer likely crystallized somewhat in the β-form. It has been shown that annealing the β-form will transform the crystals into the α-form at about 130°C.[12, 14] The crystallinity of this sample is also 30%. However, if we consider the recrystallization that occurred, the polymer was 13% β-crystalline and 17% α-crystalline. Figure 2.7 B shows the thermogram of an evaporated drop from dichloromethane. The glass transition has disappeared, or been overshadowed by the crystallization exotherm which appears at 73°C. The crystallization temperature has been shifted lower due to a more ordered amorphous phase, which crystallizes more readily since there is less order to impart. The melting endotherm appears at 170°C. Using the

same method as before, the crystallinity in this sample is 31%. Now, however, if we take into account the thermal crystallization that occurs, it accounts for 7% of the crystallinity. This means the polymer was already 24% crystalline. Furthermore there is no evidence of the β-crystalline form in this sample. While the DSC results shown here are from macroscopic evaporated drops and not from actual particles, they clearly show that PLLA undergoes solvent induced crystallization when dichloromethane or 1,4-dioxane is evaporated from a 5% (w/v) solution. Moreover, the solvent plays an important role in the degree and type of crystallization that occurs. Dichloromethane, which is a better solvent for PLLA than 1,4-dioxane, crystallizes the polymer more completely.

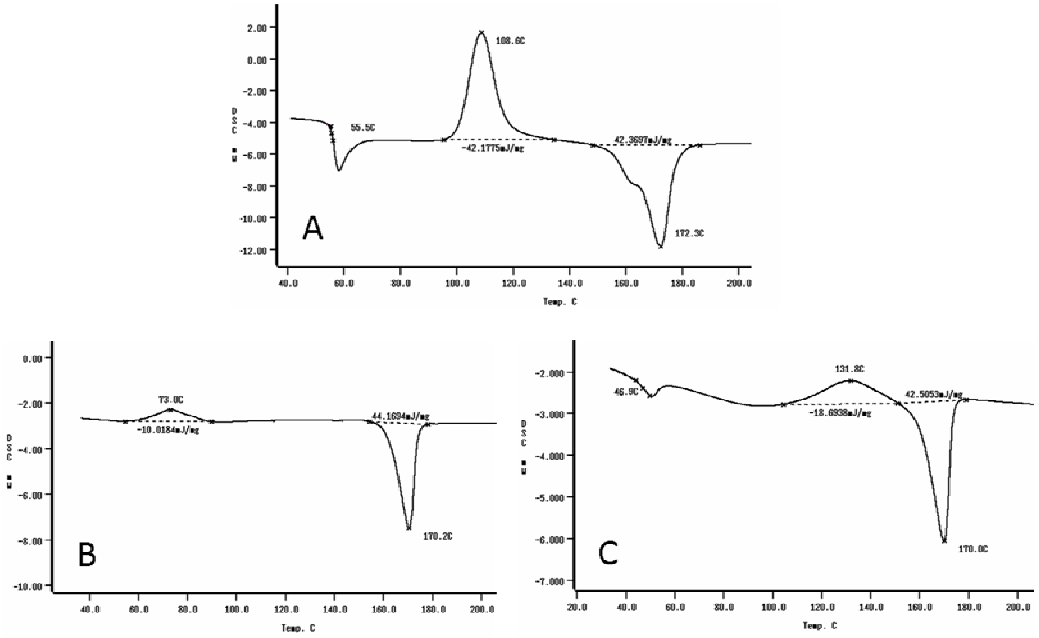

Figure 2.7 DSC thermograms of PLLA (A) as received, (B) from a solution of PLLA in dichloromethane and (C) from a solution of PLLA in 1,4 dioxane.

In addition to DSC, electron diffraction was performed to confirm crystallinity on a sample from dichloromethane. The electron diffraction experiments were carried out on actual particles as opposed to macroscopic samples. This data confirms the presence of a

crystalline structure. From the diffraction patterns obtained, calculation of the crystal lattice d spacing was performed. This confirmed which crystalline form was present; α-PLLA has unit cell parameters of a = 1.07 nm, b = 0.645 nm, and c = 2.78 nm while β-PLLA has unit cell parameters of a = 1.03, b = 1.82, and c = 0.900 nm.[15, 16] The particles were confirmed as α-PLLA and the diffraction spots were indexed by plane (Table 2.2).

Table 2.2 Calculated and observed d spacing values from TEM electron diffraction.

Index (hkl)	Observed d spacing (nm)	Calculated d spacing (nm)
(106)	0.439	0.438
(316)	0.259	0.259
(226)	0.231	0.231
(236)	0.174	0.175
(606)	0.169	0.167
(436)	0.154	0.153
(636)	0.130	0.129

Using the solvent evaporation, pressure fill PRINT method particles which are porous and semi-crystalline can be generated. While there are many uses for particles with these properties, this method does have limitations. Nanometer sized particles could not be reproducibly generated using this method. Typical fabrication resulted in some isolated particles and some scum (Figure 2.8).

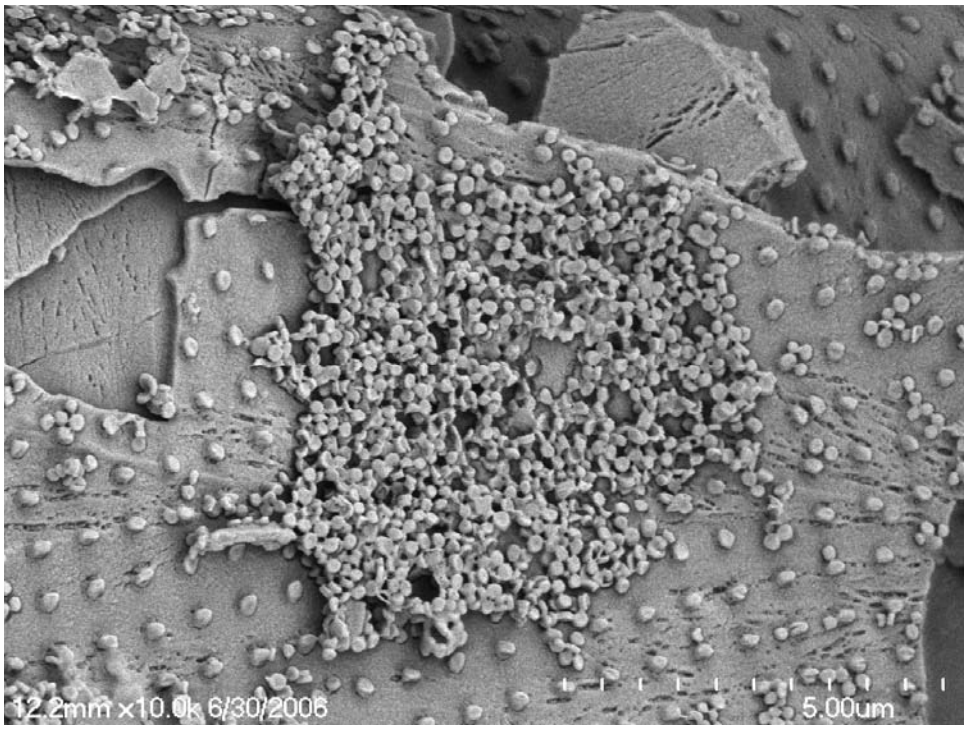

Figure 2.8 A sample with both scum and free, isolated 200nm particles; typical results for the solvent evaporation, pressure fill PRINT method of nanoparticles.

This method, as the name implies, relies heavily on the pressure contact between the mold and the substrate. If this contact is imperfect, polymer solution will remain and a scum layer will be generated. When moving from the microscale to the nanoscale the room for error is dramatically decreased. If the relief of the mold is considered, the micron sized cavities can be compressed or distorted more than the nanometer cavities so they compensate for imperfect pressure to a higher degree. The solvent evaporation, pressure fill PRINT method is therefore a good method for micron-sized particles, but in order to generate smaller particles a different method is needed.

2.3 The thermal, capillary fill PRINT method

Having found the limitations of the solvent evaporation pressure fill PRINT method, a new method was sought with the ability to fabricate both microparticles and

nanoparticles. In the second iteration of the PRINT process, capillary action is used to pull molten polymer into cavities during a film split with a high energy film. The excess polymer remains on the high energy film. This method is ideal for making microparticles and nanoparticles.

2.3.1 Experimental

2.3.1.1 Materials

Poly(lactic acid-co-glycolic acid) (PLGA50:50; 33,000 g/mol and PLGA85:15; 50,000 g/mol) was purchased from Lakeshore Biomaterials. Dimethyl sulfoxide (DMSO) and dimethylformamide (DMF) were purchased from Sigma Aldrich. Fluorocur®, 200nm x 200nm and 80nm x 360nm pre-fabricated molds were obtained from Liquidia Technologies.

2.3.1.2 Particle visualization

For visualization samples were coated with 3 nm gold palladium alloy using a Cressington 108 auto sputter coater. Images were taken at an accelerating voltage of 2 kV using a Hitachi model S-4700 scanning electron microscope (SEM).

2.3.1.3 Particle fabrication procedure

A polymer is dissolved in an organic solvent. The ideal concentration depends on the size of the particle, a larger particle requires a higher concentration. For nanoparticles a 2% (w/v) solution is best. A sheet of poly(ethylene terephthalate) (PET) is coated with

the desired composition from 150 µL solution using a #5 Mayer rod (R.D. Specialties) (Figure 2.9 A). The solvent is evaporated under heat. The film is then placed in contact with the patterned side of a mold and passed through a heated nip (ChemInstruments Hot Roll Laminator) at 100°C and 50 psi (Figure 2.9 B). The film is split immediately as it passes out of the nip. The polymer solidifies and the result is a filled mold containing isolated particles (Figure 2.9 C).

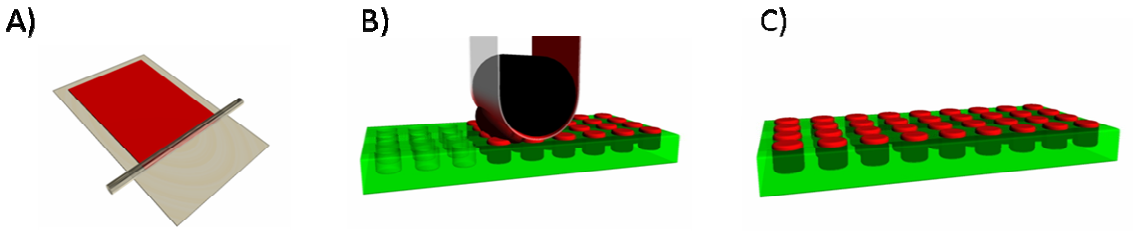

Figure 2.9 The thermal, capillary fill PRINT process. (A) A film is cast on PET. This sheet is termed the delivery sheet, (B) The delivery sheet in passed under a heated nip in contact with a mold, and (C) The mold is filled with isolated solid polymer particles.

2.3.3 Results

This method has the ability to fabricate both micro- and nanoparticles, a benefit over the solvent evaporation, pressure fill PRINT method. In addition the fidelity of template replication and homogeneity of the particles produced was increased as the particles were no longer porous and fully reproduced the shape of the template. PLLA and PLGA were investigated, though the focus fell on PLGA as the more attractive drug delivery matrix due to the higher degree of tailorability. Figure 2.10 shows the successful fabrication of 80 x 320 nm particles using this method.

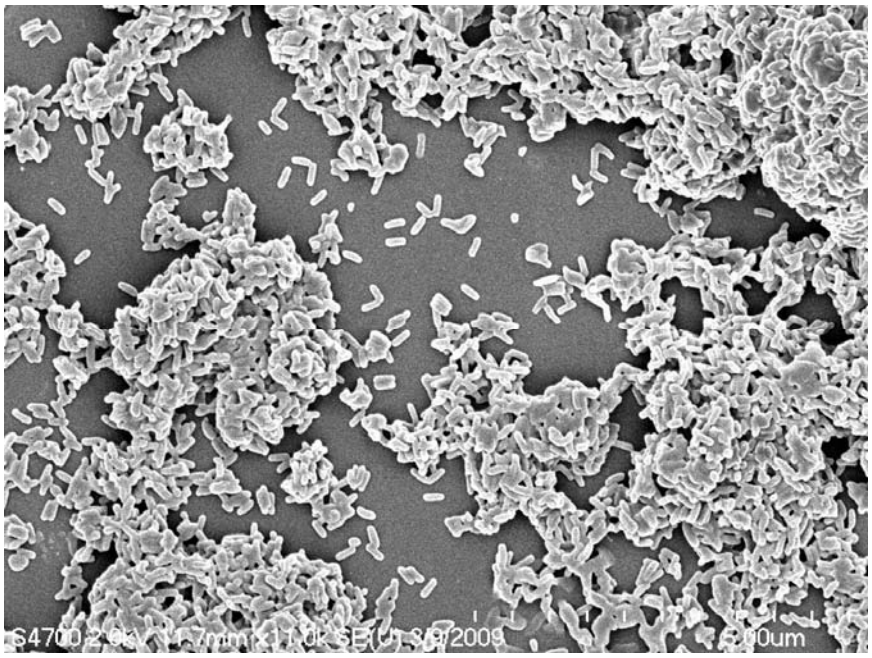

Figure 2.10 80nm x 320nm PLGA nanoparticles.

The thermal, capillary fill PRINT method is based on raising a polymer above its T_g and reaching a state of flow. While a polymer which is heated to its T_g goes from glassy to rubbery, the T_g must be exceeded in order to achieve flow. The PRINT process is typically operated at 100-130^{o}C for PLGA which has a T_g of 45-50^{o}C. There is a range of temperatures for a particular polymer because the T_g is not the only factor that affects filling. The molecular weight of the polymer directly affects the viscosity of the melt. The mold fills by capillary forces which must compete against the viscosity of the polymer melt. Once the viscosity of the melt reaches a critical level the capillary forces can no longer overcome it and the mold does not fill. In a small intermediate range, the delivery sheet is embossed with the pattern. This indicates the polymer has some mobility, but not enough to separate from the bulk film on the delivery sheet. Molecular weight measurements are made using different techniques and different standards, but inherent viscosity measurements are simple and standardized. By looking at the inherent viscosity

of a polymer, the ability of that polymer to fill the mold without a plasticizer can be determined. PLGA with an inherent viscosity <0.5 dL/g can fill the mold while polymers above require a plasticizing agent to bring down the T_g and viscosity of the mixture. This agent can be almost any small molecule or a second polymer with lower T_g. Another important consideration when choosing a polymer is whether the particle has a high enough modulus to hold its shape at room temperature. The molecular weight and PDI of the polymer plays a key roll in this characteristic, with low molecular weights having a decreased modulus. The PDI can also affect the modulus if there are significant lower or higher molecular weight fractions. In general very low molecular weight polymers (approx. <5 kDa) can be filled, but do not retain their shape. Very low molecular weight polymers are not desirable for drug delivery applications anyway because the release of cargo is too fast. Low to moderate molecular weight polymers (approx. 5 – 50 kDa) can be filled and retain their shape. And finally high molecular weight polymers (approx. >50 kDa) can not fill the mold without the addition of a plasticizing agent. The addition of a plasticizing agent is a viable options for drug delivery vehicles, though it does add a layer of complexity.

2.4 Particle Harvesting

In the final step of the PRINT process the particles must be removed from the mold and collected in solution. This is termed harvesting. There are a number of ways to harvest particles, but they all fall under two categories: mechanical or sacrificial layer harvesting. In mechanical harvesting a force is applied directly to the particles once transferred to an array. In sacrificial layer harvesting the particles are transferred in an

array onto a material which can be dissolved or melted freeing the particles with no mechanical force applied. Both methods follow the same basic steps. Particles are transferred from the mold into an array and are then collected as free, isolated particles (Figure 2.11). The difference lies is the substrate they are transferred onto.

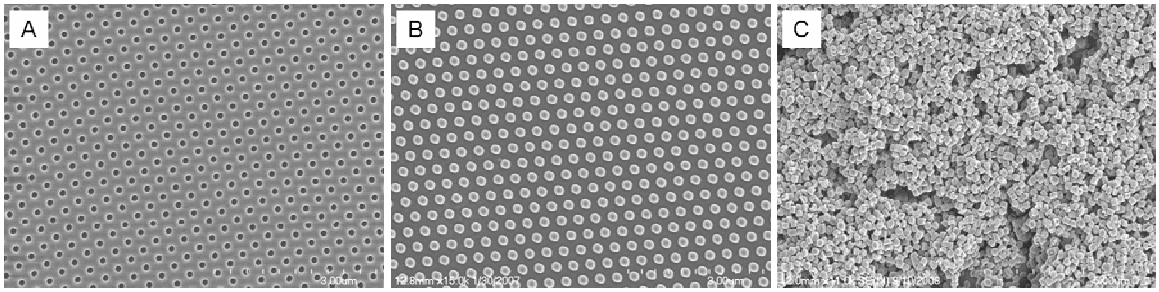

Figure 2.11 An SEM image of the (A) the empty mold after particles are removed, (B) the array of particles transferred out of the mold onto a substrate, and (C) collected free particles.

2.4.1 Mechanical Harvesting

The first methods used to remove particles from the mold where mechanical in nature. Rubbing a glass slide across the mold was used to remove particles which were crosslinked. For linear polymer particles this method was too forceful and damaged particles. A more gentle method, termed squeegee harvesting after the action of collecting the particles, was developed. This method was used for most of the *in vitro* work presented herein. In this technique particles are transferred from the mold to a solid substrate such as silicon, glass, or PET by placing the filled mold on the substrate (Figure 2.12 A) and applying heat while the two are in contact (Figure 2.12 B). This re-melts the particles which adhere to the higher energy substrate. When the mold is peeled off the particles remain stuck to the substrate (Figure 2.12 C). While the surface area contact is 5 times higher for the Fluorocur mold, the surface energy is so much lower that the particles are released to the higher surface energy film. Once the array is transferred the

particles are collected using a cell scraper and a bead of water with polyvinyl alcohol (PVOH; 22,000 g/mol) supplied by Liquidia technologies as a stabilizer (Figure 2.12 D).

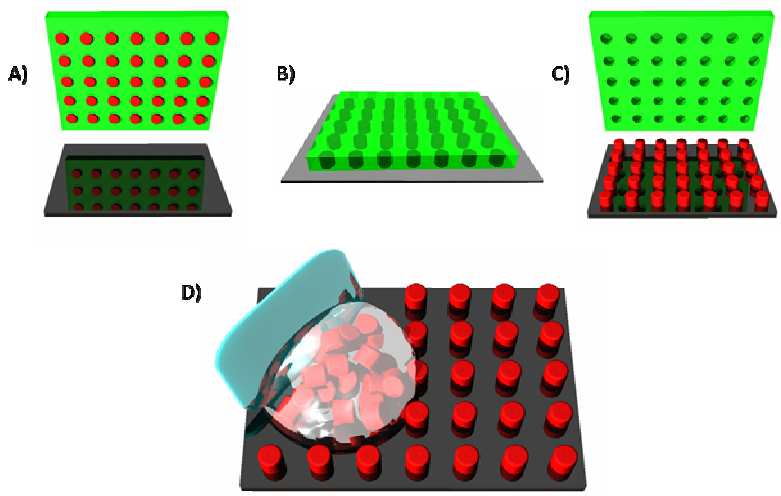

Figure 2.12 Particle harvesting via the squeegee method: (A) the mold is placed in contact with a solid substrate, (B) the mold and substrate are heated while in contact adhering the particles to the substrate, (C) when the mold is peeled back the particles are left in an array on the substrate, (D) a cell scraper (blue) and a bead of water containing stabilizer are used to mechanically collect the particles using gentle lateral force.

This process relies on the use of a stabilizer. The stabilizer lowers the surface tension which assists in the release from the substrate with lowered mechanical force. In addition the stabilizer prevents hydrophobic particle-particle interactions, which prevents aggregation.

2.4.2 Sacrificial Layer Harvesting

As transitions were made to larger scales and *in vivo* studies some evidence of aggregation was observed. It was concluded that this aggregation was due to the mechanical force applied to particles during squeegee harvesting. As particles are harvested with a cell scraper the row of particles are pushed into the next row of particles which can lead to aggregation despite the presence of stabilizer. A non-mechanical

technique was developed to overcome this challenge since the best way to prevent aggregation is to never force the particles together. In sacrificial layer harvesting the particles are removed from the mold on a water soluble sacrificial layer which is then dissolved to release the particles into solution. This eliminates mechanical force and allows the particles to be coated with stabilizer immediately. The most commonly employed sacrificial layer is poly(vinyl alcohol) (PVOH). PVOH coated poly(ethylene terephthalate) was obtained from Liquidia Technologies. The mold is placed in contact with the PVOH coated PET (Figure 2.13 A). While in contact the film and mold are heated melting both the particle and the PVOH film (Figure 2.13 B). When the mold is removed the particles remain on the harvesting layer (Figure 2.13 C). When a drop of water is placed on this harvested layer the PVOH dissolves releasing the particles and coating the particles with PVOH (Figure 2.13 D).

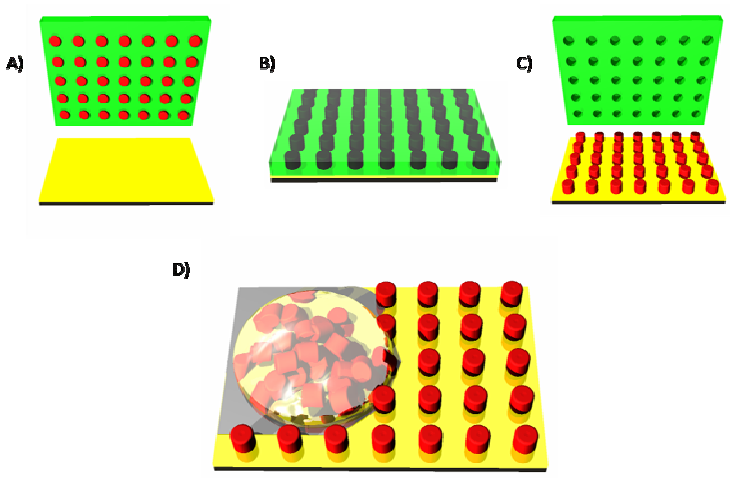

Figure 2.13 PVOH harvesting: (A) the mold is placed in contact with a solid substrate coated with PVOH, (B) the mold and coated substrate are heated while in contact adhering the particles to the substrate, (C) when the mold is peeled back the particles are left in an array on the coated substrate, (D) a bead of water is used to collect the particles without mechanical force.

2.5 PRINT process scale-up

The previously described techniques were all developed on a small scale. The scale up of the PRINT process has been critical to the expansion from small *in vitro* experiments to large *in vivo* experiments. Scale up involved the purchase and manufacturing of new equipment and advances made by Liquidia Technologies in mold fabrication. Initially molds were made by hand as needed and templates were typically AFM calibration grids or other pre-fabricated patterns of appropriate size (Figure 2.14). Particle quantities from these small templates were useful for the demonstration of the PRINT process, but not sufficient for *in vitro* applications. Slowly the size of the master was scaled-up from templates millimeters in size to 8 inch wafers which were sufficient for *in vitro* studies. As the technology progressed, fabrication of larger quantities was needed. Liquidia Technologies developed the machinery necessary to make rolls of mold in a continuous line (Figure 2.14). Using these molds cut time and cost and allowed for large batches of particles to be fabricated at a time.

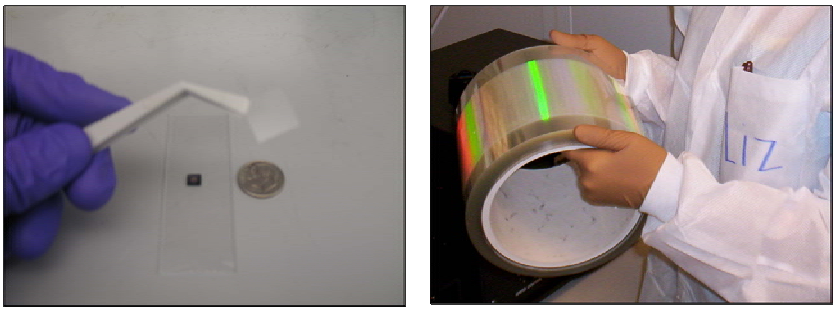

Figure 2.14 Advances in mold technology. Left: original master on a glass slide with the mold size compared to a dime. Right: a roll of 200 nm mold supplied by Liquidia Technologies.

In addition to advances made in mold fabrication, new equipment was obtained and the PRINT process became higher throughput. A hot roll laminator (HL-100) was purchased

from ChemInstruments. This piece of equipment has two rolls which create a nip point allowing a large angle of separation during filling (Figure 2.15 A). This is important because when the film is split the polymer needs to still be in the molten state in order for the polymer which has filled the cavity to separate from the bulk film. Since this nip can be run continuously, an indefinite length of mold can be filled. The particles can be transferred to the PVOH layer in the same way (Figure 2.15 B). Finally the harvesting step was upgraded to a semi-continuous roll process. A piece of equipment termed the "bead harvester" was constructed. It consists of two rolls creating a nip point. The transfer layer is passed through the nip on which a bead of water rests (Figure 2.15 C). The PVOH is immediately dissolved when the bead contacts it, releasing the particles into the bead.

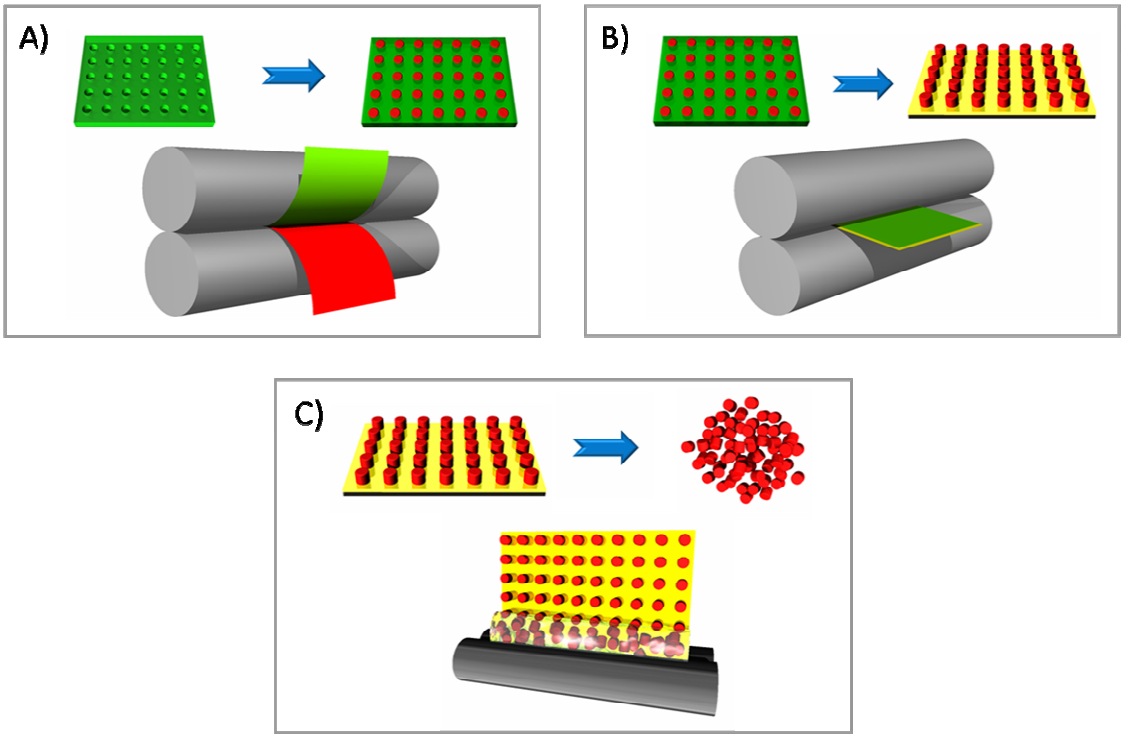

Figure 2.15 Scaled-up PRINT process. (A) a mold is filled, (B) the particles are transferred to a water soluble film, (C) the particles are collected in a bead of water.

While harvesting the particles using the bead harvester is semi-continuous and generates very stable particles, there is a large excess of PVOH present. This PVOH needs to be removed and the particles need to be concentrated. There are many filtration methods available including dialysis, centrifugation, centrifiltration, and tangential flow filtration. Centrifugation and centrifiltration are the quickest and simplest, however, they pack the particles together against the bottom of the tube or the filter membrane. As discussed previously this type of mechanical force is undesirable. Dialysis is a slow and water intensive process which tends to dilute the sample further. Tangential flow filtration is a method of filtration where the flow is parallel to the filter membrane. The pressure generated when passing the solution through the fiber membrane pushes the excess water and soluble PVOH out into a collection tube (Figure 2.16).

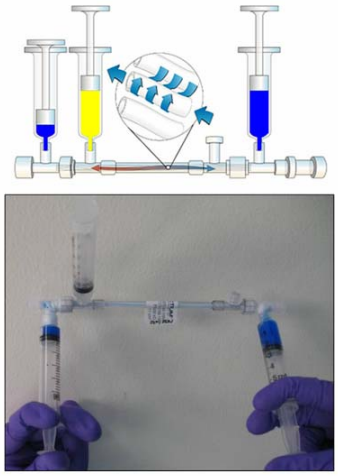

Figure 2.16 Krosflow® MicroKros (X1-500S-200) tangential flow filtration apparatus.

Krosflow® MicroKros (X1-500S-200) were purchased from Spectrum Labs. Both the PVOH and the particles are concentrated overall; however, the amount of PVOH removed becomes clear when the ratio between the PVOH and particles is compared.

Before tangential flow filtration there is ~17 times as much PVOH as particles by mass. After tangential flow filtration this is reduced to only ~2 times.

Table 2.3 A demonstration of PVOH removal and particle concentration by tangential flow filtration.

	PVOH concentration (mg/mL)	Particle concentration (mg/mL)	Ratio
Before Filtration	5	0.3	16.7
After Filtration	18	8	2.3

2.6 *In vitro* cytotoxicity of engineered PLGA PRINT nanoparticles

The first step in characterizing how PLGA PRINT nanoparticles interact with the body is *in vitro* evaluation of cytotoxicity. A drug delivery vehicle should be non-toxic so that once the therapeutic is delivered, the vehicle is safely metabolized or excreted. In addition to 100% PLGA nanoparticles, particles containing 10% poly(ethyleneimine) (PEI) were tested. The latter composition was of interest both for complexing siRNA and as a way of introducing a chemical handle on which to react PEG or targeting ligands.

2.6.1 Experimental

2.6.1.1 Materials

7,000 g/mol PLGA with a lactic acid to glycolic acid content of 50:50 was purchased from Lakeshore Biomaterials. PEI (25,000 g/mol branched) and maleic anhydride were purchased from Sigma Aldrich. Dimethyl sulfoxide (DMSO) and dimethylformamide (DMF) were purchased from Sigma Aldrich. mPEG(5K)-NHS(SS)

was purchased from Creative PEGWorks. CellTiter-Glo assays were purchased from Promega.

2.6.1.2 Particle fabrication and post-reaction with PEG

Particles were fabricated using the thermal, capillary fill method and the squeegee harvest method previously described. PEI was incorporated by simply mixing with PLGA in the precursor solution. PEGylation was accomplished by reacting particles containing PEI with an excess of mPEG(5K)-NHS(SS) for 45 minutes at pH 6.5 and room temperature. Negatively charged PEGylated particles were generated by further reacting the PEGylated particles with excess maleic anhydride under the same conditions to quench any unreacted amines. Excess reagents were then removed by tangential flow filtration.

2.6.1.3 *In Vitro* cytotoxicity

In vitro cytotoxicity was measured using an ATP-luciferase assay. All cell lines were cultured in media supplemented with 10% serum. For toxicity studies, cells were plated at 5,000 cells per well in white walled 96 well plates. Particles were dosed on cells in media supplemented with 10% serum. After 72 hours the viability of the cells was measured using a CellTiter-Glo assay and a SpectraMax M5 plate reader (Molecular Devices).

2.6.2 Results

Two cells lines to be used in subsequent biodistribution and efficacy experiments were investigated: non-small cell lung carcinoma (H460) and ovarian cancer (SKOV3). Negatively charged (-20mV) 100% PLGA particles, positively charged (+63mV) 90% PLGA / 10% PEI particles, and PEGylated (+49mV) 90% PLGA / 10% PEI particles were investigated. Figure 2.17 shows viability as a percent of untreated (control) cells. The compositions with PEI showed slightly lower viability than the compositions without due to the positive charge of the particle, but all compositions show ≥80% viability up to 125 μg/mL. These compositions were chosen for *in vivo* tolerance screening.

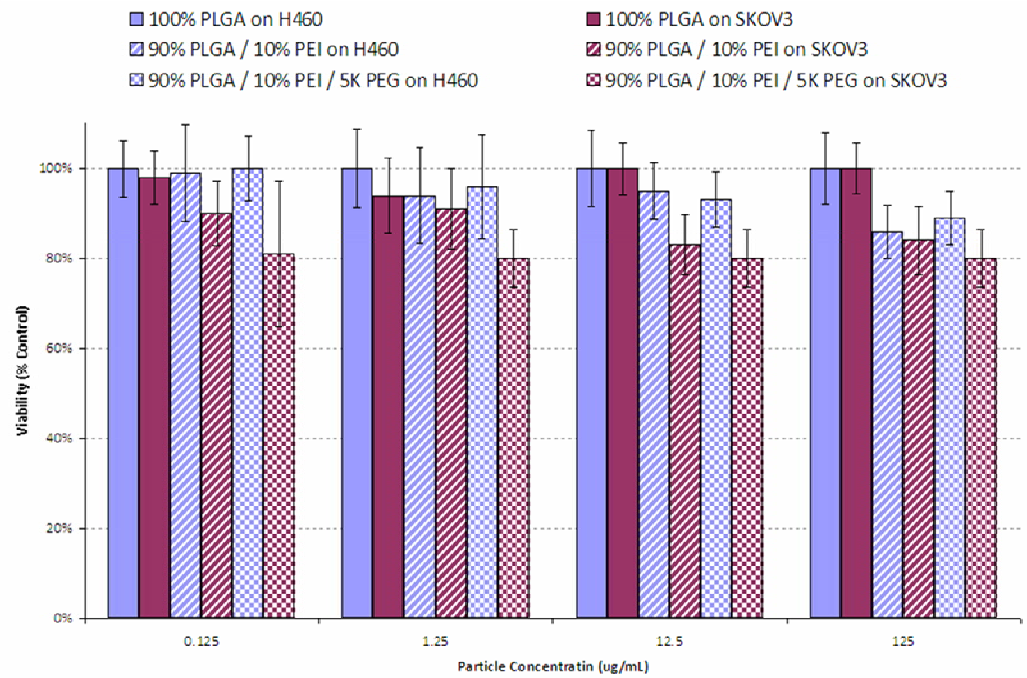

Figure 2.17 The 72 hour viability of H460 (blue) and SKOV3 (purple) cells when treated with PVOH stabilized PLGA PRINT 200 nm cylindrical particles (solid bars), 90% PLGA / 10% PEI PRINT 200nm cylindrical particles (striped bars), and PEGylated (5K) 90% PLGA / 10% PEI PRINT 200nm cylindrical particles (checkerboard bars).

2.7 *In vivo* immune response to engineered PLGA PRINT nanoparticles

In order to test how well particle injections were tolerated *in vivo*, two markers of immune response were investigated. Tumor necrosis factor alpha (TNFα) is an acute immune response cytokine produced mainly by macrophages which leads to inflammation. TNFα typically peaks at 2 hours post-administration. Interleukin 12 (IL-12) is a cytokine which can also be produced by macrophages in addition to dendritic cells and B-cells. IL-12 is a T-cell stimulating factor and typically peaks 6 hours post-administration.

2.7.1 Experimental

2.7.1.1 Materials

7,000 g/mol PLGA with a lactic acid to glycolic acid content of 50:50 was purchased from Lakeshore Biomaterials. PEI (25,000 g/mol branched) and maleic anhydride were purchased from Sigma Aldrich. Dimethyl sulfoxide (DMSO) and dimethylformamide (DMF) were purchased from Sigma Aldrich. mPEG(5K)-NHS(SS) was purchased from Creative PEGWorks. Matrigel® was purchased from BD Biosciences. IL-12 and TNFα ELISA assays were purchased from BD Biosciences.

2.7.1.2 Particle fabrication and post-reaction with PEG

Particles were fabricated as using the thermal, capillary fill method and the squeegee harvest method previously described. PEGylation was accomplished as previously described.

2.7.1.3 Measurement of immune response

All mice were handled in accordance with the University of North Carolina's Institutional Animal Care and Use Committee (IACUC) protocols. Immuno-compromised Balb/c Nude and SCID CB.17 mice were purchased from Harlan Labs. One week after arrival mice were injected with 5 million H460 or SKOV3 cells in the right or left flank. Injections of H460 cells used Matrigel® as a tumor formation aid. Once tumors formed, mice were injected I.V. with PLGA PRINT nanoparticle solutions and control solutions (n=3). Blood was collected at 2 hours by mandibular bleed and at 6 hours by cardiac puncture. Immune response was measured using TNFα and IL-12 ELISA assays read on a SpectraMax M5 plate reader (Molecular Devices).

2.7.2 Results

Figures 2.18 and 2.19 below show the TNFα and IL-12 response of mice to a variety of controls and particle compositions. Controls included mice which received no injection, injections of PBS ("control injection") and injections of dye and PVOH. None of the particle compositions tested excited an immune response statistically significant from the control groups by measure of either cytokine. This confirms what the *in vitro* cytotoxicity assay suggests: both 100% PLGA and PLGA/PEI/PEG compositions are well tolerated *in vivo*.

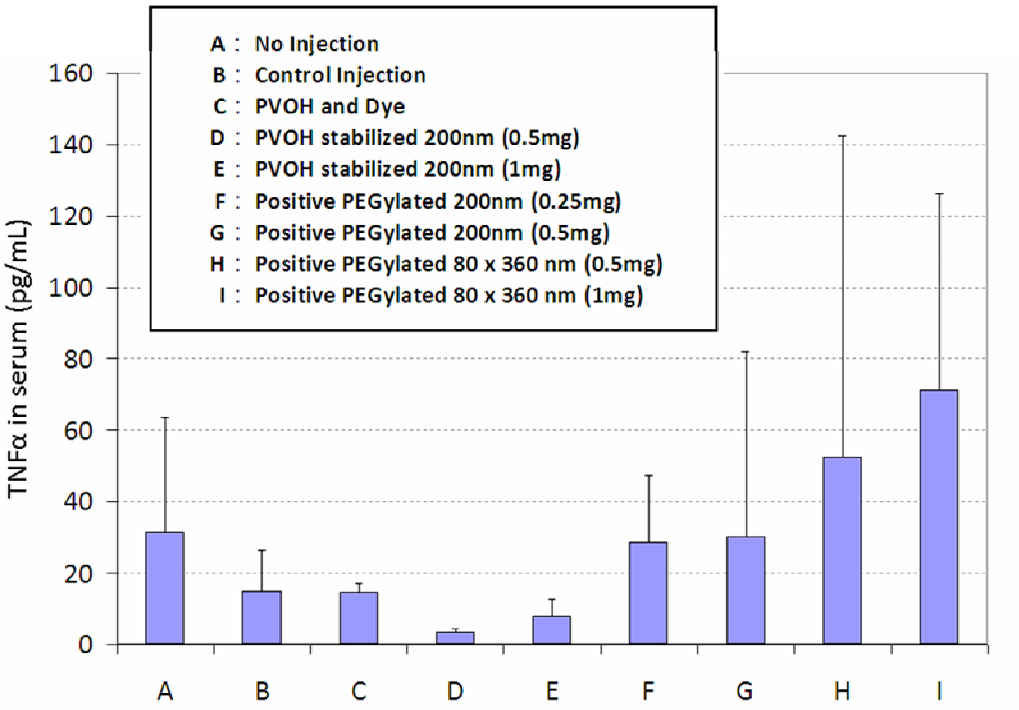

Figure 2.18 The TNFα levels in serum 2 hours after injection.

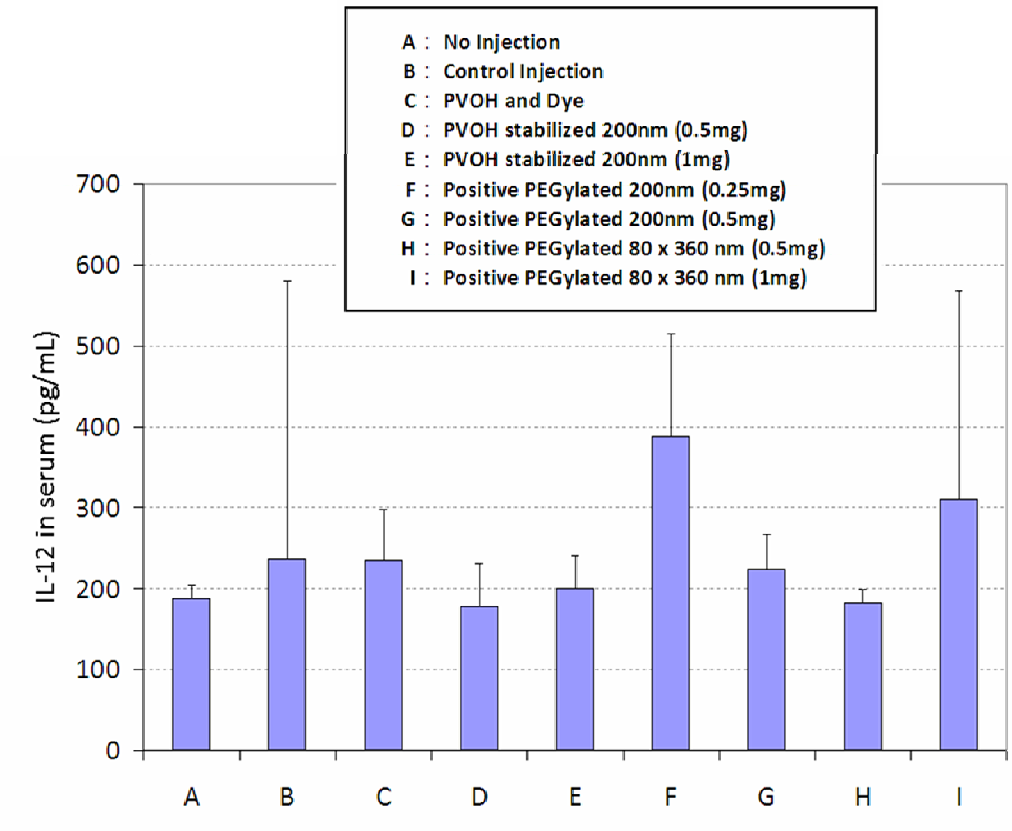

Figure 2.19 The IL-12 levels in serum 6 hours after injection.

2.8 Biodistribution of engineered PLGA PRINT nanoparticles

The biodistribution of a therapeutic determines the level of systemic exposure and the maximum concentration in the tumor. The goal of advanced drug delivery is to accumulate drug in the tumor using a drug delivery vehicle while reducing the exposure of organs which can be damaged by the therapeutic. The biodistribution of PLGA PRINT nanoparticles fabricated via the thermal, capillary fill PRINT method was investigated. Systemic administration through intravenous (IV) injection is the quickest way to gain access to the bloodstream, in which the particles must travel to reach the tumor. Inhalation, oral administration, intraperitoneal (IP) injection, subcutaneous (SC) injection, and intramuscular (IM) injection are also valid methods of administering therapeutics. While some of these methods can be preformed by the patient at home offering higher patient compliance, in each case the particle must traverse additional barriers in order to gain access the bloodstream before accumulation in the tumor can occur. To minimize the barriers to delivery, PLGA PRINT nanoparticles were administered through IV injection in all biodistribution studies. Two types of tumor models were studied: xenograft and orthotopic. A xenograft model is one in which cancer cells are injected into the back or leg of an immuno-compromised mouse. An orthotopic model is one in which cancer cells are injected where that tumor would naturally grow. The three tumor models studied were a xenograft non-small cell lung carcinoma model (H460), a xenograft ovarian cancer model (SKOV3), and an orthotopic pancreatic cancer model (ASPC-1).

2.8.1 Experimental

2.8.1.1 Materials

Poly(lactic acid-co-glycolic acid) (PLGA; 50:50; 33,000 g/mol) was purchased from Lakeshore Biomaterials. Dimethyl sulfoxide (DMSO) and dimethylformamide (DMF) were purchased from Sigma Aldrich. 1,1'-dioctadecyl-3,3,3',3'-tetramethylindodicarbocyanine perchlorate (DiD) was purchased from Invitrogen.

2.8.1.2 Particle fabrication and characterization

Particles were fabricated using the thermal, capillary fill method and the PVOH sacrificial layer harvest method previously described. DiD was incorporated at 2% total solids. For size and charge characterization, dynamic light scattering (DLS) measurements were made at 30μg/mL particle concentrations on a Malvern Instruments Nano-ZS.

2.8.1.3 Biodistribution

All mice were handled in accordance with the University of North Carolina's Institutional Animal Care and Use Committee (IACUC) protocols. Immuno-compromised Balb/c Nude and SCID CB.17 mice were purchased from Harlan Labs. One week after arrival mice were injected with 5 million H460 or SKOV3 cells in the right or left flank. Injections of H460 cells used Matrigel® (BD Biosciences) as a tumor formation aid. The orthotopic model was generated by injecting ASPC-1 cells orthotopically. Once tumors formed, mice were injected IV with PLGA PRINT nanoparticle solutions and

control solutions (n=3). At set times organs were harvested and measured using an IVIS® Kinetic Optical Imaging system. Particles were detected at an excitation wavelength of 675 nm and an emission wavelength of 720 nm with a 30 second exposure.

2.8.2 Imaging agents

Tracking particles *in vivo* can be accomplished through chemically labeling the polymer matrix or encapsulating a beacon (a dye, a magnetic contrast agent or a radioactive isotope). Animals can then be imaged whole body or organs can be individually harvested and measured. A dye was chosen to follow PLGA PRINT nanoparticles *in vivo* due to the ease of processing on communal equipment (radioactive isotopes contaminate equipment with radiation) and access to optical *in vivo* imaging systems. The first studies were carried out using a near-infrared (NIR) dye labeled PLGA. However in order to achieve a higher signal over background a physically entrapped dye was used for later studies. Using a beacon which is not chemically bound to the matrix is risking release and subsequent detection of the small molecule's biodistribution. The dye was therefore chosen to be highly hydrophobic and the release studied. Figure 2.20 shows the chemical structure of DiD, the NIR dye chosen for entrapment, as well as the release profile of DiD from PLGA particles over 48 hours. Less than 5% of the dye is released over 48 hours, twice the longest biodistribution time point studied. This makes DiD a good choice for an entrapped beacon.

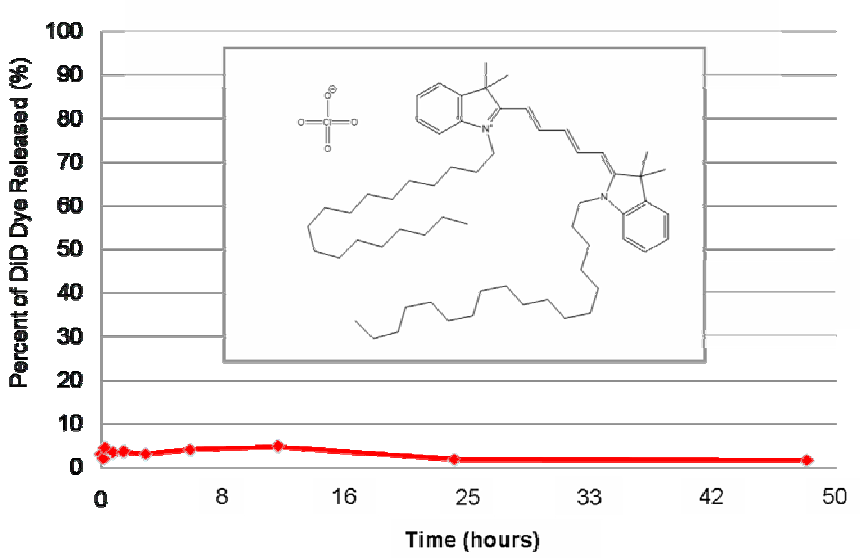

Figure 2.20 The release of DiD (inset structure) from PLGA PRINT nanoparticles.

2.8.3 Biodistribution of PLGA PRINT nanoparticles in a SKOV3 xenograft model

The particle composition chosen for further investigation was PVOH stabilized PLGA PRINT nanoparticles (Figure 2.21). This composition demonstrated promising tumor accumulation in initial biodistribution trials and the avoidance of PEI and other additives, if not necessary, is appealing for the development of therapeutics which can move through FDA screening easier due to prior art.

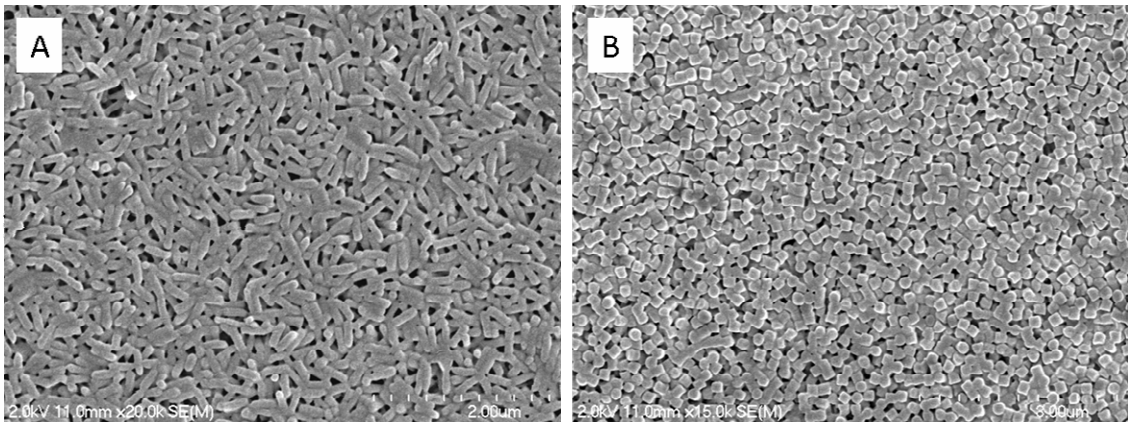

Figure 2.21 SEM images of (A) 80 x 320 nm particles and (B) 200 nm particles.

By using the sacrificial harvesting method, well stabilized samples of both sizes were generated. The PDI of both samples was <0.100, a narrow size distribution (Table 2.4). The particles exhibited a comparable, negative charge.

Table 2.4 Dynamic light scattering characterization.

Particle	Size (nm)	PDI	Zeta Potential (mV)
200 nm	242	0.084	-6
80 x 360 nm	193	0.077	-3

The biodistribution of these samples (Figure 2.22) reflects the stability of the formulation. At 24 hours post-administration 25-40% of particles are still in circulation. Additionally 10-15% of particles have accumulated in the tumor. These numbers compare favorably to other PLGA systems, especially considering previous work by other research groups has suggested that PEGylation is necessary for enhanced circulation and tumor accumulation.[17-21] In most of these cases the particles are formed from PLGA-PEG block copolymers. Using block copolymers in the PRINT process, however, yields an unstable particle due to the differences in polymer orientation. When PLGA-PEG polymers are used to fabricate particles by emulsion methods, the polymer orients so that the PLGA forms a core and the PEG is mostly on the surface (*i.e.* the PLGA is in the organic phase while the PEG stretches into the water phase). However, when PLGA-PEG polymers are used to fabricate particles using the PRINT process there is no orientation preference so when these particles are introduced to water much of the PEG is buried within the particle and stabilization is poor. For these reasons a post-reaction with PEG is needed if

PEGylated particles are desired. However, the results here suggest that PEGylation is not necessary to achieve high tumor accumulation with PLGA PRINT nanoparticles.

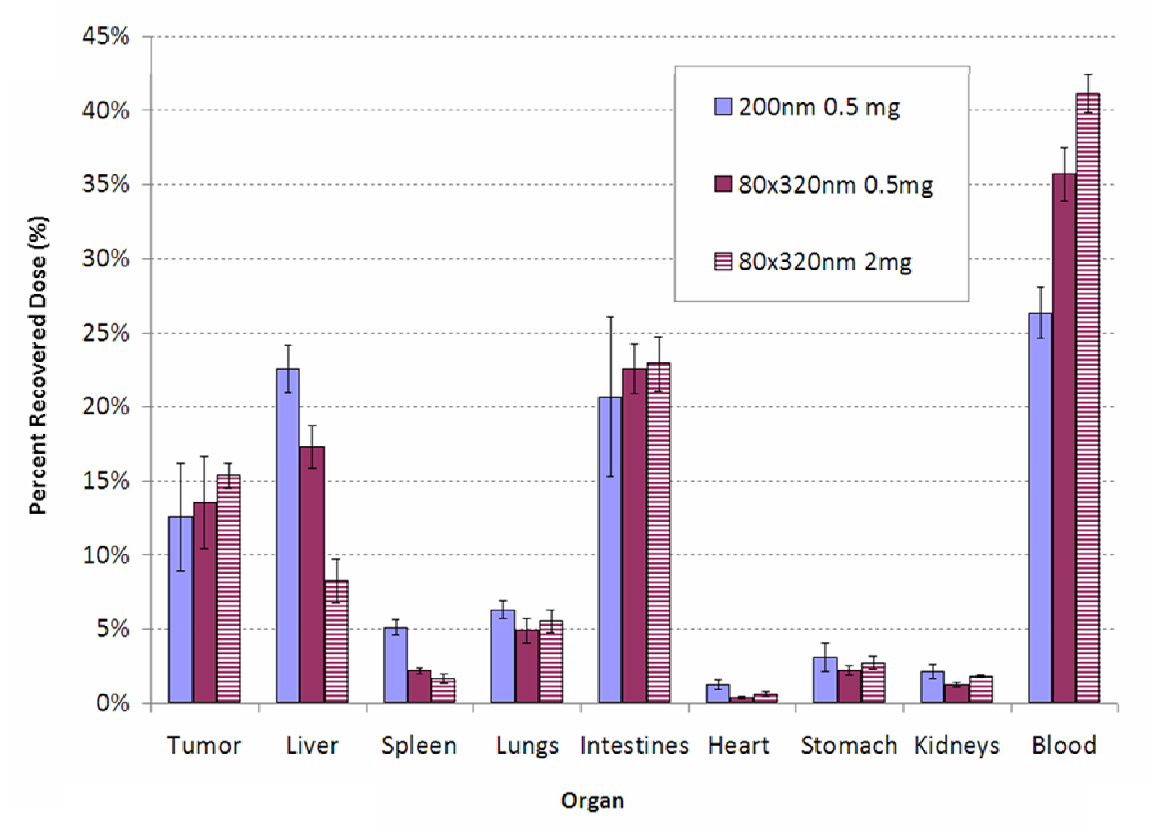

Figure 2.22 The biodistribution of PVOH stabilized 200nm (blue) and 80 x 360 nm (purple) particles 24 hours after injection in SCID mice with xenograft SKOV3 tumors.

In this study the difference between 200 nm and 80 x 320 nm particles was examined. A 200 nm particle has 3.5 times the volume of a 80 x 320 nm particle and is 2.5 times larger in the smallest (critical) dimension. Due to the smaller size the liver and spleen accumulation of 80 x 320 nm particles is reduced resulting in increased circulation in the blood. The tumor accumulation at 24 hours is the same, however, as particles are cleared from circulation over time it is expected that the 80 x 320 nm particles would show higher tumor accumulation as a result of their extended circulation. The effect of dose

was also studied on the 80 x 320 nm particles. When the dose was increased 4 times the percent of particles in circulation increased while the percent accumulation in liver decreased. This may be due to saturation of the liver at high particle doses. It should be noted that while the percent accumulation in the tumor remains the same, the total accumulation in the tumor is therefore 4 times higher. This indicates the tumor is not being saturated, even at high particle doses, which will allow for a wider dosing range.

2.8.4 Biodistribution of PLGA PRINT nanoparticles in an orthotopic ASPC-1 model

In addition to xenograft tumor models, an orthotopic model was investigated. A tumor grown subcutaneously on the leg of a mouse is the simplest, but not the most accurate, model. Tumors grown orthotopically are in the environment the tumor would naturally be in and genetically engineered mouse models (GEMM) are the most accurate with tumors spontaneously developing. The biodistribution of PVOH stabilized 80 x 320 nm particles was investigated in an orthotopic pancreatic tumor model. When compared to the xenograft model previously discussed many similarities are seen (Figure 2.23). A change in organ distribution would not be expected. What is different in this model is the accumulation in the tumor. Pancreatic tumors are dense, poorly vascularized tumors. At 4 hours very little accumulation in the tumor has occurred although it can be seen that particles are reaching the pancreas. At 24 hours, however, almost 5% of the recovered dose is to be found in the tumor. The accumulation over time is probably due to fractions remaining in circulation over longer times and to clearance from other organs. The particle accumulation in the liver, lung, and pancreas decreases over time while signal in the tumor and the intestines increases. Increased accumulation in the intestines over time

may be a sign of how the particles are cleared and excreted. This data is an indication that PLGA PRINT nanoparticles will be able to reach even dense tumors wherever they are located in the body.

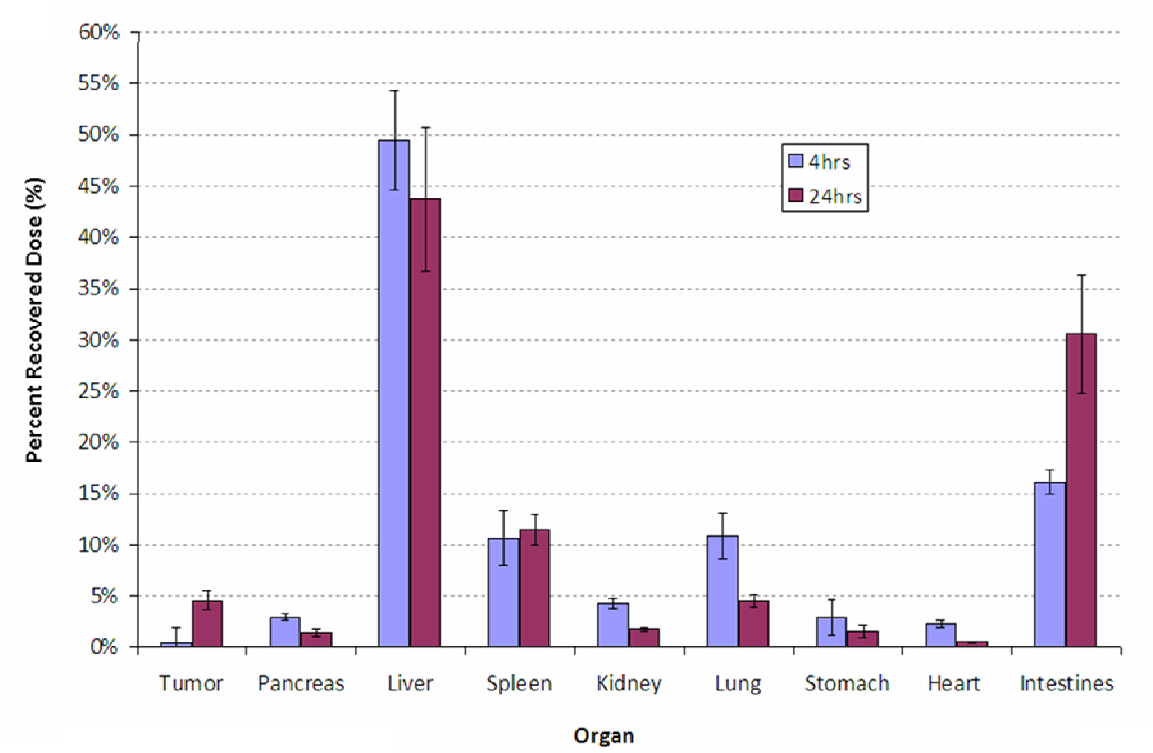

Figure 2.23 The biodistribution of PVOH stabilized 80 x 360 nm particles 4 hours (blue) and 24 hours (purple) after injection in nude mice with orthotopic pancreatic tumors.

2.9 Conclusions

The fabrication of size and shape specific particles using the PRINT process has been demonstrated. Two very different processes were developed. The solvent evaporation, pressure fill PRINT method produces microparticles with porosity and crystallinity. These particles could be used for inhalation delivery; by tailoring the size, shape, and porosity the deposition of the particle in the lung could be altered and by

tailoring the crystallinity, the release characteristics of the particle could be altered. The thermal, capillary fill PRINT method is ideal for fabricating micro- and nanoparticles. This method has been scaled up and is capable of fabricating milligram scale quantities of particles. The cytotoxicity and immune response to PLGA PRINT nanoparticles with and without the addition of PEI and PEG was shown to be low. The biodistribution of PVOH stabilized particles was shown to depend on the size of the particle, the dose administered, and the tumor model investigated. Over time particles clear from most organs with the exception of the tumor and the intestines where further accumulate is seen. High tumor accumulation and long circulation was demonstrated. Biodistribution in an orthotopic model demonstrates tumor accumulation in an environment more similar to the environment of naturally occurring tumors. These studies indicate PLGA PRINT nanoparticles would make excellent drug delivery vehicles and have the potential to improve efficacy over systemic administration.

2.10 Future Work

The investigation of a wider range of sizes and shapes will determine optimal properties for long circulation, reticuloendothelial system (RES) avoidance and high tumor accumulation. A series of masters with a critical dimension of 80 nm and aspect ratios from ~1 to ~63 are currently available. This particle series can be used to determine the effect of shape on particle biodistribution in a systematic fashion. There is already some evidence that high aspect ratio particles may evade the reticuloendothelial system more efficiently than particles with an aspect ratio of 1, warranting further study.[22] In addition to this series of shapes, smaller size masters are being generated (down to 20

nm) which will allow for a comparison of particle size with homogeneous particle populations, something not currently available. A library of available shapes and sizes with known biodistribution profiles will allow for a plug and play approach to cancer therapy. As biodistribution studies move forward a shift from so called chop and count to whole animal imaging will allow biodistribution to be tracked over longer time courses with fewer mice. In addition these methods can be used to track particles during efficacy trials and are translatable to clinical trials in humans. In order to move to clinically relevant whole animal imaging, magnetic or radioactive beacons must be incorporated in the particles for MRI or PET imaging respectively. Finally current biodistribution studies examined particle location on a whole organ scale. Future biodistribution studies will examine where particles are located within a given organ, most importantly how differences in size and shape effect tumor penetration. The PRINT platform will allow for the study of these mechanisms on a level currently unavailable and more importantly will allow for the tailoring of therapies based on their specific requirements.

References

1. Rolland, J. P.; Van Dam, R. M.; Schorzman, D. A.; Quake, S. R.; DeSimone, J. M., Solvent-resistant photocurable "liquid teflon" for microfluidic device fabrication. *Journal of the American Chemical Society* **2004,** 126, (8), 2322-2323.

2. Rolland, J. P.; Hagberg, E. C.; Denison, G. M.; Carter, K. R.; De Simone, J. M., High-resolution soft lithography: Enabling materials for nanotechnologies. *Angewandte Chemie-International Edition* **2004,** 43, (43), 5796-5799.

3. B. W. Maynor, I. L., Z. Hu, J. P. Rolland, A. Pandya, Q. Fu, J. Liu, R. J. Spontak, S. S. Sheiko, R. J. Samulski, E. T. Samulski, J. M. DeSimone, Supramolecular nanomimetics: repliaction of micelles, viruses, and other naturally occurring nanoscale objects. *Small* **2007,** 3, (5), 845-849.

4. Rolland, J. P.; Maynor, B. W.; Euliss, L. E.; Exner, A. E.; Denison, G. M.; DeSimone, J. M., Direct fabrication and harvesting of monodisperse, shape-specific nanobiomaterials. *Journal of the American Chemical Society* **2005,** 127, (28), 10096-10100.

5. R. A. Petros, P. A. R., J. M. DeSimone, Reductively Labile PRINT Particles for the Delivery of Doxorubicin to HeLa Cells. *Journal of the American Chemical Society* **2008,** 130, 5008-5009.

6. J. Y. Kelly, J. M. D., Shape-Specific, Monodisperse Nano-Molding of Protein Particles. *Journal of the American Chemical Society* **2008,** 130, (16), 5438-5439.

7. M. J. Hampton, J. L. T., J. M. DeSimone, Direct patterning of CdSe quantum dots into sub-100nm structures. *Langmuir* **2010,** 26, (5), 3012-3015.

8. J. Nunes, K. P. H., L. Mair, R. Superfine, J. M. DeSimone, Multifunctional shape and size specific magneto-polymer composite particles. *Nano Letters* **2010,** 10, (4), 1113-1119.

9. Ito, H.; Minami, A.; Tanino, H.; Matsuno, T., Fixation with poly-L-lactic acid screws in hip osteotomy - 68 hips followed for 18-46 months. **2002,** 73, (1), 60-64.

10. Xiong, Z.; Yan, Y. N.; Wang, S. G.; Zhang, R. J.; Zhang, C., Fabrication of porous scaffolds for bone tissue engineering via low-temperature deposition. **2002,** 46, (11), 771-776.

11. Gazzano, M.; Focarete, M. L.; Riekel, C.; Scandola, M., Structural study of poly(L-lactic acid) spherulites. **2004,** 5, (2), 553-558.

12. Sasaki, T.; Yamauchi, N.; Irie, S.; Sakurai, K., Differential scanning calorimetry study on thermal behaviors of freeze-dried poly(L-lactide) from dilute solutions. **2005,** 43, (2), 115-124.

13. Wang, F. J.; Wang, C. H., Etanidazole-loaded microspheres fabricated by spray-drying different poly(lactide/glycolide) polymers: effects on microsphere properties. *Journal of Biomaterials Science-Polymer Edition* **2003,** 14, (2), 157-183.

14. Ohtani, Y.; Okumura, K.; Kawaguchi, A., Crystallization behavior of amorphous poly(L-lactide). **2003,** B42, (3-4), 875-888.

15. Iwata, T.; Doi, Y., Morphology and enzymatic degradation of poly(L-lactic acid) single crystals. **1998,** 31, (8), 2461-2467.

16. Sarasua, J. R.; Arraiza, A. L.; Balerdi, P.; Maiza, I., Crystallization and thermal behaviour of optically pure polylactides and their blends. **2005,** 40, (8), 1855-1862.

17. J. Cheng, B. A. T., I. Sherifi, J. Sung, G. Luther, F. X. Gu, E. Levy-Nissenbaum, A. F. Radovic-Moreno, R. Langer, O. C. Farokhzad, Formulation of functionalized PLGA-PET nanoparticles for in vivo targeted drug delivery. *Biomaterials* **2007,** 28, 869-876.

18. Z. Panagi, A. G., G. Evangelatos, E. Livaniou, D. S. Ithakissios, K. Avgoustakis, Effect of dose on the biodistrbution and pharmacokinetics and PLGA and PLGA-mPEG nanoparticles. *International Journal of Pharmaceutics* **2001,** 221, 143-152.

19. K. Avagoustakis, A. B., Z. Panagi, P, Klepetsanis, E. Livaniou, G. Evangelatos, D. S. Ithakissios Effect of copolymer composition on the physicochemical characteristics, in vitro stability, and biodistribution of PLGA-mPEG nanoparticles. *International Journal of Pharmaceutics* **2003,** 259, 115-127.

20. H. Lee, H. F., B. Hoang, R. M. Reilly, and C. Allen, The Effects of Particle Size and Molecular Targeting on the Intratumoral and Subcellular Distribtuion of Polymeric Nanoparticles. *Molecular Pharmaceutics* ASAP.

21. F. Alexis, E. P., L. K. Molnar, and O. C. Farokzhad, Factors Affecting the Clearance and Biodistribution of Polymeric Nanoparticles. *Molecular Pharmaceutics* **2008,** 5, (4), 505-515.

22. D. A. Christian, S. C., O. B. Garbuzenko, T. Harada, A. L. Zajac, T. Minko, and D. E. Discher, Flexible Filaments for In Vivo Imaging and Delivery: Persistent Circulation of Filomicelles Opens the Dosage Window for Sustained Tumor Shrinkage. *Molecular Pharmaceutics* **2009,** 6, (5), 1343-1352.

CHAPTER 3

ENGINEERED PLGA PRINT® PARTICLES FOR THERAPEUTIC DELIVERY

3.1 Introduction

The efficacy of particles designed for advanced drug delivery must be tested in progressively more representative models, until they reach clinical trials and are administered in patients. The first two hurdles are *in vitro* cell based assays followed by *in vivo* efficacy trials in mouse models. In order to test the efficacy of PLGA PRINT nanoparticles two different therapeutic techniques were explored: RNAi therapy and chemotherapy. These two therapies have different modes of action, different delivery requirements, and different cargo sensitivities. By exploring these dissimilar systems the true versatility of the PRINT process is demonstrated.

3.2 RNAi therapy

RNAi therapy, as previously described, is a method of knocking down protein expression by delivering siRNA into the cytoplasm of cells. Since siRNA can not cross the cell membrane itself, the drug delivery vehicle must be internalized and the siRNA released intracellularly. Encapsulation of siRNA is a challenge with the conventional methods to fabricate PLGA particles because some of the hydrophilic siRNA partitions out of the polymer phase before solidification. Encapsulation of siRNA in the PLGA PRINT particle, however, is straightforward as the second phase is a hydrophobic, oleophobic perfluorinated polyether elastomer. In order to demonstrate successful intracellular delivery, knockdown in a luciferase model was explored.

3.2.1 Experimental

3.2.1.1 Particle fabrication

7,000 g/mol PLGA with a lactic acid to glycolic acid content of 50:50 was purchased from Lakeshore Biomaterials. 20,000 g/mol PLGA with a lactic acid to glycolic acid content of 75:25 was purchased from Sigma-Aldrich. 25,000 g/mol branched PEI was purchased from Sigma-Aldrich. Anti-luciferase siRNA-1 and siGENOME non-targeting siRNA #1 were purchased from Dharmacon. Particles were fabricated using the thermal, capillary fill PRINT method and harvested using the squeegee method as previously described.

3.2.1.2 Particle characterization

For particle visualization by scanning electron microscopy (SEM), samples coated with 3 nm gold palladium alloy using a Cressington 108 auto sputter coater. Images were taken at an accelerating voltage of 2 kV using a Hitachi model S-4700 SEM. For size and charge characterization, dynamic light scattering (DLS) measurements were made at 30μg/mL particle concentrations on a Malvern Instruments Nano-ZS. To determine siRNA release profiles, particles were incubated at 37^{o}C in PBS for set time intervals. Particle solutions were then passed through Ultrafree-MC Durapore PVDF 100 nm membranes (Fisher) to remove all particles. Particle supernatant and free siRNA samples were then run on a 2.5% agarose gel in 1M $CaCl_2$.

3.2.1.3 *In vitro* assays

Luciferase transfected HeLa and H460 cells were plated at 5,000 cells per well in a 96-well plate and allowed to adhere for 24 hours. Cells were then dosed with nanoparticle solutions in Opti-MEM for 4 hours in triplicate. After 4 hours the cell were washed and incubated with fresh complete media for an additional 72-96 hours. Promega's Bright-Glo™ Luciferase Assay System was used to determine luciferase expression in each well according to the standard protocol provided. The MTS assay (Promega) was used to determine viability according to the manufacture's protocol. A SpectraMax M5 plate reader (Molecular Devices) was used to measure the results of both assays.

3.2.1.4 Confocal imaging

The cells were treated with particles using the same method as for the other *in vitro* assays only in a well with a coverslip bottom. The samples were additionally stained with DRAQ5 (Biostatus Ltd) according to the manufacturers protocol in order to stain the nuclei (ex. 647nm, em. 670nm) and fixed with 4% paraformaldehyde. Images were taken on an Olympus FV500 confocal laser scanning microscope (Olympus Co Ltd).

3.2.1.5 TEM imaging

The cells were treated with particles using the same method as for the other *in vitro* assays. The samples were then treated with 2% paraformaldehyde / 2% glutaraldehyde and 1% osmium tetroxide / 1.25% ferrocyanide. To prepare for sectioning the samples were dehydrated with ethanol and embedded in Polybed 812 epoxy resin

(Polysciences Inc). After sectioning with a diamond knife, the sections were treated with 4% aqueous uranyl acetate and Reynold's lead citrate. Sections were imaged on a LEO EM910 transmission electron microscope (LEO Electron Microscopy Inc).

3.2.2 Encapsulating siRNA in PLGA PRINT particles

The key to fabricating any particle composition using the PRINT process is casting a homogeneous film, or delivery sheet. For particles which consist of more than one component the film must be examined to determine if there is any phase separation. Any heterogeneity in the film will lead to heterogeneity in the particles. Figure 3.1 shows two films with heterogeneity (A and B) and one film appropriate for use in the PRINT process (C).

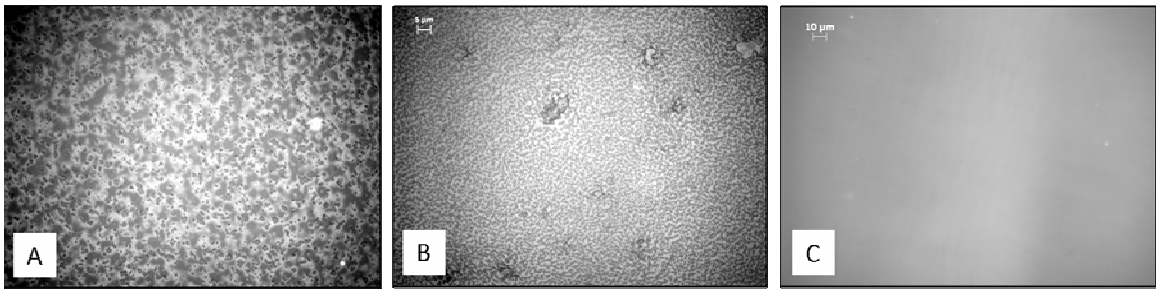

Figure 3.1 Examples of films cast from PLGA/PEI/siRNA solutions. (A and B) heterogeneous films and (C) a homogeneous film.

For most systems any solvent(s) in which all components are miscible can be used to cast the delivery sheet. For siRNA a judicious choice of solvent must be made since siRNA is only highly soluble in water. Furthermore if complexes between siRNA and PEI are generated, their size must be controlled. If simply mixed, siRNA and PEI form large complexes that precipitate out of solution. In order to generate small complexes, mixing the siRNA and PEI at an interface between two miscible solvents was required. The

solvents chosen were DMF and DMSO due to their high water miscibility and good solvent characteristics for both PLGA and PEI. First the polymers are mixed in DMSO, while the siRNA is dissolved in water. The siRNA/water is then diluted with DMF and added on top of the polymer/DMSO solution slowly in order to create two phases (Figure 3.2 A). The ratio of the DMF phase to the DMSO phase is 4:1. This two-phase solution is then mixed slowly until completely homogeneous (Figure 3.2 B). This technique generates complexes which are on average 8-10 nm. This film can then be cast (Figure 3.2 C) resulting in a homogeneous film and particles.

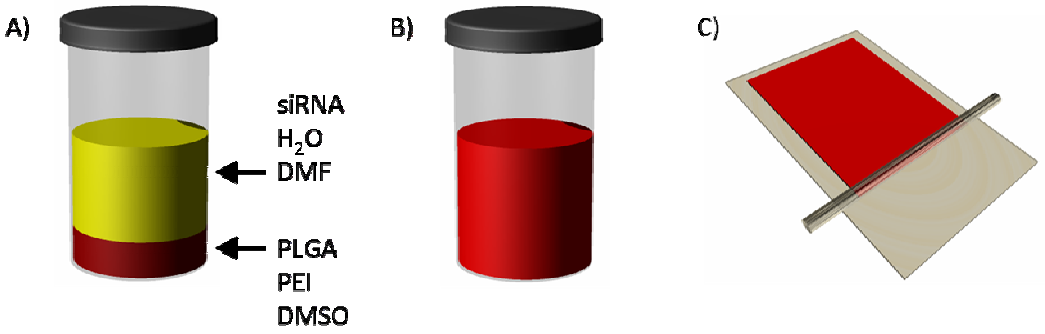

Figure 3.2 The generation of homogeneous PLGA/PEI/siRNA films. (A) a two-phase solution where yellow is DMF with siRNA/water and dark red is DMSO with PLGA/PEI, (B) the two phases are then mixed until completely homogeneous, and (C) the film is then cast from this solution.

Particles were successfully fabricated from a wide range of compositions. By varying the amount of PEI and siRNA incorporated, the zeta potential of the particle was tailored. Particles were generated with zeta potentials from -25mV to +60mV. Figure 3.3 shows monodisperse 200 nm particles which have a zeta potential of +40mV. These particles are very stable in solution due to static repulsion and therefore do not require a stabilizer; this is one of the rare cases in which PVOH is not included in the harvesting procedure.

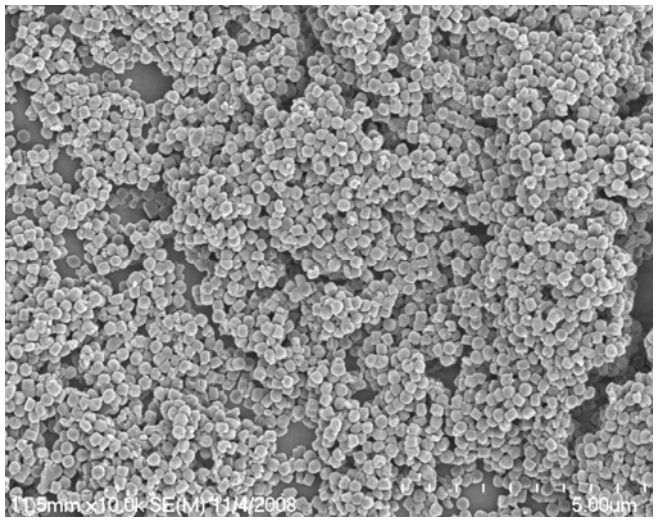

Figure 3.3 SEM of 200 nm PLGA PRINT particles containing 10% PEI and 5% siRNA.

3.2.3 siRNA release from PLGA PRINT nanoparticles

Once particles were successfully fabricated, the release of siRNA was investigated. In order for the particles to be effective drug delivery agents, they must be able to release siRNA and the siRNA must have remained unharmed by the processing conditions. The thermal, capillary fill PRINT method does heat the delivery sheet to 100^{o}C, but the time any one location on the film is heated this high is only 1-2 seconds. In addition the siRNA is at that point complexed with PEI and imbedded in a solid polymer film which may provide additional protection. To investigate the release of siRNA, gel electrophoresis was used. The supernatant from particles incubated at 37^{o}C in PBS from 0-72 hours was investigated (Figure 3.4). This time course was chosen as most *in vitro* knockdown studies were focused on a 72 hour incubation.

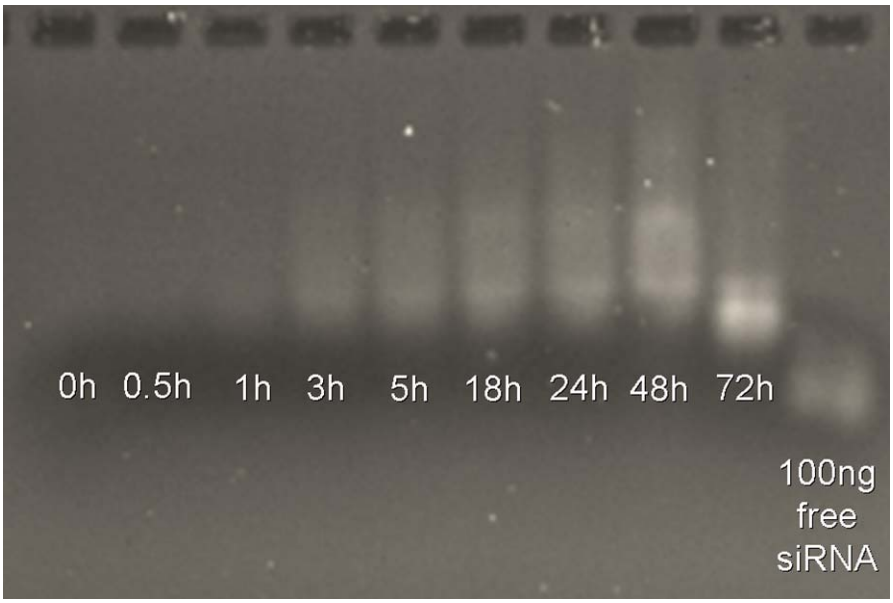

Figure 3.4 The release of siRNA from 200 nm PLGA/PEI particles over 72 hours.

The gel shows siRNA is continually released from the particles over the full 72 hours. The final lane is free siRNA equal to the total amount of siRNA in each particle sample (*i.e.* representative of 100% encapsulation and 100% release from the particle). The particles appear to have released all the siRNA by 72 hours. Interestingly the siRNA from the particles does not travel quite as far down the gel as the free siRNA. This would indicate the siRNA is slightly larger or slightly less negative, retarding its motion down the gel. This indicates there could be some residual PEI. Salt ($CaCl_2$) was added to each lane to break up the complex, but the bands remained slightly higher than the free siRNA. The smear seen with the particle samples as opposed to the single band seen with free siRNA is also an indication that some siRNA is still bound. The lack of any smaller fragments confirms the siRNA is not being degraded in the process.

3.2.4 Cellular internalization and particle degradation

Once particles which could encapsulate and successfully release siRNA were fabricated, cellular internalization was investigated. As previously mentioned, using an encapsulated hydrophobic dye is a very popular method, but can lead to false positives as the dye can be taken up into the lipophilic cell membrane.[1] Instead of relying on a questioned technique, internalization of particles was examined with a Cy3-labeled siRNA and was confirmed by TEM. First confocal studies were carried out knowing that the dye-labeled siRNA could not cross the cell membrane alone. Figure 3.5 shows the uptake of 200 nm particles in HeLa cells at 2 hours. The cells dosed with negatively charged particles (-24mV, no PEI) show no internalization, while cells dosed with positively charged particles (+34mV, 10% PEI) show the presence of particles within the cells. This confirms that PEI (a positive charge) is necessary for internalization.

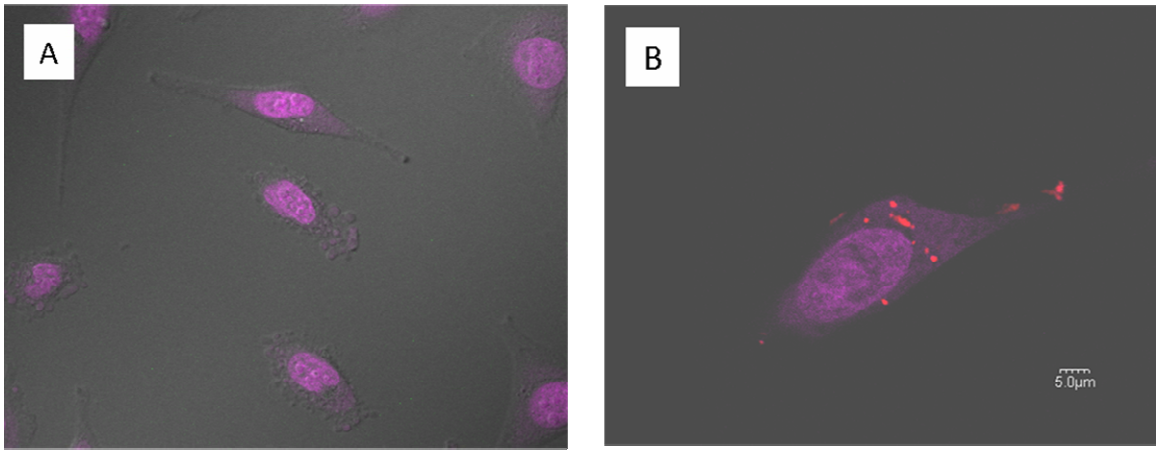

Figure 3.5 The internalization of (A) -24mV PLGA/siRNA particles and (B) +34mV PLGA/PEI/siRNA particles. The nucleus is stained purple while the particles contain Cy3-labeled (red) siRNA.

The same samples were then examined by TEM to confirm internalization of particles. Figure 3.6 shows particles being endocytosed by a HeLa cell. The particles are rounded, which is expected since the particles which are PLGA ($T_g = 45^oC$) and PEI ($T_g = -47^oC$) have been at 37^oC for 4 hours and a sphere is the minimal energy shape. The particles have a granulated appearance which is probably due to the PEI/siRNA complexes.

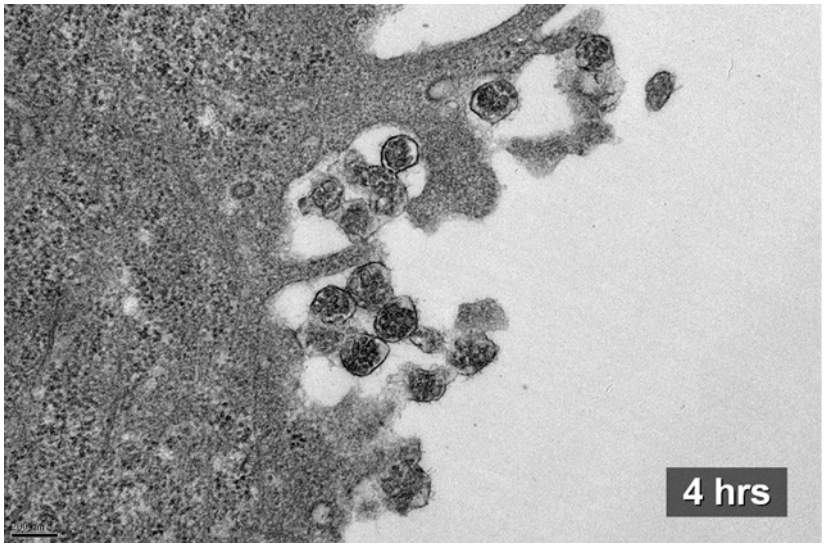

Figure 3.6 TEM image of a HeLa cell internalizing PLGA/PEI/siRNA particles.

In addition many particles were seen in intracellular compartments (Figure 3.7). The cell appears to combine dozens of particles in one vesicle and these vesicles locate near the nucleus. From 4 to 24 hours the particles start to loose their structure and definition. Over 72 hours the particles are completely broken down by the cells, however, polymer can still be still in vesicles. It is likely that during this process, PEI/siRNA complexes are escaping the vesicles due to their high positive charge.

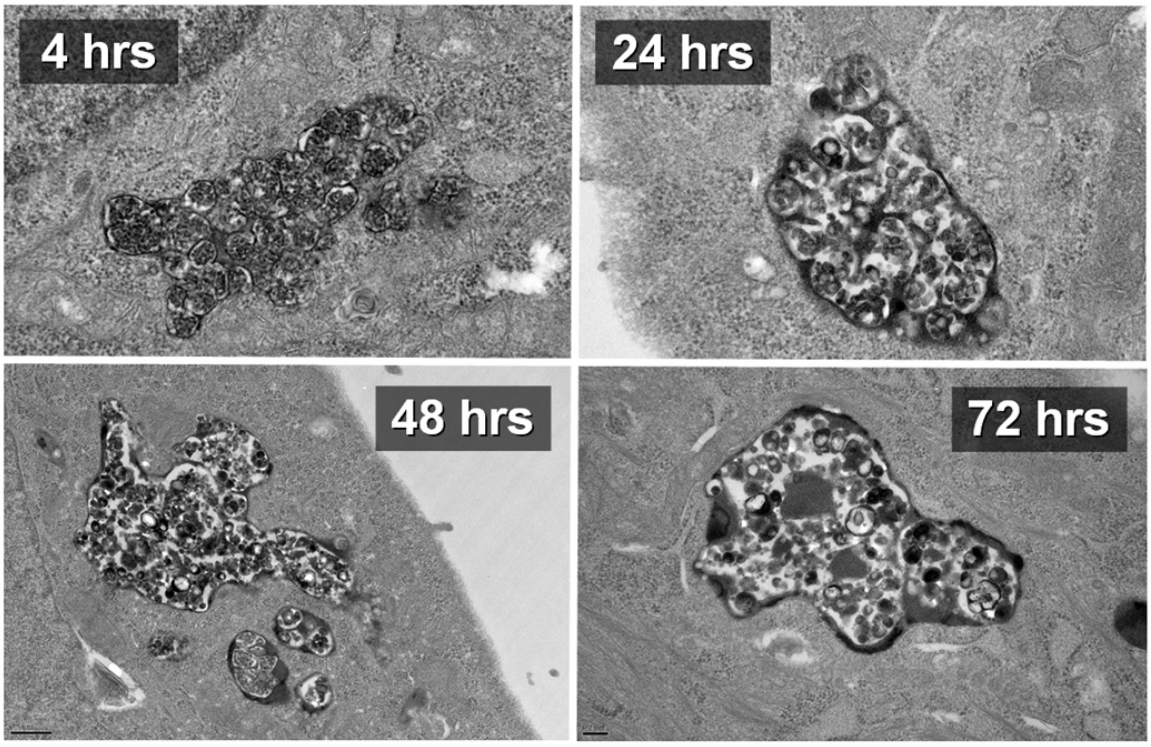

Figure 3.7 The degradation of PLGA/PEI/siRNA particles over 72 hours.

By using a dye-labeled siRNA, which can't cross the cell membrane alone, and confirming with TEM, definitive proof of particles internalization was obtained.

3.2.5 *In vitro* knockdown

The culmination of these tests is an assay for efficacy. The simplest way to test efficacy of a siRNA system is with a reporter protein and the most commonly used reporter is luciferase. In this model cells are stably or transiently transfected with luciferase. When treated with the substrate for luciferase, luciferin, these cells luminesce. Luciferase knockdown on HeLa-Luc (luciferase expressing cervical cancer) and H460-Luc (luciferase expressing non-small cell lung carcinoma) was demonstrated (Figure 3.8).

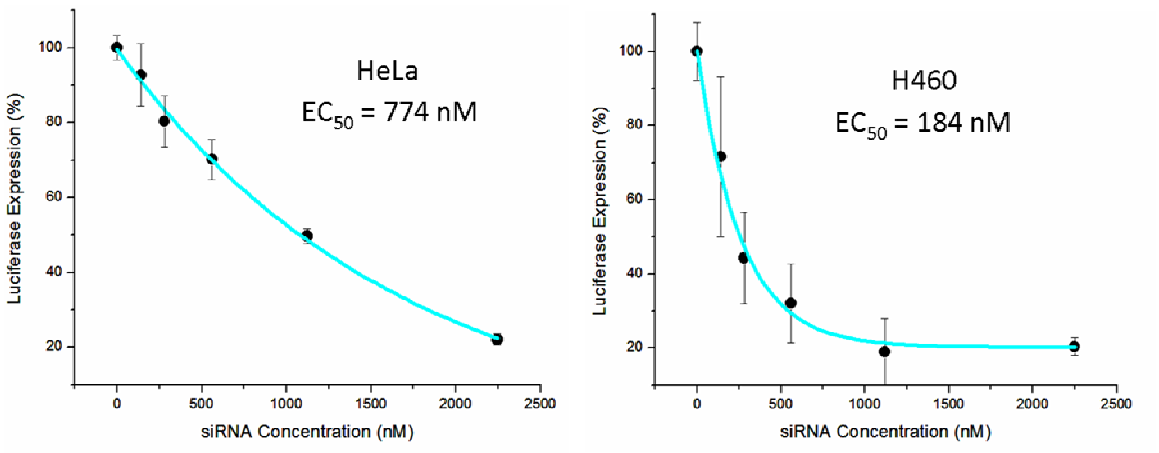

Figure 3.8 Delivery of anti-luciferase siRNA. Expressed as a percent of control (untreated) cells.

Appropriate controls are necessary when looking at protein knockdown since cell death could also cause reduced expression. Viability assays showed the particles caused no toxicity and particles containing irrelevant siRNA show no significant reduction in luciferase expression (data not shown). These controls confirm any effect is due to the delivery of active siRNA. Particles containing anti-luciferase siRNA show significant dose dependent knockdown. H460 cells were more easily affected by the particles due to a lower overall expression of luciferase. The doses required for knockdown are two to three orders of magnitude higher the most effective siRNA delivery systems reported: lipidoids reported by Love et al. in 2010.[2] Three different lipidoid formulations show >80% knockdown at single digit nM doses. These systems have already shown efficacy in mice and nonhuman primates at low siRNA doses. Comparison to the EC_{50} values of other PLGA nanoparticles is made difficult by the tendency to report knockdown at only one dose. Katas et al. reported 0-99% knockdown based on different PLGA/PEI compositions at an siRNA dose of 27nM on HEK 293 cells and 10-65% knockdown from the same particles and dose on CHO K1 cells.[3] This along with our own work

demonstrates how important the specific cell line is to the efficacy of the particle. Tahara et al. reported 0-60% knockdown based on PLGA and chitosan modified PLGA compositions at an siRNA dose of 50nM on A549 cells.[4] These two examples illustrate PLGA/PEI PRINT nanoparticles are slightly above other reported particle systems. The most likely reason for this is the particle's inability to escape the endosome. Recall from the TEM studies (Figure 3.8) that polymer remains trapped in the vesicle even at 72 hours. This vesicle has most likely matured into a lysosome in which any remaining siRNA will be degraded. The fraction of siRNA which escaped the endosome earlier leads to the knockdown observed, but dosing is slightly above averages reported due to incomplete endosomal escape. Confocal studies with dye-labeled siRNA were used to confirm this hypothesis. High concentrations of siRNA were observed concentrated in vesicles out to 72 hours. The amount of diffuse fluorescence (siRNA in the cytosol) can not be measured because it is low compared to the signal from the vesicles. This does not necessarily indicate the particles would not show efficacy *in vivo*. It is crucial to acknowledge the pros and cons of using *in vitro* screening to select formulations for *in vivo* administration. The particles release siRNA over the full 72 hours which may not be the optimal release profile for *in vitro* studies were particles have been shown to internalize in the first 15-30 minutes. For *in vivo* studies the release profile of the particle may be more appropriate since the particle must make its way to the tumor, enter and transverse the tumor tissue, and be internalized. In this situation the particle may be "primed" by this travel time and release more siRNA during the critical pH window in the endosome. Furthermore the PRINT process allows the release rates to be systematically tailored so if not optimal a different composition could be explored.

3.2.6 Conclusions

The PRINT process has been demonstrated as an effective tool for the fabrication of siRNA containing PLGA particles. High cell uptake was achieved through the incorporation of PEI in the particle matrix, giving the particles a positive charge. The degradation of the particles *in vitro* over 72 hours was shown to be rapid, however, some polymer and siRNA remains in the vesicle. The particles exhibit no toxicity *in vitro* and dose dependent knockdown in an *in vitro* luciferase model has been demonstrated.

3.2.7 Future Work

3.2.7.1 Decreased EC_{50} with lipid coated compositions

In order to achieve lower EC_{50} a slightly different formulation is under investigation. Since the best knockdown currently reported is with lipid containing systems, lipids were added to the PLGA PRINT system. The purpose of the lipid is to achieve cellular internalization and to aid in endosomal escape. Lipids were successfully added to the PLGA particle matrix, however, like with adding PEG into the particles matrix, many of the lipids are buried inside the particle. In order to get the highest benefit from the lipids used, the PLGA/siRNA particle was first fabricated and then lipids were simply added to the harvesting medium. The lipids coated the PLGA particles due to the hydrophobic nature of PLGA and the amphiphilic nature of lipids. The characterization of 80 x 320 nm PLGA/siRNA particles coated with a 1:1 mixture of DOTAP:DOPE is shown in Table 3.1 below.

Table 3.1 The characterization of 80 x 320 nm PLGA PRINT nanoparticles coated with lipid.

Lipid concentration (mg/mL)	Size (nm)	Zeta Potential (mV)
0	212	-6
0.1	220	+11
0.5	240	+15

These particles were then tested for internalization using a dye-labeled DNA of the same sequence as the anti-luciferase siRNA (Figure 3.9) and flow cytometry. Particles without lipid coating showed no uptake as expected. The lipid coating resulted in cellular internalized with higher lipid concentrations resulting in higher internalization. Lipid coatings above 0.5 mg/mL display cytotoxicity due to a high concentration of free lipid, which disrupts cell membranes.

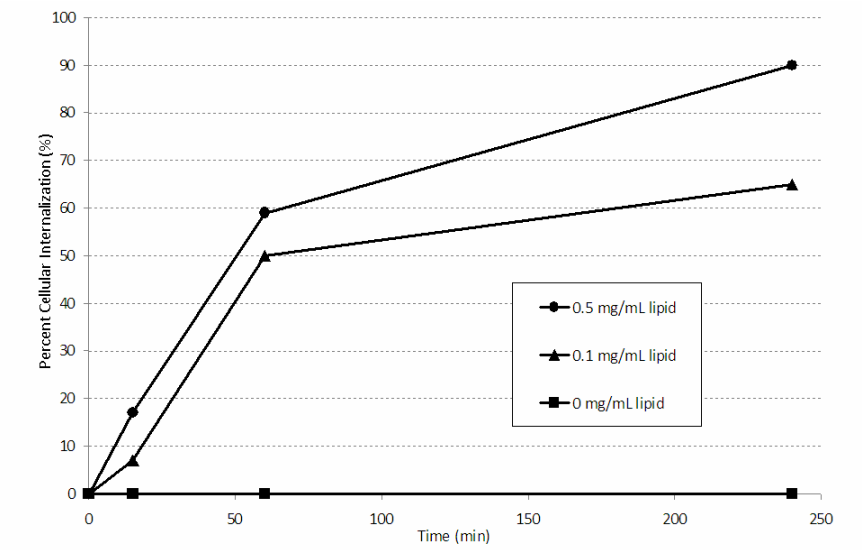

Figure 3.9 The internalization of lipid coated 80 x 320 nm PLGA PRINT nanoparticles as a function of time.

Finally the *in vitro* efficacy of these particles were tested (Figure 3.10). Not only were the particles successful in knocking down luciferase expression, but EC_{50} values were similar to the values reported in the literature for lipidoids. Particles coated with 0.25 mg/mL lipid had an EC_{50} of 7nM and particles coated with 0.2 mg/mL lipid had an EC_{50} of 15nM.

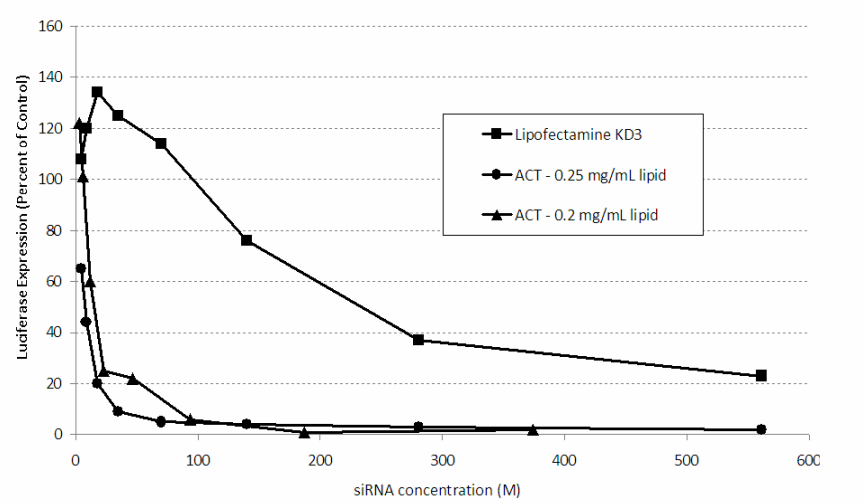

Figure 3.10 Knockdown of luciferase in HeLa-Luc cells by 80 x 320 nm lipid coated PLGA/siRNA nanoparticles.

This composition shows great promise for *in vivo* efficacy and can easily be tailored, using different lipids and different ratios / concentrations of lipid to find an optimal coating.

3.2.7.2 Therapeutic siRNA and *in vivo* knockdown

The knockdown of a reporter gene such as luciferase is an easy screening tool and can be used *in vivo*, but moving to the knockdown of a relevant, therapeutic gene is a more attractive choice. Currently under investigation is the knockdown of the androgen

receptor in the prostate cancer cell line LNCaP. This receptor is implicated in treatment resistant prostate cancers. Once *in vitro* knockdown of this gene is successful, the *in vivo* efficacy can be tested by monitoring mRNA levels and tumor progression in mice with xenograft LNCaP tumors. Using the lessons learned from biodistribution experiments will be crucial to choosing the best size and shape to deliver particles to the tumor most effectively. Once siRNA delivery with PLGA PRINT nanoparticles is demonstrated *in vivo*, combination therapies with chemotherapeutics can be explored.

3.3 Chemotherapy

The second therapy investigated with the PLGA PRINT nanoparticle system was chemotherapy. The purpose of chemotherapy is not to correct the cancerous cells' function as in RNAi therapy, but to destroy the cell and allow the body's natural clearance mechanisms rid the body of the tumor cell by cell. Docetaxel and its need for a drug delivery vehicle were previously described. The requirements of the docetaxel delivery system are different from the siRNA delivery system. The key difference being cellular internalization is not required for efficacy. There are also aspects of the PRINT process that are different. The incorporation of small molecules instead of nanometer-sized complexes allows for a higher loading of therapeutic. And in the case of small molecules all components can be mixed without a special protocol. The chemotherapeutic delivery system therefore quickly succeeded *in vitro* above currently reported systems and *in vivo* investigations were begun.

3.3.1 Experimental

3.3.1.1 Particle Fabrication

Poly(lactic acid-co-glycolic acid) (PLGA; 50:50; 33,000 g/mol) was purchased from Lakeshore Biomaterials. PLGA (85:15; 50,000 g/mol) was purchased from Polysciences. Dimethyl sulfoxide (DMSO) and dimethylformamide (DMF) were purchased from Sigma Aldrich. HPLC grade acetonitrile (ACN) and water were purchased from Fisher Scientific. Docetaxel was purchased from LC Laboratories. Fluorocur®, 200nm x 200nm and 80nm x 360nm pre-fabricated molds and polyvinyl alcohol (PVOH; 22,000 g/mol) were obtained from Liquidia Technologies. Particles were fabricated using the previously described thermal, capillary fill PRINT method and either squeegee harvested (*in vitro* studies) or bead harvested (*in vivo* studies).

3.3.1.2 Particle characterization

To accurately determine particle concentration, thermogravimetric analysis (TGA) samples were prepared by pipetting 20 μL of particle solution into a sample pan and monitoring the weight on a Perkin Elmer Pyris 1 TGA under the following heating steps: 25-100oC at 10oC/min, 15 minute hold, 100-500oC at 10oC/min. For particle visualization by scanning electron microscopy (SEM), samples were prepared by pipetting 50 μL of particle solution onto a woven mesh filter (BioDesign Inc. Cell Microsieve 5μm) and then rinsing with Milli-Q filtered water. Samples were dried and coated with 3 nm gold palladium alloy using a Cressington 108 auto sputter coater. Images were taken at an accelerating voltage of 2 kV using a Hitachi model S-4700 SEM.

For size and charge characterization, dynamic light scattering (DLS) measurements were made at 30μg/mL particle concentrations on a Malvern Instruments Nano-ZS.

3.3.1.3 Docetaxel encapsulation and release by HPLC

Encapsulation efficiency was measured using an Agilent Technologies Series 1200 HPLC with a C18 reverse phase column (Zorbax Eclipse XDB-C18, 4.6x150mm, 5 micron). A mobile phase of water and acetonitrile on a gradient from pure water to pure acetonitrile over 10 minutes with a flow rate of 1 mL/min was employed with a detection wavelength of 210nm. A five minute hold at pure acetonitrile was employed after the initial gradient to wash out the polymer. The docetaxel peak appeared at 8.9 minutes and the PLGA peak appeared at 11.1 minutes. The ratio of the peaks in the precursor solution was compared to the ratio of the peaks in the particle to determine encapsulation. Particles (200nm x 200nm) were harvested and mixed 1:1 with acetonitrile to dissolve the particles for injection. Using the same HPLC method as was used to measure encapsulation efficiency, release profiles were measured for all four PRINT docetaxel compositions. Particles (200nm x 200nm) were incubated in PBS at 37^{o}C for set periods. Aliquots were removed and spun down. The supernatant was removed and the pellet was dissolved in acetonitrile. HPLC was used to determine the docetaxel content remaining.

3.3.1.4 *In vitro* cytotoxicity

H460 cells, a non-small cell lung carcinoma, were cultured in RPMI media supplemented with 10% serum. For toxicity studies, cells were plated at 5,000 cells per well in white walled 96 well plates. Particles (200nm x 200nm) and the standard of care,

Taxotere, were dosed on cells in RPMI media supplemented with 10% serum at twelve ten-fold dilutions of docetaxel concentration. After 72 hours the viability of the cells was measured using a CellTiter-Glo assay (Promega) and a SpectraMax M5 plate reader (Molecular Devices).

3.3.1.5 *In vivo* efficacy

All mice were handled in accordance with the University of North Carolina's Institutional Animal Care and Use Committee (IACUC) protocols. Immuno-compromised Balb/c Nude and SCID CB.17 mice were purchased from Harlan Labs. One week after arrival mice were injected with 5 million SKOV3 cells in the right or left flank. Once tumors formed, mice were injected I.T. with PLGA PRINT nanoparticle solutions and control solutions (n=5). Tumor volumes were then monitored initially every day and then every 2-3 days.

3.3.1.6 PK determination

The same method used for biodistribution studies was used to treat mice for PK determination. Blood samples and organ harvest occurred at 0.083 (n=2), 1 (n=2), 6 (n=3) and 24 (n=3) hours. The Taxotere treatment group consisted of sampling at 0.083, 0.25, 0.5 1, 1.5, 2, 4, 6, 7, 16 and 24 hrs (n=3 all). Simple protein precipitation using acetonitrile was used to extract docetaxel from plasma and tumor samples. A validated LC-MS/MS assay was used to measure the total docetaxel concentration in plasma and tumor samples.[5]

3.3.2 High Drug Loading

In addition to exquisite control over the physical properties of the particle, the PRINT process allows for complete control over particle composition. The "second phase" in this process is a perfluoropolyether network which is both oleophobic and hydrophobic so partitioning into this material is low.[6] This has led to the ability to achieve good encapsulation with loadings much higher than possible with traditional methods. In the literature (Table 1.2) maximum docetaxel loading is 15% with encapsulation widely varying dependant not only on the particular fabrication method, but on the specific parameters used. PLGA PRINT particles 200nm x 200nm can be loaded with 0 – 40% docetaxel (w/w) using the same processing parameters for all compositions. Encapsulation efficiency is >90% for all compositions. Others have cited lowered encapsulation efficiency as drug loading increases[7], however, with the PRINT process loading does not affect encapsulation nor does it affect the particle's physical properties. The largest dimension of the 200nm x 200nm cylinder is approximately 280nm and the smallest 200nm which is reflected in the size measured by dynamic light scattering (DLS) and is consistent across all compositions (Table 3.2).

Table 3.2 Encapsulation efficiency of PLGA PRINT nanoparticles at varying drug loadings (w/w) and physical characterization by DLS.

Theoretical Loading	Encapsulation Efficiency (%)	Size (nm)	Zeta Potential (mV)
0%	--	263 ± 5	-22.6 ± 0.6
10%	93 ± 11	256 ± 10	-19.8 ± 0.8
20%	95 ± 5	246 ± 2	-22.3 ± 0.3
30%	99 ± 7	247 ± 4	-19.6 ± 0.3
40%	99 ± 3	251 ± 1	-21.8 ± 0.2

The charge is negative, typical of PLGA nanoparticles, and is also consistent across all compositions. SEM shows the particles are a homogeneous size and shape within and between compositions (Figure 3.11). The ability to create the same outward physical properties with different compositions in a homogeneous population of particles is going to generate investigations into interesting dosage questions that traditional methods can not explore. One interesting and unexplored question is the difference in delivering the same drug dose in different particle doses. For example, to compare the efficacy of administering 1 mg of 20% docetaxel particles versus 0.5 mg of 40% docetaxel particles. This is a comparison other methods simply can not investigate because the loadings are not achievable with traditional methods and even if they were the particle's physical properties would not be identical, clouding the results. The availability of more dosing options can provide a better chance of increasing efficacy in patients.

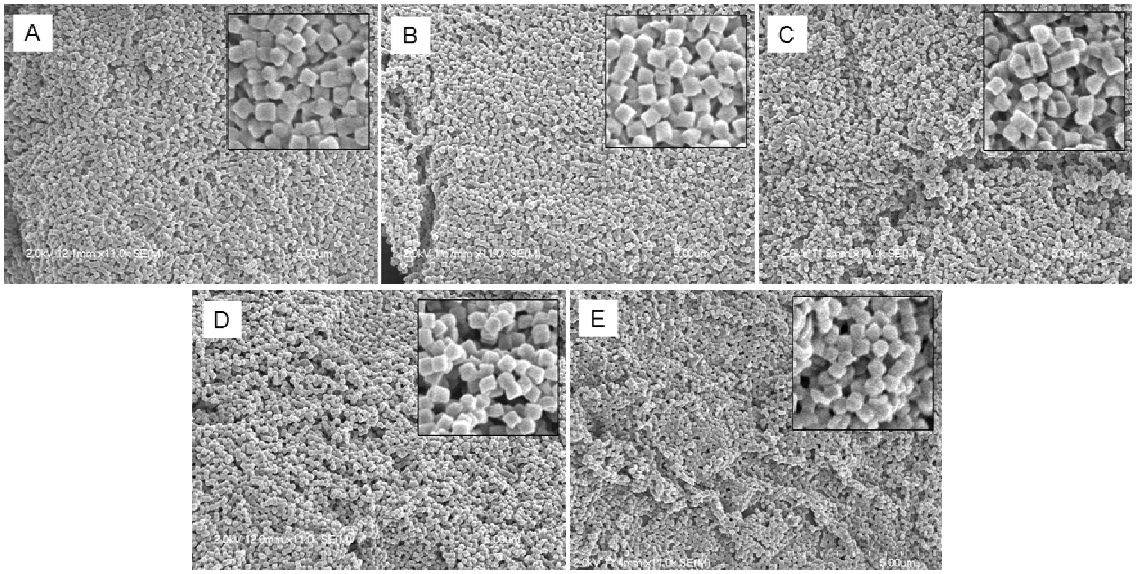

Figure 3.11 SEM images of cylindrical 200nm x 200nm PLGA PRINT nanoparticles containing varying amounts of docetaxel: A) 0%, B) 10%, C) 20%, D) 30%, E) 40%. Inset images are a magnification of a portion of the image to the same scale for more detail.

3.3.3 Release Profiles

As with siRNA the release of active docetaxel from the particle is also of high importance. The main concern with docetaxel is heat induced degradation during the melt filling step of the PRINT process. This was investigated by HPLC (Figure 3.12).

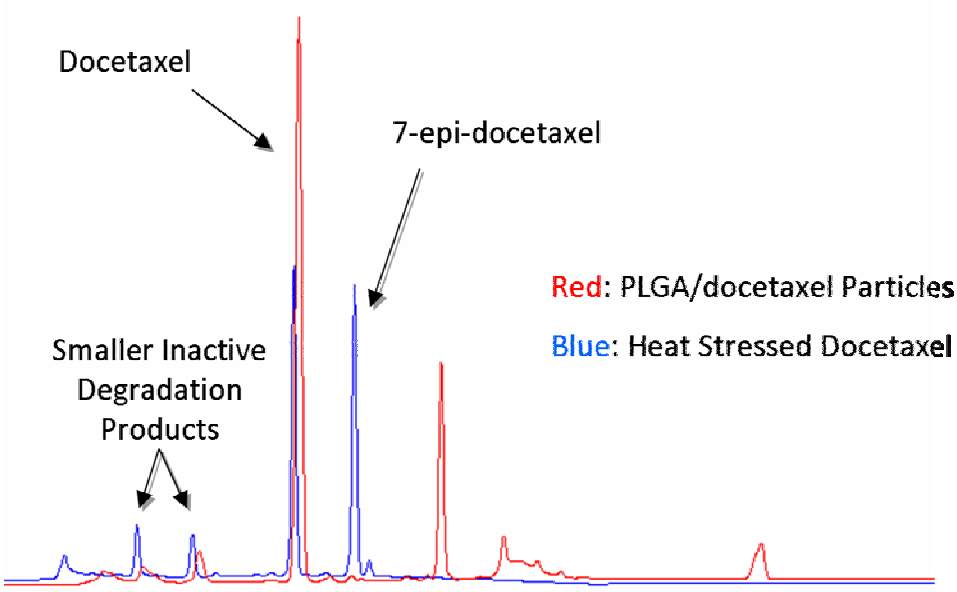

Figure 3.12 The HPLC trace of heat stressed docetaxel (blue) and PLGA/docetaxel particles (red).

The main heat degradation product of docetaxel is 7-epi-docetaxel which comes out later in the solvent gradient. 7-epi-docetaxel is still active against microtubule depolymerization, however, it is less cytotoxic than docetaxel. There are also two smaller, fragment degradation products which come out earlier in the gradient are and inactive.[8, 9] All these degradation products can be seen in the blue trace, docetaxel which was heated to 100°C for 1 minute. When particles containing docetaxel are then compared, no 7-epi-docetaxel is seen (red trace). All latter peaks in the red trace are identified components of the particle. Having shown the docetaxel remains intact

throughout the PRINT process, HPLC was used to measure the release of docetaxel from PLGA particles under sink conditions (Figure 3.13). The PLGA chosen for *in vitro* cytotoxicity experiments was one with a fast release profile. All compositions show similar release and complete release is achieved in 24 hours. The release rates of the particles should therefore have no effect on the cytotoxicity across compositions measured at 72 hours.

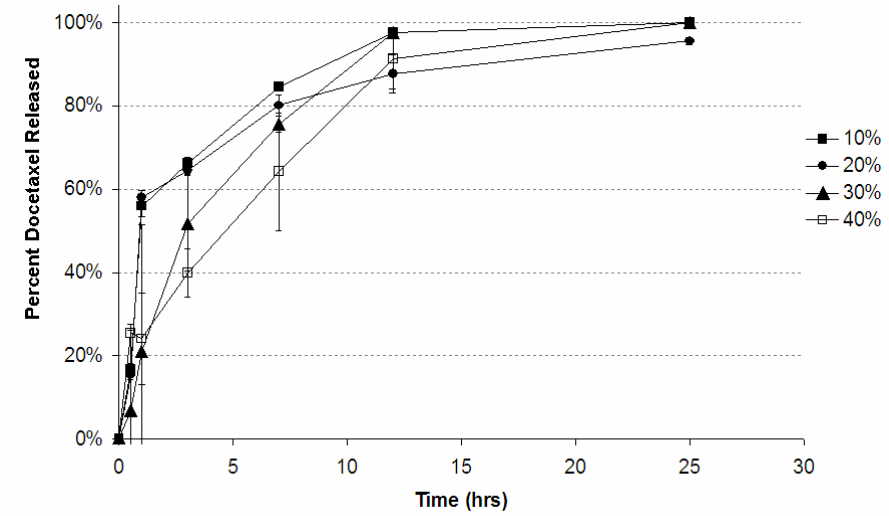

Figure 3.13 Release profiles of PLGA nanoparticles containing 10-40% docetaxel at pH 7.4 and 37°C.

The particles exhibit the typical burst rate seen in the literature with PLGA nanoparticles (Table 1.3). Importantly the particles completely release docetaxel. Some formulations reported in the literature show incomplete release even at low time points.[7] Interestingly the highest loading of docetaxel exhibits a slightly slower release. This may be attributed to the hydrophobic nature of docetaxel and the increased docetaxel-docetaxel interactions of the particle with higher loading.

3.3.4 *In vitro* drug delivery efficacy

Uptake studies had previously confirmed that negatively charged PLGA PRINT nanoparticles are not internalized by cells (Figure 3.6). The efficacy of these particles then depends on their ability to release docetaxel which will then be internalized by cells or their ability to transfer docetaxel directly across the cell membrane while in contact with cells. A comparison of toxicity among particles containing 0 – 40% docetaxel on H460 non-small cell lung cancer is shown in Figure 3.14 below.

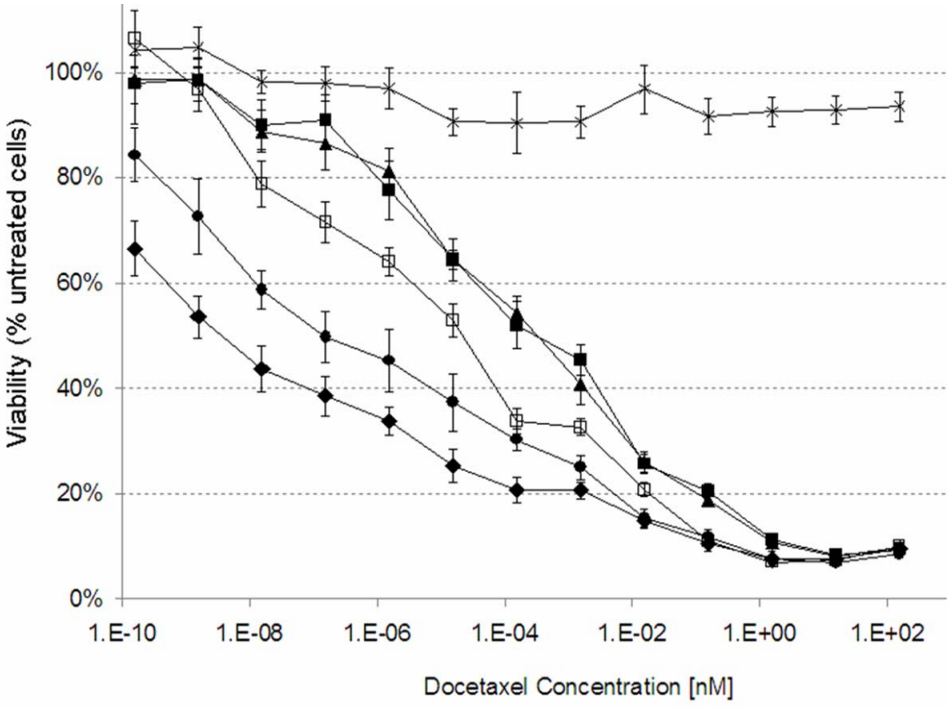

Figure 3.14 H460 cell viability after 72 hour exposure to Taxotere® and PLGA PRINT nanoparticles containing various docetaxel weight percents: 0% docetaxel (x), 10% docetaxel (■), 20% docetaxel (▲), 30% docetaxel (●), 40% docetaxel (♦), and Taxotere® (□). Blank particles (0%) were dosed at equal particle concentrations to 10% docetaxel containing particles (i.e. the highest particle dose).

Particles without drug are non-toxic as expected from the biocompatible, bioabsorbable nature of the polymer and previous toxicity experiments. PLGA PRINT nanoparticles

containing docetaxel exhibit dose dependant toxicity and are toxic in sub-picomolar docetaxel concentrations. This demonstrates the wide dosing range at which the particles may have efficacy *in vivo*. The particles are compared to the standard of care therapy, Taxotere®. Slightly lower toxicity compared to this standard is seen with particles containing 10% and 20% docetaxel while particles containing 30% and 40% docetaxel show higher toxicity at the same docetaxel concentration (Table 3.3).

Table 3.3 IC_{50} values for docetaxel loaded PLGA PRINT Nanoparticles and Taxotere.

	IC_{50} [nM]
Taxotere	1.2 x 10-5
10% Docetaxel PLGA PRINT	2.8 x 10-4
20% Docetaxel PLGA PRINT	2.6 x 10-4
30% Docetaxel PLGA PRINT	2.7 x 10-7
40% Docetaxel PLGA PRINT	5.3 x 10-9

These results demonstrate not only that the PRINT process allow for high encapsulation of docetaxel, but that the docetaxel is released from the particle, can be delivered to its desired cellular target, and is unharmed by the processing conditions. Since release rates are equal for all four PRINT docetaxel compositions, it suggests higher docetaxel loadings could be important to increase efficacy at a lower total dose and further investigation into the effects of higher loadings on toxicity, something until now impossible to study, are warranted. In addition the IC_{50}s of docetaxel PLGA PRINT nanoparticles are orders of magnitude lower than any values reported in the literature which range from 1 nM to 105 nM.[10-13]

3.3.5 *In vivo* drug delivery efficacy

The *in vivo* efficacy docetaxel PLGA PRINT nanoparticles was investigated in a xenograft SKOV3 mouse model. To test efficacy without the added complexity of biodistribution, intratumoral (I.T.) injections were employed. This is an investigation of the particles' ability to release docetaxel *in vivo* where it will reach its intracellular target and actively block cell division; thereby delaying the growth of the tumor or in the best case, leading to regression. Each mouse was injected with three doses (0.2 mg of docetaxel per dose) every other day of Taxotere, docetaxel containing PLGA particles, or an equal mass of blank (drug free) particles. The tumor volumes (4 mice each) are shown in Figure 3.15 below.

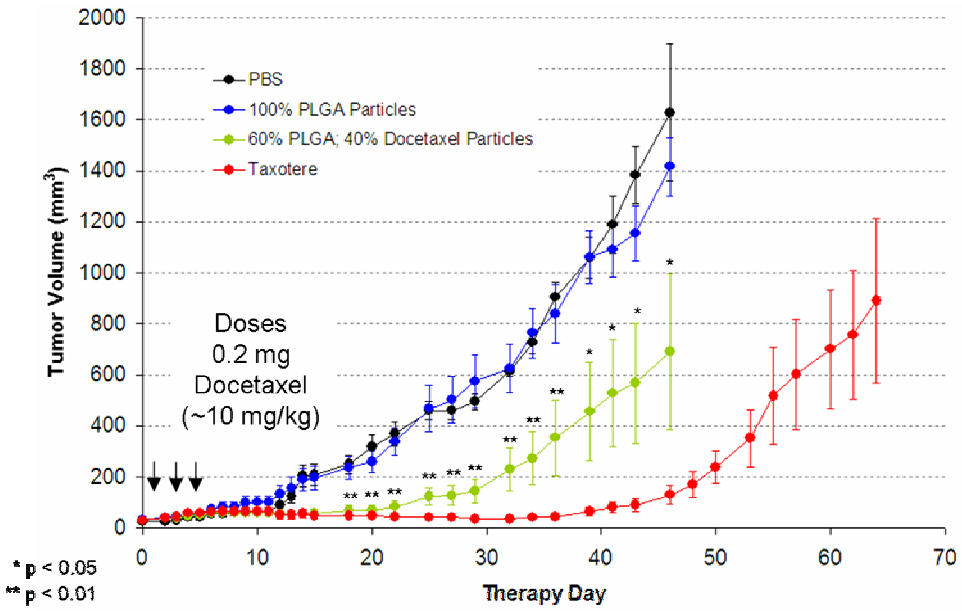

Figure 3.15 The in vivo efficacy of 40% docetaxel PLGA PRINT nanoparticles in SKOV3 mouse model (*p<0.05, **p<0.01).

The mice injected with 100% PLGA particles and the mice injected with PBS show identical tumor progression over 45 days. This demonstrates neither the particle injection

nor the PLGA affects tumor progression. The mice treated with docetaxel containing PLGA PRINT nanoparticles show a 15 day delay in progression which is significant out to day 45 after which there are fewer than 4 mice remaining. The group treated with Taxotere shows a longer delay of an additional 15 days. No treatment was able to prevent progression all together or achieve regression. In fact once progression began the rate of growth is similar between all groups. The benefit of Taxotere over PLGA nanoparticles is likely due to their size and therefore their mobility in the tumor tissue. DLS measurement showed Taxotere is actually a nanoparticle suspension with particles measuring 14 nm (PDI 0.2) and -2 mV. The smaller particle probably penetrates through the tumor tissue, away from the injection site more easily than the 200 nm PLGA PRINT particle.[14] This allows the Taxotere to reach a higher volume of the tissue and delay progression more effectively. Nevertheless the PLGA PRINT nanoparticles have clearly demonstrated their ability to deliver docetaxel *in vivo* and effect the progression of a rapidly growing tumor.

3.3.6 Pharmacokinetics of docetaxel *in vivo*

To design a particle which will have the highest efficacy when administered I.V. we turned to pharmacokinetics (PK). By studying which particles deliver the most docetaxel to the tumor, a good estimate of the optimal formation for *in vivo* efficacy can be obtained. Two formulations were investigated in the initial PK study. The first was the formulation used previously in the I.T. efficacy study: 40% docetaxel in a 50:50 PLGA (33,000 g/mol). The second was a slower release formulation: 40% docetaxel in an 85:15 PLGA (50,000 g/mol). The difference in release is 1 day versus over 1 week (Figure 3.16).

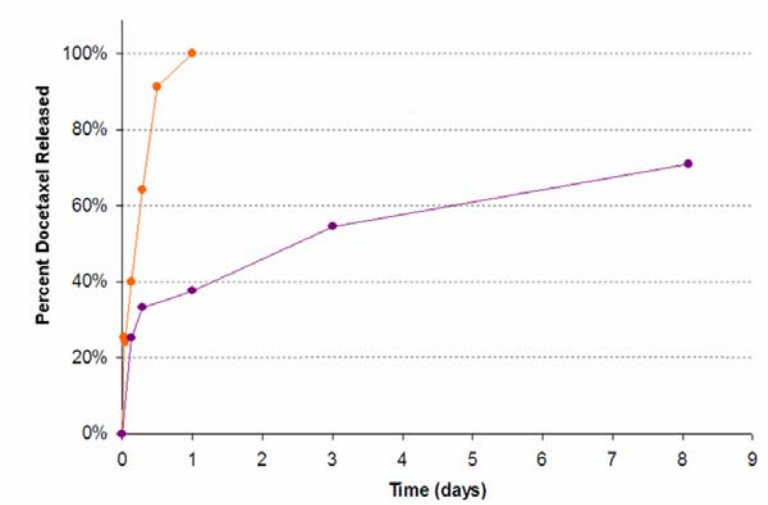

Figure 3.16 The release of docetaxel from two different PLGA polymers: orange is a 50:50, 33kDa PLGA and purple is a 85:15, 50kDa PLGA.

There are no physical differences in the particle formulations (Table 3.4) which indicates the particle itself should have the same biodistribution. This is one of the many benefits of the PRINT method. The formulation can be tailored one variable at a time.

Table 3.4 The physical properties of PLGA PRINT nanoparticles from different PLGA polymers.

PLGA Polymer	Size (nm)	PDI	Zeta Potential (mV)
50:50	225 ± 3	0.031	-8
85:15	227 ± 1	0.041	-3

Any difference in PK must, therefore, be due to a difference in release profile. It would be expected that the 50:50 PLGA particle may be releasing docetaxel in the blood stream before the particle accumulates in the tumor, while the 85:15 PLGA particle will lose less docetaxel before reaching the tumor. As hypothesized, the particle with a slower release profile showed higher docetaxel accumulation in the tumor. And both PLGA PRINT compositions showed higher tumor accumulation than Taxotere (Figure 3.17).

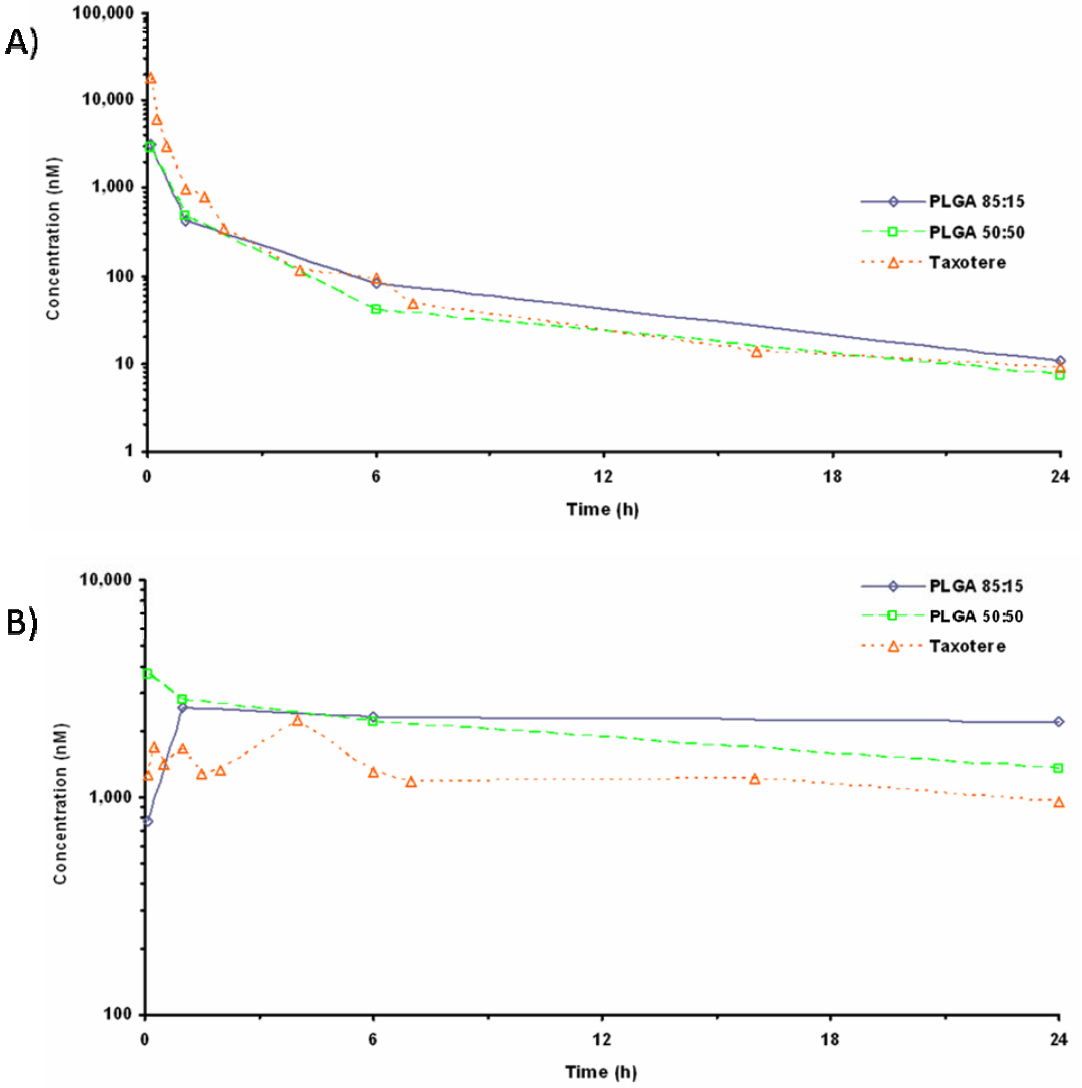

Figure 3.17 The PK profiles of two PRINT compositions compared to Taxotere over 24 hours. Concentrations in (A) plasma and (B) tumor.

This initial study indicates the 85:15 PLGA composition would be more effective when administered I.V. The plasma clearance can be characterized by the area under the curve (AUC). Table 3.5 shows the AUC values for Taxotere, PLGA PRINT nanoparticles, and some PLGA formulations from the literature.

Table 3.5 AUC values for Taxotere and PLGA nanoparticles.

Injection	Fabrication Method	Composition	Size (nm)	PDI	$AUC_{0-\infty}$ (h•nM)	Ref
Taxotere	--	--	14	0.2	8,172	--
Nanoparticle	PRINT	50:50 PLGA	225	0.031	3,605	--
Nanoparticle	PRINT	85:15 PLGA	227	0.041	4,140	--
Nanoparticle	Emulsion	50:50 PLGA	175	0.24	67,781	[12]
Nanoparticle	Emulsion	75:25 PLGA	102	0.15	70,545	[10]

The formulations reported in the literature are smaller and much more heterogeneous in size than the PRINT compositions which probably leads to the enhancement in circulation. Smaller particles and more importantly the smaller fractions of a heterogeneous particle population (<100nm) are less likely to be cleared by the liver and spleen. This suggests a smaller PRINT particle should be investigated. Before *in vivo* efficacy trials are begun, however, the PK of more compositions needs to be tested. The efficacy trial takes months to complete while a PK experiment can be conducted in one day. Obviously the PK study is a valuable screening tool and full advantage should be taken.

3.3.7 Conclusions

The fabrication of PLGA nanoparticles with high and efficient docetaxel loadings has been demonstrated. The physical properties of these particles remain constant even while the chemical composition is altered. These particles have shown toxicity *in vitro* higher than currently studied PLGA emulsion formulations with some indication that high loadings increases efficacy. In an efficacy study, particles delayed the progression of SKOV3 xenograft tumors. This was the first demonstration of *in vivo* anti-tumor efficacy

by PRINT nanoparticles; higher efficacy compositions are sure to follow. PK investigation is underway to choose the next compositions for *in vivo* efficacy testing.

3.3.8 Future Work

The ultimate goal of advanced drug delivery with PLGA PRINT nanoparticles is a fully tailorable system whereby a doctor can choose a desired chemotherapeutic or combination of therapeutics and a desired PK/PD profile for the specific needs of a patient.

3.3.8.1 PK studies with more sizes, shapes and compositions

To achieve a fully tailorable system, compositions with different sizes, shapes, and release profiles as well as different doses and dosing regimes must be thoroughly explored. The first hurdle is the fabrication of smaller particles with highly efficient loadings. While 200 nm particles show >90% encapsulation efficacy, initial test on 80 x 320 nm particles showed much lower loading. It was hypothesized that while no x,y phase separation occurs in the films, some separation in the z-direction could occur as demonstrated in Figure 3.18 below.

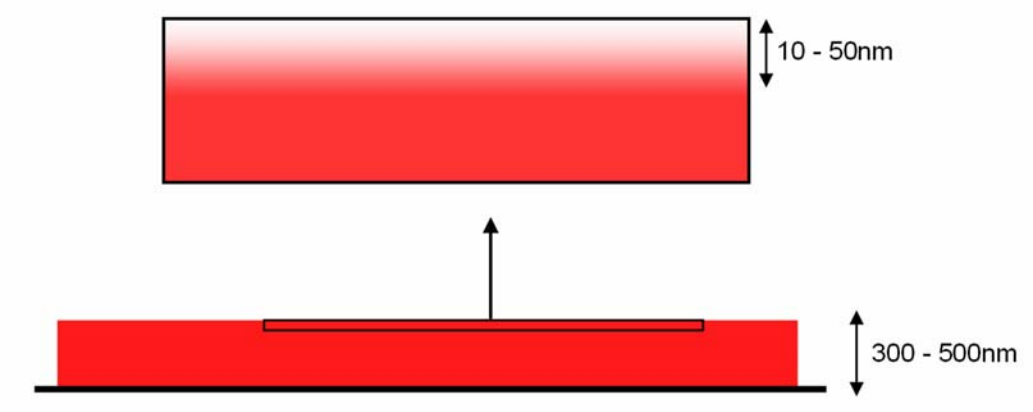

Figure 3.18 A cutaway view of a PLGA/docetaxel film which is typically 300-500 nm in depth. The docetaxel is represented by the red color which is depleted in the first 10-50 nm on the very surface of the film.

To test if this separation was occurring, the film was explored using time of flight secondary ion mass spectrometry (TOF SIMS). In this method a sample beam and a sputtering beam alternate, giving a depth profile of the film. Figure 3.19 shows the depth profile of a 40% docetaxel PLGA film cast from DMF/DMSO. Region I is the surface of the film where ubiquitous surface contamination strongly influences secondary ion yield. Region II is the bulk of the film and region III is the interface of the film with the PET substrate. A depletion of docetaxel is clearly seen near the surface of the film. In order to make smaller particles with high loadings this issue must be solved. Some progress has already been made, increasing encapsulation efficiency from ~10% to ~70%.

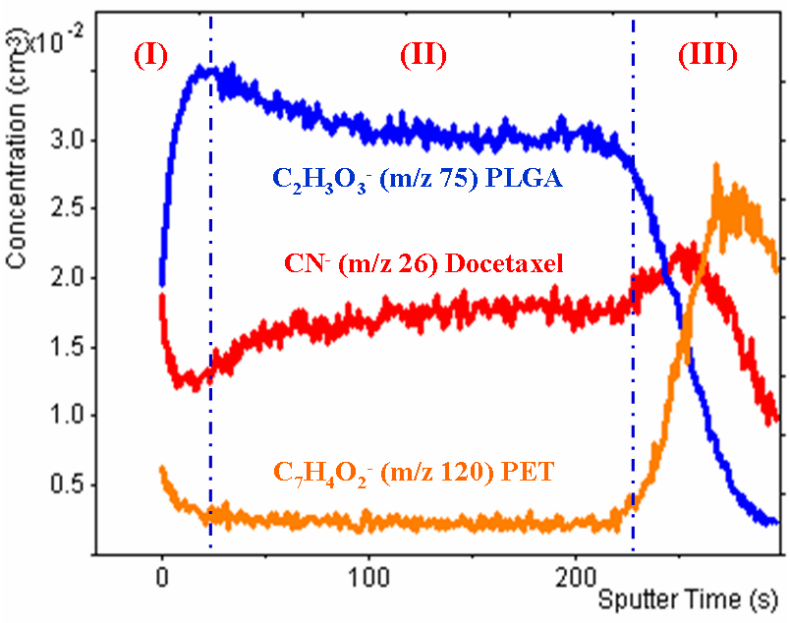

Figure 3.19 TOF SIMS depth profile of PLGA/docetaxel film.

Once this issue is fully solved, the comparison of particles from the 80 nm differing aspect ratio series and the smaller aspect ratio of 1 series discussed previously can be explored. Since tumor penetration will be an important issue for this delivery system, information gathered from biodistribution studies will be very instructive. Different PLGA polymers will also need to be explored to vary the release rate of the particle. This can be used to maintain a therapeutic concentration of drug in the tumor for a desired length of time. Finally targeting of this system is also underway and the effect on biodistribution, tumor penetration, and drug PK/PD will be another layer of complexity to explore.

3.3.8.3 Combinations of gene therapy and chemotherapy

A combination of siRNA and chemotherapy should be investigated once both are fully developed. Several groups have already demonstrated the improved efficacy of the

combination over either single component.[15-17] Genes targeted by these groups included inhibitor of apoptosis proteins (IAPs) which serve a pro-survival function and are often upregulated in cancer cells; focal adhesion kinases (FAKs) which affect cell migration, invasion, and proliferation and whose upregulation in cancer is a predictor of poor prognosis; and epidermal growth factor receptor (EGFR) which triggers proliferation, angiogenesis, and metastasis and is upregulated in many cancers. Combination therapy with PLGA PRINT nanoparticles will be very straightforward as all components can be mixed into a single particle or components can be administered together in separate particles which can have the same physical properties. This is an advantage over current methods which can not tailor physical properties independent of composition and which can not easily encapsulate cargos with different philicities. Furthermore the limited amount of cargo other particle technologies are capable of loading certainly limits the ability to encapsulate effect quantities of multiple cargos. The PRINT process allows for the fabrication of highly engineered PLGA particles, beyond any currently available technologies, showing great promise as a tailorable drug delivery system. While the future plans for PLGA PRINT nanoparticles are not just imagined, but already underway; the future of this work is truly limitless.

References

1. P. Xu, E. G., L. Tong, C. B. Highley, D. R. Errabelli, T. Hasan, J. Cheng, D. S. Kohane, Y. Yeo, Intracellular Drug Delivery by poly(lactic-co-glycolic acid) Nanoparticles, Revisited. *Molecular Pharmaceutics* **2008,** 6, (1), 190-201.

2. K.T. Love, K. P. M., C. G. Levins, K. A. Whitehead, W. Querbes, J. R. Dorkin, J. Qin, W. Cantley, L. L. Quin, T. Racie, M. Frank-Kamenetsky, K. N. Yip, R. Alvarez, D. W. Y. Sah, A. de Fougerolles, K. Fitzgerald, V. Koteliansky, A. Akinc, R. Langer, D. G. Anderson, Lidid-like materials for low-dose, in vivo gene silencing. *PNAS* **2010,** 107, (5), 1864-1869.

3. H. Katas, E. C., H. O. Alpar, Preparation of polyethyleneimine incorporated poly(D,L-lactide-co-glycolide) nanoparticles by spontaneous emulsion diffusion method for small interfering RNA delivery *International Journal of Pharmaceutics* **2009,** 329, 144-154.

4. K. Tahara, H. Y., N. Hirashima, Y. Kawashima, Chitosan-modified poly(D,L-lactide-co-glycolide) nanospheres for improving siRNA delivery and gene-silencing effects. *European Journal of Pharmaceutics and Biopharmaceutics* **2010,** 74, 421-426.

5. W. C. Zamboni, S. S., E. Joseph, R. A. Parise, M. J. Egorin, J. L. Eiseman, Tumor, tissue, and plasma pharmacokinetic studies and antitumor response studies of docetaxel in combination with 9-nitrocamptothecin in mice bearing SKOV3 human ovarian xenografts. *Cancer Chemotherapeutic Pharmacology* **2008,** 62, 417-426.

6. Rolland, J. P.; Van Dam, R. M.; Schorzman, D. A.; Quake, S. R.; DeSimone, J. M., Solvent-resistant photocurable "liquid teflon" for microfluidic device fabrication. *Journal of the American Chemical Society* **2004,** 126, (8), 2322-2323.

7. S. Murugesan, S. G., R. K. Averinei, M. Nahar, P. Mishra, N. K. Jain, PEGylated Poly(lactide-co-glycolide) (PLGA) Nanoparticulate Delivery of Docetaxel: Synthesis of Diblock Copolymers, Optimization of Preparation Variables on Formulation Characteristics and In Vitro Release Studies. *Journal of Biomedical Nanotechnology* **2007,** 3, 52-60.

8. B. M. Rao, A. C., M. K. Srinivasu, M. L. Devi, P. R. Kumar, K. B. Chandrasekhar, A. K. Srinivasan, A.S. Prasad, J. Ramanatham, A stability-indicating HPLC assay method for docetaxel. *Journal of Pharmaceutical and Biomedical Analysis* **2006,** 41, 676-681.

9. D. Kumar, R. S. T., S. K. Deolia, M. Mitra, R. Mukherjee, A. C. Burman, Isolation and characterization of degradation impurities in docetaxel drug substance and its formulation. *Journal of Pharmaceutical and Biomedical Analysis* **2007,** 43, 1228-1235.

10. M. Senthilkumar, P. M., and N. K. Jain, Long circulating PEGylated poly(D,L-lactide-co-glycolide) nanoparticulate delivery of docetaxel to solid tumors. *Journal of Drug Targeting* **2008,** 16, (5), 424-435.

11. F. Esmaeili, M. H. G., S. N. Ostad, F. Atyabi, M. Seyedabadi, M. D. Malekshahi, M. Amini, and R. Dinarvnand, Folate-receptor-targeted delivery of docetaxel nanoparticles prepared by PLGA-PEG-folate conjugate. *Journal of Drug Targeting* **2008,** 16, (5), 415-423.

12. F. Esmaeili, R. D., M. H. Ghahremani, S. N. Ostad, H. Esmaily, and F. Atyabi, Cellular cytotoxicity and in-vivo biodistribution of docetaxel poly(lactide-co-glycolide) nanoparticles. *Anti-Cancer Drugs* **2010,** 21, (1), 43-52.

13. O. C. Farokhzad, J. C., B. A. Teply, I. Sherifi, S. Jon, P. W. Kantoff, J. P. Richie, and R. Langer, Targeted nanoparticle-aptamer bioconjugates for cancer chemotherapy in vivo. *PNAS* **2006,** 103, (16), 6315-6320.

14. H. Lee, H. F., B. Hoang, R. M. Reilly, and C. Allen, The Effects of Particle Size and Molecular Targeting on the Intratumoral and Subcellular Distribtuion of Polymeric Nanoparticles. *Molecular Pharmaceutics* ASAP.

15. C. Gill, C. D., A. J. O'Neill, R. W. G. Watson, Effects of cIAP-1, cIAP-2, and XIAP triple knockdown on prostate cancer cell susceptibility to apoptosis, cell survival, and proliferation. *Molecular Cancer* **2009,** 8, (39), 1-12.

16. J. Halder, C. N. L. J., S. K. Lutgendorf, Y. Li, N. B. Jennings, D. Fan, G. M. Nelkin, R. Schmandt, M. D. Schaller, A. K. Sood Focal Adhesion Kinase Silencing Augments Docetaxel-Mediated Apoptosis in Ovarian Cancer Cells. *Clinical Cancer Research* **2005,** 11, (24), 8829-88-36.

17. S. M. Thomas, M. J. O., M. L. Freilino, S. Strychor, D. R. Walsh, W. E. Gooding, J. R. Grandis, W. C. Zamboni, Antitumor Mechanisms of Systemically Administered Epidermal Growth Factor Receptor Antisense Oligonucleotides in Combination with Docetaxel in Squamous Cell Carcinoma of the Head and Neck. *Molecular Pharmacology* **2007,** 73, (3), 627-638.